People's Democratic Republic of Algeria

Ministry of Higher Education and Scientific Research

A. MIRA-BEJAIA University

Faculty: Nature and Life Sciences

Department: Food Sciences

Attached Laboratory or Research Unit:

Biomathematics, Biophysics, Biochemistry and Scientometry Laboratory (L3BS)

THESIS

SUBMITTED FOR THE DEGREE OF

DOCTORATE

Domain: Nature and Life Sciences **Field: Food Sciences**

Specialty: Food Product Quality and Safety

Presented by

Sabrina IDIR

Subject

Anthocyanin-Rich Extracts: Composition, Stability and Formulation

Defended on: February 15, 2026 **Before a jury composed of:**

First name and last name	Title			
Mr. Khodir MADANI	Professor	Bejaia	University	Chair
Ms. Sabiha ACHAT	Professor	Bejaia	University	Supervisor
Mr. Olivier DANGLES	Professor	Avignon	University	Co-supervisor
Mr. Lotfi MOUNI	Professor	Bouira	University	Examiner
Mr. Farouk REZGUI	Professor	Bejaia	University	Examiner
Mr. Farouk MOUKAH	National Vice President	Algerian Confederation of Employers		Guest

Academic Year: 2025/2026

République Algérienne Démocratique et Populaire

Ministère de l'Enseignement Supérieur et de la Recherche Scientifique

Université A.MIRA-BEJAIA

جامعة بجاية
Tasdawit n Bgayet
Université de Béjaïa

Faculté : Sciences de la Nature et de la Vie.

Département : Sciences Alimentaires.

Laboratoire ou unité de recherche de rattachement : Laboratoire de Biomathématiques, Biophysique, Biochimie et Scientométrie (L3BS)

THÈSE

EN VUE DE L'OBTENTION DU DIPLOME DE DOCTORAT

Domaine : Sciences de la Nature et de la Vie. **Filière : Sciences Alimentaires.**

Spécialité : Qualité des Produits et Sécurité Alimentaire.

Présentée par

Sabrina IDIR

Thème

Extraits riches en anthocyanes : Composition, stabilité et formulation

Soutenue le : 15 février 2026 **Devant le Jury composé de :**

Nom et Prénom	Grade		
Mr. MADANI Khodir	Prof.	Univ. de Bejaia	Président
Mme. ACHAT Sabiha	Prof.	Univ. de Bejaia	Rapporteur
Mr. DANGLES Olivier	Prof.	Univ. d'Avignon	Co-Rapporteur
Mr. MOUNI Lotfi	Prof.	Univ. de Bouira	Examinateur
Mr. REZGUI Farouk	Prof.	Univ. de Bejaia	Examinateur
Mr. MOUKAH Farouk	Vice-Président National	Confédération Algérienne du Patronat	Invité

Année Universitaire : 2025/2026

ٱلْـحَمْدُ لِلَّهِ ٱلَّذِي بِنِعْمَتِهِ تَتِمُّ ٱلصَّالِحَاتُ، وَبِفَضْلِهِ تَتَنَزَّلُ ٱلرَّحَمَاتُ،
وَبِقُدْرَتِهِ تَتَحَقَّقُ ٱلْغَايَات
ٱلْـحَمْدُ لِلَّهِ عَلَى تَمَامِ ٱلنِّعْمَةِ وَكَمَالِ ٱلْفَضْل

à mes parents, à mes frères et sœurs, aux NOLDINES, à mes amis, pour le soutien qu'ils m'ont apporté et pour leur présence tout au long de ces années.

Remerciements / Acknowledgements

À la fois projet scientifique et parcours personnel, cette thèse est le fruit d'une collaboration enrichissante et de défis constructifs et riches en enseignements.

En premier lieu, je remercie chaleureusement Sabiha Achat, ma directrice de thèse, pour la confiance qu'elle m'a témoignée, sa disponibilité constante, son exigence bienveillante et sa rigueur scientifique. Son accompagnement attentif, tout en me laissant une grande liberté dans mes choix scientifiques, a été pour moi une source d'inspiration et a largement contribué à mon développement personnel et scientifique.

Je tiens à exprimer ma profonde reconnaissance à Olivier Dangles, dont la supervision avisée a été un atout inestimable dans la concrétisation de cette thèse. Expert en physico-chimie des anthocyanes, il a su, par son expertise et son approche bienveillante, clarifier les concepts complexes et me former dans ce domaine, ce qui a largement contribué à l'aboutissement de ce travail. Son encadrement a profondément façonné mon regard scientifique et m'a permis de développer un réel enthousiasme pour cette thématique.

I extend my sincere thanks to Dr. Luís Cruz for welcoming me, despite time constraints, to the FoodPhenolLab of LAQV-REQUIMTE at the Faculty of Sciences of the Porto University (FCUP) for a short-term internship. Under his supervision, I was able to enhance my knowledge and technical skills, which laid a solid foundation for the successful completion of this work.

Je remercie sincèrement les membres du jury, Pr. KHODIR Madani, Pr. MOUNI Lotfi, Pr. REZGUI Farouk, et Mr. MOUKAH Farouk pour l'honneur qu'ils m'ont fait en acceptant d'évaluer ce travail.

Et enfin, je souhaite remercier chaleureusement l'ensemble des membres du laboratoire 3BS, où j'ai passé la majeure partie de ces dernières années. Merci aux doctorants, enseignants, ingénieurs et amis pour leur accueil, leur aide au quotidien, leur bonne humeur et tous les moments partagés. Merci aussi à toutes celles et ceux qui, de près ou de loin, ont contribué, à la réalisation de ce travail.

Abstract

Anthocyanins are natural red–purple–blue pigments of interest as alternatives to synthetic dyes. However, their sensitivity to pH, temperature, dioxygen, light, and matrix composition limits their industrial applications, particularly under near-neutral conditions.

In this work, anthocyanin-rich extracts from eggplant peel (EPP), pomegranate juice (PGJ), and blood orange juice (BOJ) were enriched and characterized by HPLC-MS and UV–visible spectroscopy. Their composition, hydration susceptibility (reversible color loss), thermal stability (irreversible degradation), and metal-binding capacity were investigated as key determinants of color diversification and stabilization. BOJ and EPP were more resistant to hydration than PGJ. All extracts formed Al^{3+} complexes at pH 5, reversing hydration equilibria and regenerating color: EPP produced blue complexes, whereas BOJ and PGJ produced purple ones. At 50 °C, BOJ showed the highest stability, while EPP degraded rapidly.

To better approximate food-like environments, the extracts were encapsulated in alginate–pectin beads at pH 4 and 5. Encapsulation efficiency ranged from 17.9 to 82.1 %, with the highest values for EPP and PGJ and the lowest for BOJ. Thermal stability was greatest for BOJ, followed by PGJ, with EPP being the least stable. Al^{3+}–anthocyanin complexes provided the highest encapsulation efficiency and were especially stable at pH 5, with pectin further improving thermal resistance.

BOJ, the most stable extract in both liquid and encapsulated forms, contains flavonoids, particularly flavones, whose planar structures promote strong π-stacking with anthocyanins, enhancing color stability by limiting hydration and the accumulation of thermally sensitive chalcones. Conversely, PGJ experienced greater color loss due to abundant hydration-prone anthocyanidin 3,5-diglucosides, only modestly protected by endogenous ellagitannins. The faster degradation of EPP anthocyanins likely results from their higher sensitivity to autoxidation driven by caffeoyl derivatives, which, although they mitigate hydration-induced color loss, can accelerate thermal breakdown.

Finally, incorporation into hard candies confirmed practical relevance: acidified formulations produced vivid red hues, while non-acidified ones yielded purple tones for BOJ and EPP and nearly colorless PGJ. Despite lower color vividness than Allura Red, natural extracts were perceived as more authentic and were thus well appreciated by consumers.

Keywords: *Eggplant, Pomegranate, Blood orange, Anthocyanin, Copigment, Aluminum Encapsulation.*

Résumé

Les anthocyanes sont des pigments végétaux responsables des teintes rouge–pourpre–bleue et représentent une alternative prometteuse aux colorants synthétiques. Leur stabilité, fortement dépendante du pH, de la température, du dioxygène, de la lumière et de la composition matricielle, limite toutefois leur application industrielle, notamment en milieu neutre.

Dans ce travail, des extraits riches en anthocyanes de pelure d'aubergine (EPP), jus de grenade (PGJ) et jus d'orange sanguine (BOJ) ont été enrichis et caractérisés par HPLC-MS et UV-Vis afin d'évaluer composition, stabilité thermique (dégradation irréversible), hydratation (perte de couleur réversible) et complexation métallique comme facteurs de stabilisation des couleurs. BOJ et EPP se sont révélés plus résistants à l'hydratation que PGJ. Tous les extraits ont formé des complexes avec Al^{3+} à pH 5, inversant l'équilibre d'hydratation et régénérant la couleur : EPP produisait des complexes bleus, tandis que BOJ et PGJ donnaient des complexes pourpres. À 50 °C, BOJ présentait la plus grande stabilité, alors qu'EPP se dégradait rapidement.

Pour mieux simuler les environnements alimentaires, les extraits ont été encapsulés dans des billes d'alginate–pectine à pH 4 et 5. L'efficacité d'encapsulation variait de 17,9 à 82,1 %, avec les valeurs les plus élevées pour EPP et PGJ et les plus faibles pour BOJ. La stabilité thermique était toutefois la plus élevée pour BOJ, suivie de PGJ, EPP étant le moins stable. Les complexes Al^{3+}–anthocyanes présentaient la meilleure efficacité d'encapsulation et une stabilité accrue à pH 5, l'ajout de pectine renforçant encore la résistance thermique.

BOJ, l'extrait le plus stable en solution comme encapsulé, contient des flavonoïdes, notamment des flavones, dont la structure plane favorise de fortes interactions π-empilement avec les anthocyanes, limitant l'hydratation et la formation de chalcones thermosensibles. À l'inverse, PGJ a montré une perte de couleur plus marquée en raison de la présence abondante d'anthocyanidines 3,5-diglucosides, très sensibles à l'hydratation et faiblement protégées par les ellagitannins endogènes. La dégradation plus rapide des anthocyanes d'EPP s'explique par leur sensibilité accrue à l'autoxydation induite par les dérivés caféoylés.

Enfin, l'incorporation dans des bonbons durs a confirmé la pertinence pratique : les formulations acidifiées présentaient de vives teintes rouges, tandis que les non acidifiées donnaient des tons pourpres pour BOJ et EPP, et presque incolores pour PGJ. Malgré une couleur moins vive que l'Allura Red, les extraits naturels ont été perçus comme plus authentiques et en conséquence étaient bien appréciés par les consommateurs.

***Mots-clés** : Aubergine, Grenade, Orange sanguine, Anthocyane, Copigmentation, Aluminium, Encapsulation.*

ملخص

الأنثوسيانين هي أصباغ نباتية طبيعية مسؤولة عن الألوان الحمراء–الأرجوانية–الزرقاء وتشكل بديلاً واعدًا للأصباغ الاصطناعية. غير أن حساسيتها تجاه درجة الحموضة والحرارة والأكسجين والضوء وتكوين المصفوفة تحد من استخدامها الصناعي، خصوصًا في البيئات شبه المحايدة.

في هذا العمل، تم توصيف المستخلصات الغنية بالأنثوسيانين من قشر الباذنجان (EPP) وعصير الرمان (PGJ) وعصير البرتقال الدموي (BOJ) باستخدام HPLC-MS والتحليل الطيفي بالأشعة فوق البنفسجية والمرئية، لدراسة تركيبها، وقابليتها للترطيب (فقدان اللون القابل للعكس)، واستقرارها الحراري (تحلل غير قابل للعكس) ، وقدرتها على الارتباط بالمعادن كعوامل رئيسية لاستقرار الالوان. أظهر كل من BOJ وEPP مقاومة أعلى للترطيب مقارنة بـPGJ. جميع المستخلصات شكّلت مركبات مع Al^{3+}عند درجة حموضة 5 مما عكس توازن الترطيب وأعاد توليد اللون: أنتج EPP مركبات زرقاء، بينما شكّل BOJ وPGJ مركبات أرجوانية. عند 50 °م، أظهر BOJ أعلى استقرار حراري، في حين تدهور EPP بسرعة.

لمحاكاة الظروف الغذائية، تم تغليف المستخلصات في حبيبات من الألجينات والبكتين عند درجة حموضة 4 و5. تراوحت فعالية التغليف بين 17.9 و82.1٪، وكانت الأعلى لـEPP وPGJ والأدنى لـBOJ. ومع ذلك، كان الاستقرار الحراري الأكبر لـBOJ، يليه PGJ، بينما كان EPP الأقل استقرارًا. أظهرت مركبات أنثوسيانين–Al^{3+} فعالي أفضل للتغليف واستقرارًا مرتفعًا عند درجة حموض 5، مع تعزيز البكتين للمقاومة الحرارية.

يحتوي BOJ، الأكثر استقرارًا في الشكلين السائل والمغلف، على فلافونويدات، خصوصًا الفلافونات، التي تعزز هياكلها المستوية التراصّ π القوي مع الأنثوسيانين، عبر الحد من الترطيب وتكوّن الكالكونات الحساسة للحرارة. بالمقابل، فقد PGJ لونه بدرجة أكبر بسبب وفرة أنثوسيانيدين 3,5-ديجلوكوزيدات شديدة القابلية للترطيب وضعف حمايتها بالإيلاجيتانينات الذاتية. ويُعزى التحلل الأسرع لأنثوسيانين EPP إلى حساسيتها العالية للأكسدة الذاتية الناتجة عن المشتقات الكافيينية.

أخيرًا، أكّد دمج المستخلصات في الحلوى الصلبة أهميتها التطبيقية: إذ أنتجت التركيبات المحمضة ألوانًا حمراء زاهية، بينما أعطت غير المحمضة ألوانًا أرجوانية لـBOJ وEPP، وشبه عديمة اللون بالنسبة لـPGJ. رغم أن حيوية الألوان أقل من Allura Red، فقد اعتُبرت المستخلصات الطبيعية حقيقية أكثر ونالت استحسان المستهلكين.

الكلمات المفتاحية :الأنثوسيانين، الباذنجان، الرمان، البرتقال الدموي، التصبغ المشترك، الألمنيوم، التغليف.

Valorization

The present results have been communicated through the following academic contributions, listed in chronological order:

Publications in peer-reviewed journals

- Idir, S., Achat, S., Cruz, L., & Dangles, O. (2025). Anthocyanin-rich extracts: Susceptibility to color loss by hydration and thermal degradation, influence of metal ions and endogenous copigments. *Food Chemistry*, *481*, 144004.

  https://doi.org/10.1016/j.foodchem.2025.144004.

Oral communications at international conferences

- SABRINA IDIR, SABIHA ACHAT, OLIVIER DANGLES (2022). Antioxidant activity and stability of anthocyanins rich extract. The First Virtual International Seminar on Bioressources, Nutrition, and Health (ISBNH 2022). University of Abdelhamid Ibn Badis-Mostaganem-Algeria. (28th and 29th November 2022).

- Idir Sabrina, Achat Sabiha, Djenad Fatima, Achat Yasmine, Beddar Siham, Cruz Luis, Dangles Olivier (2024). Color Stability of Eggplant Peel Anthocyanin-Rich Extract: Effect of Hydration, Thermal Degradation, Metal Ions, and Endogenous Copigments. 2nd Tunisian-Algerian International Scientific Congress. Applied Sciences for sustainable Development (2nd SISTA-SADD). Orient Palce-Sousse, Tunisia. (December 19, 20 & 21, 2024).

Posters presented at national conferences

- IDIR Sabrina, ACHAT Sabiha, DANGLES Olivier, HAMMIROUNE Abdelghani, DJENAD Fatima (2023). SCREENING OF PHYTOCHEMICAL COMPOSITION AND ANTIOXIDANT ACTIVITY OF SOME ANTHOCYANINS RICH EXTRACT. 5th Natural and Life Sciences Days, A. Mira University – Bejaia, Algeria (December 6–7, 2023).

Table of Contents

Abbreviations and symbols

A	Neutral quinonoid base
A	Absorbance
A^-	Anionic quinonoid base
ACN	Anthocyanin
A_f	Final absorbance
A^G/Alg	Alginate
AH	Antioxidant
AH^+	Flavylium cation
AHC	Agglomerative Hierarchical Clustering
A_i	Initial absorbance
B	Hemiketal
BOJ	Blood orange juice
C 3,5DG	Cyanidin 3,5-O-diglucoside
C3G	Cyanidin 3-O-glucoside
C3MG	cyanidin 3-O-(6”-malonyl)glucoside
CAGR	Compound Annual Growth Rate
Cc	Cis- chalcones
CFR	Code of Federal Regulations
CIE	Commission Internationale de l’Éclairage.
CNCA	Codex Alimentarius National Committee.
CR	Color Regeneration
Ct	Trans-chalcones
D3G	Delphinidin-3-O-glucoside
D3R	Delphinidin-3-O-rutinoside
DPPH	1,1-diphenyl-2-picrylhydrazyl.
EDTA	Ethylenediaminetetraacetic acid
EPP	Eggplant peel.
ESI	ESI Electrospray Source Ionisation.
FD&C	Food, Drugs, and Cosmetics.
FDA	U.S. Food and Drug Administration.
GA	Gallic Acid.
HMF	5-hydroxymethylfurfural.
HPLC	High pressure liquid chromatography.
HSB	Hue, Saturation, Brightness.
HSL	Hue, Saturation, Lightness.
HSV	Hue, Saturation, Value.
$K\hat{}a$	Acidity constant at pseudo-equilibrium.
$K\hat{}_h$	Hydration constant at pseudo-equilibrium.
K'_a	Acidity constant at full equilibrium.
K'_h	Hydration constant at full equilibrium.
K_a	Acidity constant.
K_i	Isomerization constant.
k_{obs}	Apparent first-order rate constant of hydration.
K_t	Tautomerization constant.
MS	Mass spectrometry.

MW	Molecular weight.
NaAlg	Alginate de sodium.
P/Pec	Pectin
PCA	Principal component analysis.
PGJ	Pomegranate juice.
PREFMAP	External preference mapping
RC	Residual Color.
RGB	Red, Green, Blue.
SCF	Scientific Committee for Food.
SECO	Secoisolariciresinol.
SIN	Système International de Numérotation.
$t_{1/2}$	half-life.
TAC	Total anthocyanins content.
TPC	Total polyphenol content.
ε	Molar absorption coefficient.
λ_{max}	Wavelength of maximal absorption.

List of figures

List of tables

List of appendices

« La difficulté n'est pas de voir ce que personne n'a jamais vu, mais de penser comme personne n'a jamais pensé au sujet de quelque chose que tous voient ».

Arthur Schopenhauer

Introduction

Introduction

Food colorants represent a major class of food additives, playing a strategic role in product competitiveness by ensuring visual appeal and influencing consumer preferences. The global food colorants market was valued at USD 3.1 billion in 2023 and is projected to reach USD 4.8 billion by 2030, with a compound annual growth rate (CAGR) above 6%. Confectionery, beverages, and dairy remain the most colorant-intensive sectors, where appearance is a key determinant of consumer acceptance.[1]

Historically, natural pigments such as saffron, turmeric, and paprika were widely employed, dating back to ancient Egyptian civilization **(Singh et al., 2023)**. The discovery of synthetic dyes, starting with mauveine in 1856 by Henry Perkin, revolutionized the food industry by enabling large-scale production of more stable and cost-effective colorants **(Cova et al., 2017).** Azo dyes, a common class of synthetic colors, offered high coloring strength, attractive hues, and superior stability. However, the massive use of petrochemical-derived dyes has raised long-standing health concerns, including neurobehavioral effects in children and carcinogenic potential in animal models. Consequently, regulatory agencies have progressively tightened safety frameworks **(Barciela et al., 2023).**

Synthetic dyes are now experiencing a global decline, with avoidance particularly marked in Europe, Asia, the Middle East, the United States, and Africa. The U.S. Food and Drug Administration (FDA) has announced the phase-out of six widely used synthetic dyes by 2026, including Red 40 (Allura red AC), Yellow 5 (Tartrazine), Yellow 6 (Sunset yellow FCF), Blue 1 (brilliant blue FCF), and Blue 2 (Indigotine). While Europe has restricted Scarlet GN, Ponceau GR, and Orange RN[2,3]. These regulatory measures, combined with rising consumer mistrust, have

[1] https://www.grandviewresearch.com/industry-analysis/food-colorants-market
[2] https://www.fda.gov/news-events/press-announcements/hhs-fda-phase-out-petroleum-based-synthetic-dyes-nations-food-supply
[3] Official Journal of the European Union, Commission Regulation (EU) 2020/1819 of 2 December 2020, amending Annex II to Regulation (EC) No 1333/2008 as regards the use of colours in salmon substitutes, OJ L 403, 3 December 2020, p. 7–10.

accelerated the shift toward natural alternatives, which currently account for approximately 38% of the global food colorants market[4].

Currently, the European Union authorizes 13 natural colorants, while the United States permits 26 exempt-from-certification colors, reflecting regional regulatory differences. Widely used natural pigments include carotenoids such as β-carotene (E160a) and lycopene (E160d), spirulina extracts (E161g), and anthocyanins (E163). These pigments not only support clean-label trends but also align with sustainability goals by reducing reliance on synthetic chemicals. Leading companies have already adopted such solutions; for example, Nestlé replaced synthetic blue with spirulina extract in its candies in 2008, demonstrating both technical feasibility and consumer acceptance **(Renita et al., 2023).**

Anthocyanins are water soluble pigments, representing one of the most promising classes of natural colorants. Widely distributed in fruits, vegetables, and flowers, these polyphenols flavonoid compounds confer a broad palette of colors ranging from orange-red to blue-violet **(Dangles, 2024)**. Beyond their visual appeal, anthocyanins have attracted increasing attention for their potential health-promoting effects, including antioxidant, anti-inflammatory, and cardioprotective activities **(Krga & Milenkovic, 2019)**. In the USA, they are approved by the FDA when derived from fruit or vegetable juices (21 CFR 73.250 and 73.260), while in the EU they are classified as E163 and authorized in various food products **(Rodriguez-Amaya, 2019)**.

In recent decades, joint efforts between academic and industrial research have greatly advanced the understanding of anthocyanin chemistry **(Denish et al., 2021).** These collaborations have not only deepened knowledge of their structural diversity, color expression, and reactivity, but also stimulated innovation in their stabilization and application as natural food colorants.

At the molecular level, anthocyanins are O-glycosides of a tricyclic polyphenolic chromophore known as anthocyanidin, which exists as the flavylium cation under strongly acidic conditions (pH < 2). Their remarkable structural diversity arises from B-ring substitution patterns, the number and position of glycosyl groups, and possible acylation with aliphatic or phenolic acids **(Dangles,**

[4] https://www.marketgrowthreports.com/market-reports/food-colors-market-106235.

2024). This complexity is further amplified by the multiple reversible transformations of the flavylium ion as pH increases. Consequently, anthocyanins exist in a dynamic equilibrium between colored (flavylium and quinonoid bases) and colorless species (hemiketal and cis/trans-chalcones), the latter generally predominating under the mildly acidic conditions typical of plant tissues and foods **(Cruz et al., 2022; Dangles & Fenger, 2018; Pina, 2014)**. To counter this intrinsic instability, plants rely on protective mechanisms that shift the equilibrium toward the colored species or prevent water addition to the flavylium ion. Copigmentation through π–stacking interactions with colorless phenols exemplifies the first strategy, while metal binding to catechol-substituted anthocyanins represents the second **(Trouillas et al., 2016)**.

Beyond these natural processes, Technological approaches such as encapsulation have been increasingly applied in food science to enhance the stability of anthocyanins and extend their potential as natural colorants. Encapsulation provides a physical barrier against light, oxygen, and temperature fluctuations, thereby preserving pigment integrity, intensifying visible color, and improving resistance to thermal and photochemical degradation. In addition, it offers advantages such as controlled release, improved bioavailability, and the possibility of masking or preserving flavor and aroma. Micro- and nanoencapsulation strategies thus constitute promising tools for the formulation of functional and health-oriented food products **(Guo et al., 2018; Oancea, 2021; Tan et al., 2021)**.

The rich physical chemistry of ACNs has been extensively investigated with pure pigments **(Cruz et al., 2022; Trouillas et al., 2016)**, which are difficult to extract and purify in substantial amounts. Extension of these works to anthocyanin-rich extracts is highly desirable, as a) only extracts (not pure ACNs) are amenable to industrial development for obvious economic reasons, b) extracts may contain other components, especially colorless phenols, contributing to color stability by acting as copigments, antioxidants, UV-filters… So far, color studies involving extracts rich in ACNs and copigments are typically limited to reporting extract composition and global spectral or colorimetric parameters, as well as apparent first-order rate constants of color loss, without distinguishing the reversible and irreversible components **(Müller-Maatsch et al., 2016; Oancea, 2021; Pereira et al., 2024)**.

This thesis is based on the central hypothesis that the rigorous physicochemical models developed for purified anthocyanins can be adapted to anthocyanin-rich extracts, thus applying to the pool of ACNs in interactions with the endogenous copigments (instead of individual ACNs). Thereby providing new insights into pigment stabilization within the extract. It is specifically proposed that the composition of the plant matrix, including coexisting flavonoids, phenolic acids, and polysaccharides, plays a decisive role in modulating anthocyanin behavior. Interactions within the matrix may influence the physicochemical constants governing their equilibrium, while during encapsulation, interactions with polysaccharides further contribute to modulating their stability. Such interactions may therefore either enhance or compromise pigment persistence, depending on the structural characteristics of both the anthocyanins and the surrounding components, in realistic food-like systems.

Building on this hypothesis, the objectives of the thesis are fourfold:

1. Characterization of anthocyanin-rich extracts

- To isolate and semi-purify anthocyanin-rich extracts from selected plant sources (pomegranate juice, blood orange juice, eggplant peel).
- To determine their anthocyanin composition, copigment content.

2. Evaluation of physicochemical stability

- To determine the equilibrium constants of the anthocyanin multistate and compare them with those of purified anthocyanins reported in the literature, so as to outline the possible influence of the plant matrix on the hydration equilibrium governing the partition of anthocyanins between colored and colorless forms.
- To quantitatively assess the metal–anthocyanin binding capacity of the extracts at the relevant food pH of 5, and to investigate their thermal stability under moderate heating at pH 5, by analyzing the percentage values of reversible (color loss) and irreversible (pigment loss) degradation.

3. Encapsulation strategies

- To encapsulate the extracts within polysaccharide-based systems (alginate and pectin), and to evaluate encapsulation efficiency and the protective effect provided by the matrices.

4. Application in model food systems

- To apply anthocyanin-rich extracts in confectionery products (hard candies) as a proof of concept in model food systems, and to analyze their coloring performance and stability under relevant technological conditions, with the aim of identifying the most promising sources and formulations for use as natural food colorants. in comparison with synthetic dyes.

Chapter I. Literature review

1. Food Colorants and Industry Marketing Strategies

Food quality is generally assessed on three basic criteria: nutritional composition, innocuity and sensory properties. color stands out as a key indicator of overall food quality, as it strongly influences consumer perception from the very first visual contact, thereby affecting both product acceptability and market success **(Durazzo et al., 2022).**

The food industry uses colorants not only to enhance visual appeal, ensure color uniformity, and offset degradation caused by environmental factors such as light, oxygen, temperature, and storage, but also to serve marketing objectives, such as reinforcing product identity and creating visually distinctive or appealing products. In current practice, color application serves three main purposes: (1) in products where color is naturally provided by the raw materials themselves, such as fruits and vegetables, the objective is to preserve the visual appeal and purity of naturally occurring pigments like carotenoids, chlorophylls, and polyphenols, without the use of additives. This approach is typically applied to minimally processed foods, including frozen fruits, fruit purées, juices, and ready-to-cook vegetable meals; (2) in other cases, colorants are intentionally added to restore, enhance, or standardize color that may be altered during processing or limited by formulation constraints. This is common in products such as beverages, sauces, and flavored yogurt; and (3) color is also used to create a distinctive product identity, particularly in novelty or "fun" foods such as confectioneries, ice creams, and vividly colored beverage **(Dikshit & Tallapragada, 2018).**

1.1. General concepts of food colorants

Definition

According to the FDA (U.S. Food and Drug Administration), a color additive, or food colorant, is "*any dye, pigment or substance which, when added to or applied to a food, drug or cosmetic, or to the human body, is capable (alone or by reaction with other substances) of imparting color.*"[5]

[5] FDA (2021). Overview of Food Ingredients, Additives & Colors. U.S. Food and Drug Administration. https://www.fda.gov/food/food-ingredients-packaging/overview-food-ingredients-additives-colors.

Type of colorants

Colorants differ in their origin, chemical structure, solubility and applications. In terms of origin, colorants are divided into natural categories, identical to natural, synthetic and inorganic colorants. Natural colorants are derived from biological sources such as plants, insects and micro-organisms. For instance, pigments such as anthocyanins, carotenoids and chlorophylls, which are extracted from fruits, vegetables and other natural resources. Naturally identical colorants are synthetic versions of natural pigments, such as β-carotene, which are chemically produced to mimic the structure and function of natural pigments. Synthetic colorants, produced entirely by chemical processes, are not found in nature. Inorganic colorants, such as titanium dioxide and calcium carbonate, are derived from mineral sources **(Novais et al., 2022).**

Dyes or pigments

Colorants are either dyes or pigments, although these two terms are often used indiscriminately, Pigments, however, consist of small particles that are partially insoluble in those media in which they are applied. This means that pigments must be attached to a substrate by using additional compounds, such as polymers in paints, plastics or melts. Dyes, on the other hand, are applied to various substrates (textiles, leather, paper, hair etc) from a liquid in which they are completely, or at least partly, soluble. In contrast to pigments, dyes must have a specific affinity to a given substrate **(Gürses et al., 2016)**.

Coloring foods or food colors

In the European Union, there is a clear legal distinction between coloring foods and food additives classified as colors. This distinction is based on the extraction method and the concentration of coloring compounds. Coloring foods are defined by whether the extraction is nonselective (retaining the natural composition of the source) or selective (concentrating specific pigments). The classification is further determined by calculating enrichment factors and applying a threshold value to decide whether a product is considered a "coloring food" or a food additive. In contrast, the regulatory approach in the United States does not differentiate between colorings derived from whole foods and those that are synthetically produced or selectively extracted. U.S. regulations prioritize the safety of the coloring material for consumption, regardless of its origin or processing. However, the approved colors are divided into two groups: certified colors which are all artificial and those exempt from certification that contain pigments obtained from natural

sources, of which some can also be produced by synthesis. Although exempt colors are not subject to batch certification, they must comply with strict identity and usage specifications. Furthermore, unlike certified FD&C colors, which are approved for general use in all foods, most exempt colors are limited to specific applications, and fewer than half are authorized for unrestricted use in food **(Stich, 2016).**

1.2. Synthetic colorants

About 70% of synthetic dyes have the azo chromophore, produced globally. These dyes are synthesized through a straightforward diazotization and coupling process, with modifications applied to optimize color properties, yield, and particle size, thereby enhancing dispersibility **(Benkhaya et al., 2020)**. The most common azo dyes in the food industry include carmoisine (E112, FD&C Red 10), ponceau 4R (E124, FD&C Red 3), allura red (E129, FD&C Red 40), tartrazine (E102, FD&C Yellow No. 5), sunset yellow (E110, FD&C Yellow 6), and quinoline yellow (E104, FD&C Yellow 10). These dyes are widely used to color jams, candies, confectionery, ice cream, jellies, alcoholic beverages, and soft drinks, among other products **(Alegbe & Uthman, 2024)**. Synthetic food colorants are popular among food manufacturers due to their high purity, tinting strength, stability, brightness, uniformity, reproducibility in production, and lower cost compared to natural colorants **(Martins et al., 2016).** Azo dyes can enhance the quality, color, flavor, and preservation of foods, yet may also pose health risks due to their metabolism and the oxidative stress they may induce **(Kola-Ajibade et al., 2021)**. Recent studies have confirmed interactions between human serum albumin, azo dyes, and hemoglobin **(Barciela et al., 2023).** Notably, tartrazine has been linked to obsessive-compulsive behaviors and DNA damage in animal studies **(Zand et al., 2023)**. While the European Parliament mandates labeling for products containing these dyes to indicate potential adverse effects on children's attention and activity, some azo dyes, such as Amaranth (E123, FD&C Red No. 2), are banned in the U.S. due to concerns about carcinogenicity. To address health concerns, highly specific methods have been developed to detect synthetic food colorants and evaluate their potential medium- and long-term side effects and toxicity **(Miller et al., 2022).**

1.3. Natural colorant

Natural colorants are primarily sourced from plants, animals, and minerals. Inorganic pigments**,** 84% of natural colorants, include aluminum (for silver-gray), gold, iron oxides (yellow, red, brown,

black), titanium dioxide (white), and calcium carbonate (for opacity). These are widely used in confectionery, chocolate, gums, and bakery products. Organic colorants (16%) consist of 75% dyes and 25% pigments, some derived by modifying biological materials (e.g., caramel, vegetable carbon). Nature-identical colors, such as carotene and riboflavin, are synthesized to match natural sources. The most prominent animal-derived colorants include sepia from cuttlefish, crimson from Kermes louse, Tyrian purple from shellfish, and carminic acid from cochineal insects **(Yadav et al., 2023)**.

Plant-Based Colorants stem from compounds like tannins, anthocyanins, betalains, flavonoids, carotenoids, and chlorophylls, these natural colorants often result from a combination of compounds rather than a single constituent **(Rodriguez-Amaya, 2019)** :

- **Anthocyanins** (E163): Polyphenolic pigments providing red to blue hues, the main sources used in food industry are grapes, elderberry, black carrots and blackcurrant.
- **Betalains** (E162): Red-violet to yellow-orange pigments, with betanin from beets commonly used to replace Allura red (E129).
- **Chlorophylls and Chlorophyllins** (E140 and E141): Green pigments extracted from alfalfa, used in dairy, soups, beverages, and as color adjusters in cheese.
- **Carotenoids** (E 160): These pigments, including β-carotene, annatto, paprika, and lutein, range from yellow to red and are used in a variety of products from baked goods to beverages.
- **Curcumin** (E100): Derived from turmeric, it provides a bright yellow but is unstable in high water conditions, making it ideal for candies and gum.
- **Riboflavin** (Vitamin B2): A yellow colorant used in cereals, sweets, and ice cream, though limited due to its odor and taste.

1.4. Food color regulation

European Union (EU) regulatory

In the European Union (EU), the Scientific Committee for Food (SCF) is responsible for supervising the safety of colorants and food additives. The SCF ensures that the regulations defined by the European Commission are implemented in the national legislation of EU member states. Regulation (EC) No 1333/2008 specifies the food color additives permitted based on technological

need, practical use, and current scientific knowledge. It includes food categories and a positive list of authorized colorants in the EU, along with their maximum permitted levels and instructions for use **(Lehto et al., 2017)**. All approved food additives (listed in Annexes II and III to Regulation (EC) No 1333/2008) must comply with the specifications laid down in Regulation (EU) No 231/2012. These specifications include the additive's name and synonyms, chemical and physical characteristics, origin or source, manufacturing process, and identification criteria (such as specific wavelengths for spectrophotometric analysis). Purity requirements are also defined, including a minimum content of coloring matter for most additives, except for caramel colors and anthocyanins, which are of natural origin and have inherently variable compositions **(Martins et al., 2016)**.

United States (US) regulatory

In the United States, the regulation of food colorants falls under the jurisdiction of the Food and Drug Administration (FDA), specifically under Title 21 of the Code of Federal Regulations (CFR). Nine synthetic colorants are permitted for general use, subject to certification, while 35 colorants derived from vegetable, animal, mineral sources, or synthetic equivalents of naturally occurring compounds are exempt from certification. Notably, three synthetic colorants approved in the U.S. are prohibited in the EU, while nine food colorants legal in the EU are not authorized in the U.S. **(Durazzo et al., 2022)**

Beyond the EU and the U.S., other countries such as China, India, Japan, and Thailand have their own regulatory frameworks for food coloring, each with unique standards and requirements. These national regulations are also influenced by the Codex Alimentarius, an international food standards body that provides guidelines for food safety and quality but does not always align with national laws or consumer expectations **(Lehto et al., 2017)**.

Anthocyanin's regulation

In the USA, anthocyanins are approved by the FDA as food colorants when derived from fruit or vegetable juices, under regulations 21 CFR 73.250 and 73.260. In the EU, they are classified as E163 and authorized for use in various food products. Their application includes a maximum level of 200 mg/kg in fruit-flavored breakfast cereals, either alone or combined with cochineal (E120) and beetroot red (E162). Alternatively, their use is allowed *quantum satis*, provided they comply with purity standards concerning residual solvents and heavy metals, as specified in EU Regulation

No. 1129/2011. Authorized sources in the EU include: 163(ii) Grape skin extract (Enociania, Eno); 163(iii) Blackcurrant extract; 163(iv) Purple corn color; 163(v) Red cabbage color; 163(vi) Black carrot extract; 163(vii) Purple sweet potato color; 163(viii) Red radish color; 163(ix) Elderberry color; and 163(x) Hibiscus color. Aluminum lakes derived from these extracts are also permitted **(EFSA Panel on Food Additives and Nutrient Sources added to Food (ANS), 2013).**

Algerian regulatory

In Algeria, the use of food additives is further governed by Executive Decree No. 12-214 of May 15, 2012 (Official Journal No. 30, May 16, 2012)[6], which sets out the terms and conditions for their use in food intended for human consumption. Issued jointly by the Ministries of Commerce, Health, Industry, and Agriculture, the decree includes three annexes: Annex I lists authorized food additives, Annex II specifies the food categories in which they may be used, and Annex III outlines the permitted maximum levels. The national list remains more restrictive than those of the Codex Alimentarius or the European Union, although periodic updates, guided by the Codex Alimentarius National Committee (CNCA), established by Executive Decree No. 05-67 of January 30, 2005, and led by the Ministry of Commerce, aim to align it with international standards. Among the permitted colorants, anthocyanins are listed under the International Numbering System (SIN) as 163, with 163(ii) specifically referring to grape skin extract.

2. Visual Perception and Analytical Methods for Color Evaluation

2.1. Optical basis of color in materials

The perception of color results from a complex interplay between the physical properties of light, the chemical nature of pigments, and the physiological mechanisms of the human visual system. When radiation from the visible spectrum (400–700 nm) reaches an object, specific wavelengths are selectively absorbed by the pigments on its surface, while others are reflected or transmitted depending on the medium, reflected in the case of solids and liquids or transmitted through transparent substances like gases or clear materials. The unabsorbed light then enters the eye through the cornea and lens, where the image is focused on the retina. The iris regulates the

[6] https://www.joradp.dz/FTP/JO-FRANCAIS/2012/F2012030.pdf

amount of light that passes through, adjusting according to illumination levels. Once on the retina, light activates two types of photoreceptors, rods, which are sensitive to light intensity, and cones, which are responsible for clear vision and color perception. This activation triggers a photochemical response in the visual pigments, initiating a cascade of neural signals transmitted to the cerebral cortex. Thus, the final perception of color arises not only from the spectral characteristics of light and the pigment's selective absorption but also from the physiological and psychological processing within the observer's brain **(Cairone et al., 2020).**

Achromatic colors, white, gray, and black, arise when light is reflected or absorbed uniformly across the visible spectrum (400–700 nm). White appears when light is completely and diffusely reflected, gray when a constant portion is absorbed, and black when all light is absorbed. In contrast, chromatic colors emerge when specific wavelengths of light are selectively absorbed or reflected, as illustrated in **Figure 1 (Tilley, 2020)**.

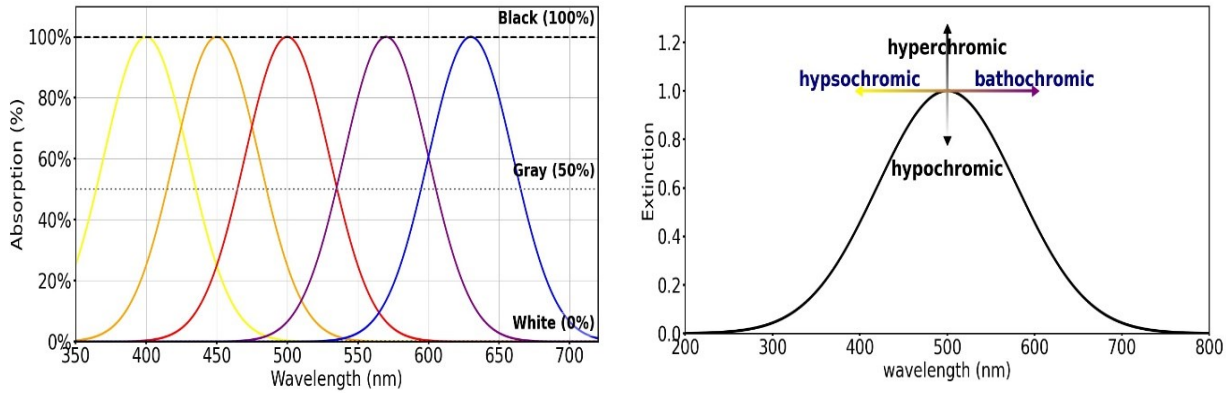

Figure 1. Left: schematic representation of the light absorption of colors, where achromatic colors are shown with dashed lines and chromatic colors with solid lines. Right: illustration of possible wavelength shifts and changes in the extinction of absorption bands **(Zollinger, 2003).**

When multiple colorants with different absorption spectra are combined, the resulting subtractive mixture often produces less vivid colors due to overlapping absorption bands. In extreme cases, such mixtures can appear black, as a result of near-complete absorption across the visible range. Additive color mixing, on the other hand, involves combining light from different sources to create new spectral profiles. When these combined spectra approximate that of sunlight, white or colorless light is perceived. While the specific wavelengths absorbed primarily determine color perception, the shape and intensity of the absorption bands also play a significant role in how colors are perceived by the human eye **(Zollinger, 2003).**

2.2. Color measurement

Essential in both industrial and scientific contexts, colorimetry provides a reliable method for describing and analyzing colors by measuring light absorption and reflection spectra, including those of dyes, pigments, and various colored material **(Choudhury, 2014).**

- *Colour specification systems*

The color estimation system can be of two types: Visual system and Instrumental methods **(Dutta et al., 2023)**. One of the earliest systems, proposed by Alfred Munsell in 1905, introduced a three-dimensional color space resembling a sphere, where each color has a specific position **(Figure 2,a).** This model defines color using three key attributes: Hue (the type of color, such as red, green, or blue), Value (the lightness or darkness, from black to white), and Chroma (the saturation or intensity of the color). While the Munsell system was a major step toward standardizing color classification, it relies on human perception and lighting conditions, making it subjective **(Dimitrova et al., 2022).** To address these limitations, a transition was made toward instrumental methods, where color models are used as visualizations of multidimensional spaces depicting the color spectrum. These methods use devices such as colorimeters or spectrocolorimeters that quantify color precisely. One of the most widely used systems in this context is the CIE system, developed by the Commission Internationale de l'Éclairage (CIE). It is based on mathematical models and tristimulus values (X, Y, Z), which can reproduce any visible color by combining the three primary colors: red, green, and blue (RGB). Among the most popular derivatives of the CIE system is the CIELAB model (or CIE L*a*b*), which provides a perceptual representation of color that closely matches human vision. This model defines color using three coordinates: L* (lightness), a* (green–red axis), and b* (blue–yellow axis). Another important model is HSV (Hue, Saturation, Value) — or its variants HSB (Brightness) and HSL (Lightness) **(Figure 2,b)**. These models offer a more intuitive, cylindrical representation of colors derived from the RGB space. This organization better reflects how humans perceive and adjust color attributes, especially in design and visualization tools. Unlike the Munsell system, CIELAB is entirely based on instrumental measurements, making it an objective, standardized, and industry-oriented approach, especially relevant in the food sector **(Pridmore, 2011; Shamey, 2023).**

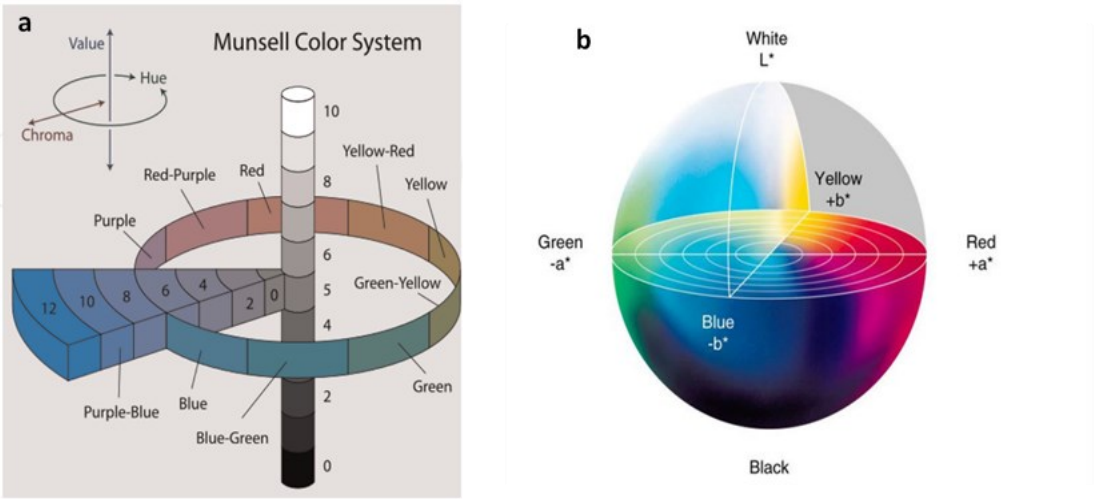

Figure 2. Munsell visual system **(Dutta et al., 2023)** (a), CIELAB color system **(Shamey, 2023)** (b).

- *Spectrophotometers*

  A spectrophotometer is a precise optical instrument used to measure the intensity of light absorbed, transmitted, or reflected by a sample across a range of wavelengths. It typically includes a light source, a dispersing element (such as a monochromator), an optical system, a detector, and a signal processor that converts light into an electrical signal. In transmission mode, it measures the light passing through transparent or liquid samples; in reflection mode, it analyzes light reflected from solid or opaque materials. When the energy of incident light matches the excitation energy of a molecule's electrons, specific wavelengths are absorbed, while the remaining light is transmitted or reflected. The resulting variation in light intensity across wavelengths is displayed as a spectrum, which provides insights into molecular composition, reactions, and optical properties such as color. These measurements, though intrinsic to the sample and independent of lighting or observation conditions, can be translated into standardized color coordinates, based on a defined illuminant and observer angle, highlighting the importance of standardization in colorimetric analysis. Their ability to deliver wavelength-specific data makes spectrophotometers ideal for research and development applications **(Dutta et al., 2023; Karuppaiah et al., 2023).**

- *Colorimeters*

  Colorimeters are simpler instruments designed to measure the color of both primary radiation sources, which emit their own light, and secondary radiation sources, which reflect or transmit external illumination. Unlike spectrophotometers, they do not scan across wavelengths but instead use optical filters to mimic the human eye's three types of cone cells, following the trichromatic theory of vision. A standard tristimulus colorimeter includes: (1) a light source to illuminate the sample, (2) three filters aligned with the L, M, and S cone sensitivities, and (3) a detector that captures the filtered light and converts it into electrical signals. This process yields tristimulus values (X, Y, Z) or directly provides data in the CIELAB color space (L*, a*, b*)**,** which closely correlates with human color perception. These instruments simulate the visual response of a standard observer under a standard illuminant, meaning that the output may vary depending on the specific device and its configuration. Their ruggedness, simplicity, and ease of use make them especially suitable for routine quality control applications, particularly in industries such as food, textiles, and plastics, where consistent color evaluation is essential **(Choudhury, 2014; Pathare et al., 2013).**

3. Polyphenols: Structural Diversity and Functional Relevance

Polyphenols are a large and structurally heterogeneous family of secondary metabolites derived from plants. They are defined by the presence of one or more hydroxyl groups directly attached to aromatic rings, which gives rise to their distinct reactivity and biological functions. Although the term "polyphenol" implies the presence of multiple phenolic groups, it is commonly used in a broader sense to include compounds with simpler structures, phenolic acids, to highly polymerized tannins, as long as they originate from plant phenolic metabolism **(Šamec et al., 2021; Singla et al., 2019).** In the plant kingdom, polyphenols play essential roles in defense against biotic and abiotic stresses, including ultraviolet (UV) radiation, pathogens, and herbivores. They also contribute to pigmentation, attract pollinators, reinforce cell walls, and participate in plant signaling **(Hasanuzzaman et al., 2020; Zagoskina et al., 2023)**. In food science and human health, polyphenols have attracted considerable attention due to their broad biological activities. These include antioxidant, anti-inflammatory, antimicrobial, and anticancer effects, as well as modulation of enzyme function and signaling pathways **(Dias et al., 2021; Medini et al., 2014; Olszowy,**

2019; Verma et al., 2020). Their presence in fruits, vegetables, grains, and beverages such as tea, coffee, and wine contributes not only to sensory properties like color, astringency, and bitterness, but also to the nutritional and therapeutic value of plant-derived foods **(De Mejia et al., 2020; Singh et al., 2023).**

3.1. Polyphenols classes

Structurally, polyphenols are primarily biosynthesized via two major pathways: the shikimate-derived phenylpropanoid pathway, which produces most phenolic acids and flavonoids, and the acetate/malonate polyketide pathway, responsible for certain simple phenols and stilbenes **(Cheynier et al., 2013; Shen et al., 2022; Zagoskina et al., 2023)**. The variability in their structure is not merely chemical but also determines their solubility, stability, reactivity, and bioavailability. At the core of polyphenol chemistry lies the aromatic ring substituted with hydroxyl groups. There is no consensus regarding their classification **(Belščak-Cvitanović et al., 2018)**. Depending on the number and arrangement of these rings and their substituents, the most widely adopted approach subdivides phenolics into two main groups: flavonoids and non-flavonoid polyphenols, a scheme commonly used in the literature **(Figure 3 & Figure 4) (Durazzo et al., 2019; Singla et al., 2019).**

Flavonoids represent the most structurally diverse and extensively studied class of polyphenols. They share a common C6–C3–C6 skeleton composed of two aromatic rings (A and B) linked by a three-carbon bridge, which typically forms a closed heterocyclic pyran ring (C) **(Figure 3).**

This configuration gives rise to the characteristic phenyl-benzopyran structure of flavonoids. Variations in the oxidation state, hydroxylation pattern, glycosylation, and degree of saturation of the central ring give rise to several subclasses: anthocyanins, flavanols, flavanones, flavonols, flavones, and isoflavones **(Cuyckens & Claeys, 2004; de Araújo et al., 2021)**. Non-flavonoids encompass a wide range of compounds lacking the C6–C3–C6 backbone. The most prominent are phenolic acids, which typically contain a single aromatic ring and are classified into hydroxybenzoic acids (C6–C1) and hydroxycinnamic acids (C6–C3) **(Gómez-Caravaca et al., 2014; Lourenço Neto et al., 2018)**, Other notable non-flavonoid phenolic compounds include xanthones, stilbenes, lignans, and tannins, which contain at least two aromatic rings, with tannins possessing more than two **(Figure 4) (Quideau et al., 2011).**

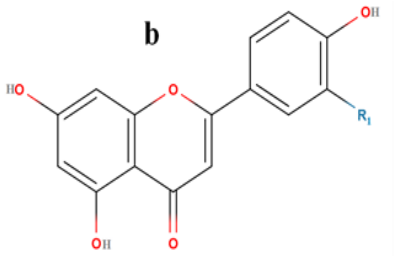

Flavones	
	R1
Apigenin	H
Luteolin	OH

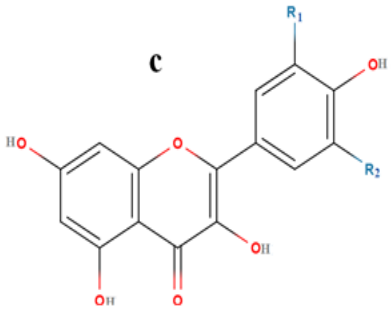

Flavonols		
	R1	R2
Quercetin	OH	H
Kaempferol	H	H
Myricetin	OH	OH
Laricitin	OH	OCH_3

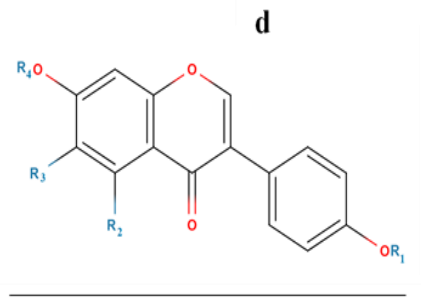

Isoflavones				
	R1	R2	R3	R4
Daidzin	H	H	H	glc
Glycitin	H	H	OCH_3	glc
Genistin	H	OH	H	glc

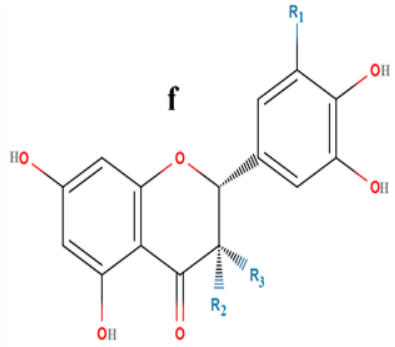

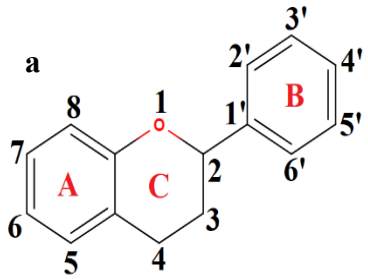

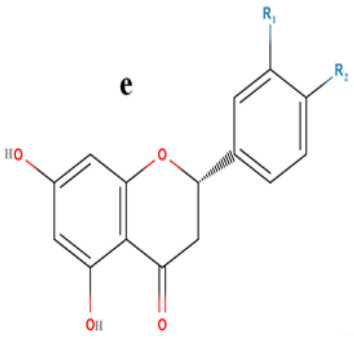

Flavan-3-ols			
	R1	R2	R3
(+)-Catechin	H	OH	H
(-)-Epicatechin	H	H	OH
(+)-Gallocatechin	OH	OH	H
(-)-Epigallocatechin	OH	H	OH
(+)-catechin-3-O-gallate	H	OH	Gallic acid
(-)-Epicatechin-3-O-gallate	H	H	Gallic acid

Flavanones		
	R1	R2
Naringenin	H	OH
Hesperetin	OH	OCH3

Figure 3. Basic chemical structure of the flavonoid subfamily. R_1, R_2, and R_3 represent substituents in some examples of phenolic flavonoid compounds. The general structure of flavonoids consists of benzene rings A and B linked by a heterocyclic pyran ring (a); Flavones (b), flavonols (c), isoflavones (d), flavanones (e) and flavan-3-ols (f). The general and detailed structures of the anthocyanin subclass are presented in Section 4.1.**(El Rayess et al., 2024).**

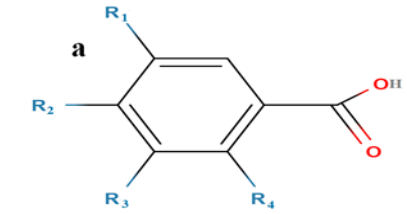

	Hydroxybenzoic acid			
	R1	R2	R3	R4
Gallic acid	OH	OH	OH	H
Vallinic acid	H	OH	OCH3	H
Protocatechiuc acid	H	OH	OH	H
Syringic acid	OCH3	OH	OCH3	H

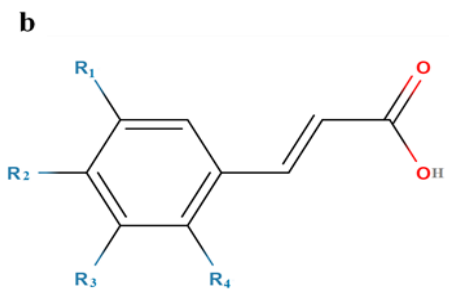

	Hydroxycinnamic acid			
	R1	R2	R3	R4
Caffeic acid	H	OH	OH	H
ρ-coumaric	H	H	OH	H
Ferulic acid	H	OCH3	OH	H
Sinapic acid	H	OCH3	OH	OCH3

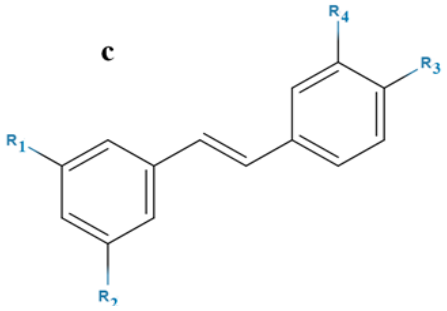

	Stilbene			
	R1	R2	R3	R4
trans-resveratrol	OH	OH	OH	H
Piceatannol	OH	OH	OH	OH

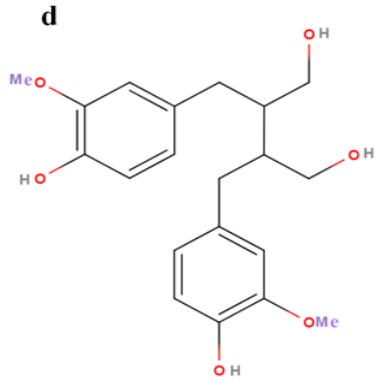

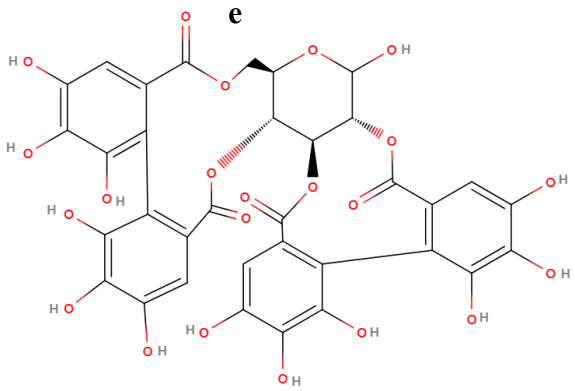

Figure 4. Basic chemical structure of the non-flavonoid subfamily. R_1, R_2,R_3 and R_4 represent substituents in some examples of non- flavonoid compounds. Hydroxybenzoic acid (a), Hydroxycinnamic acid (b), Stilbene (c), Secoisolariciresinol (SECO) (d), Pedunculagin (e) **(Bach Knudsen et al., 2020; El Rayess et al., 2024; Snarska et al., 2024).**

4. Anthocyanins: From Molecular Reactivity to Color Stabilization

At the molecular level, anthocyanins are intrinsically reactive compounds with electrophilic, nucleophilic, and electron-donating properties. This reactivity contributes to their broad color range but also to their marked instability in solution **(Dangles & Fenger, 2018; Di Meo et al., 2012; Trouillas et al., 2016).** Therefore, the effective use of anthocyanin-rich plant extracts as food colorants requires a thorough understanding of their degradation pathways and the natural stabilization mechanisms developed by plants, such as copigmentation and metal complexation, potentially acting in synergy. Food-grade biopolymers, including proteins and polysaccharides, may also serve as suitable carriers for the development of ready-to-use anthocyanin formulations **(Song et al., 2022)**. This section discusses color degradation and stabilization mechanisms in relation to anthocyanin structure and environmental conditions, and highlights key challenges in their application as natural food colorants.

4.1. Structural features and reversible forms

4.1.1 Anthocyanins structure and derivatives

Anthocyanins are water-soluble flavonoid pigments characterized by a hydroxylated 2-phenylbenzopyrylium ion chromophore (flavylium cation) **(Figure 5).** They are predominantly found in the cell sap of higher plants, flowers, fruits, vegetables, seed coats, leaves, stems, tubers, and roots, where they are responsible for vivid red, purple, and blue hues **(Zeng et al., 2022)**. Structurally, they differ from other flavonoids by the presence of two double bonds in the heterocyclic C-ring and a positively charged oxygen atom, features that contribute to their pH-dependent coloration **(Rodriguez-Amaya, 2019)**.

The basic framework of anthocyanins consists of three essential components **(Morata et al., 2019)**:

- **Anthocyanidin**, the aglycone chromophore composed of the typical A-, B-, and C-rings, bearing hydroxyl (–OH) and/or methoxyl (–OCH_3) groups.
- **Glycosidic residues**, generally mono- (e.g., glucose, galactose, rhamnose, and arabinose), disaccharides (e.g., rutinose, sambubiose, and sophorose) commonly found in plants, or occasionally trisaccharides, attached via O-β-glycosidic bonds to hydroxyl groups on the chromophore. Glycosylation is systematic at the C3-OH position, frequent at C5-OH, and occasionally observed at other OH positions.

- **Acyl groups**, such as acetyl, malonyl, and hydroxycinnamoyl derivatives (often bearing additional –OH or –OCH_3 substituents), esterified to the sugar moieties, typically at the C6-OH position.

Variations in substitution patterns, particularly on the B-ring of the aglycone, define the different anthocyanidins. About 35% of naturally occurring anthocyanidins have been identified, with six, cyanidin, delphinidin, malvidin, pelargonidin, peonidin, and petunidin, accounting for approximately 92% of all reported anthocyanins **(Figure 5) (Andersen & Jordheim, 2010**). Simple glycosides, such as anthocyanidin 3-O-glucosides and 3,5-O-diglucosides, are the most common forms in foods, while acylated derivatives, especially with hydroxycinnamic acids (HCAs), are prevalent in floral pigmentation and dark-colored vegetables **(Dangles, 2024)**.

Glycosylation and acylation are the primary sources of structural diversity, with more than 700 anthocyanin derivatives reported **(Figure 5). (Feitosa et al., 2023; Wallace & Giusti, 2015)** . These substitutions influence color expression, stability, interactions with other molecules, bioavailability, and potential health benefits **(Belwal et al., 2020; B. Zhang et al., 2020).** Anthocyanins absorb light maximally in the visible range (510–530 nm) and in the ultraviolet range (270–280 nm) under acidic conditions, when the heterocyclic oxygen is protonated. Additional spectral shifts may occur due to conjugation with substituents on the aromatic rings **(Pina, 2014; Trouillas et al., 2016).** While anthocyanins serve ecological roles in plants, such as photoprotection and attraction of pollinators, they are also important dietary polyphenols **(Albuquerque et al., 2018; Belwal et al., 2020; De Pascual-Teresa et al., 2010; Dias et al., 2021; Krga & Milenkovic, 2019)**.

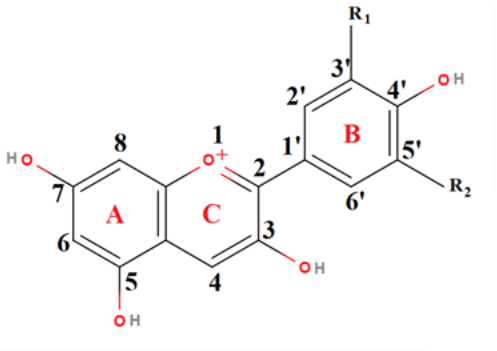

	Anthocyanins	
	R_1	R_2
Cyanidin	OH	H
Malvidin	OCH_3	OCH_3
Delphinidin	OH	OH
Pelargonidin	H	H
Petunidin	OCH3	OH
Peonidin	OCH3	H

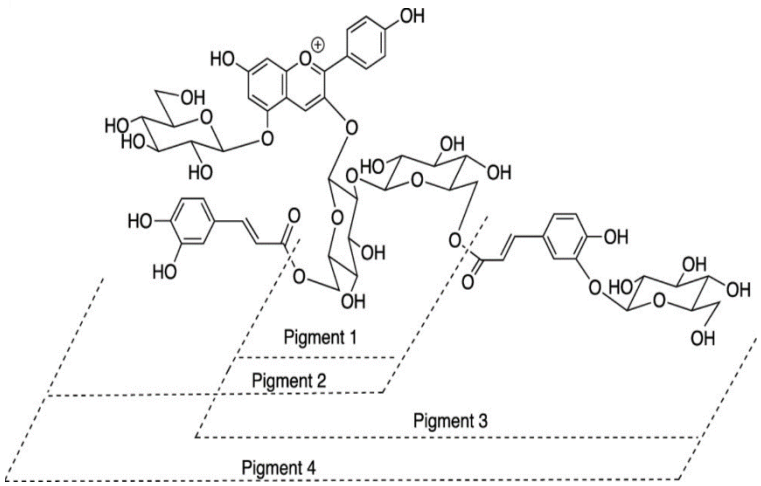

Figure 5. left: Structure of the six common anthocyanidin aglycone find in nature. Right: Polyacylated anthocyanins originally reported by Dangles et al. **(1993b),** adapted from Cruz et al.**(2022).**

4.1.2 Reversible color Loss and the role of pH

Although anthocyanins are frequently described in the literature by their flavylium cation form, this structural representation, when made without considering the influence of pH on anthocyanin speciation, may lead to misinterpretation of experimental observations **(Cruz et al., 2022)**. In aqueous systems, whether within plant vacuoles or food matrices, anthocyanins typically exist in mildly acidic conditions (pH 3–6), a range that promotes rapid and reversible color loss due to structural rearrangements **(Trouillas et al., 2016).**

At sufficiently acidic condition (pH < 3), the flavylium cation (AH^+) is the predominant species. This red-colored form is stabilized through charge delocalization around the O1 atom in the pyrylium ring, conferring both chromatic intensity and chemical stability. However, as pH increases toward neutral values, the flavylium cation undergoes a sequence of pH-dependent, reversible transformations, namely deprotonation **(Figure 6)**, hydration, and subsequent tautomerization - isomerization reactions **(Figure 7)**, resulting in a dynamic network of

interconvertible species **(Mendoza et al., 2019; Mendoza & Pina, 2021; Pina, 2014**). Each of these species contributes differently to the observed color and chemical stability of the solution:

- Flavylium cation (AH^+) – red, dominant at very low pH
- Quinoidal bases (A and A^-) – purple to blue, formed by proton dissociation
- Hemiketal (B) – colorless, formed via nucleophilic addition of water
- Cis- and trans-chalcones (Cc and Ct) – colorless to faint yellow, formed via tautomerization and isomerization of the hemiketal.

These transformations are illustrated by the following reaction scheme:

$$AH^+ \rightleftharpoons A \rightleftharpoons B \rightleftharpoons C$$

The relative distribution of these forms depends on the thermodynamic equilibrium of the system and shifts according to experimental conditions, notably pH and temperature. These constants vary according to anthocyanin structure, temperature, ionic strength and solvent polarity **(Basílio & Pina, 2016; Pina et al., 2012)**.

i. **Deprotonation (acid–base equilibria)**

The first transformation that occurs with rising pH is proton loss from the flavylium cation. The phenolic hydroxyl groups on the flavylium structure, especially at positions C7, C5, and C4′, become deprotonated due to the electron-withdrawing effect of the pyrylium ring, which increases the acidity of these groups. The C7-OH group is the most acidic ($pKa_1 \approx 4$), and its deprotonation yields the neutral quinonoid base (A), which absorbs light at longer wavelengths (λmax shifts by ~20–30 nm compared to AH^+), turning the solution from red to purple. At higher pH (around 7), a second proton is lost from the C4′-OH group ($pKa_2 \approx 7$), generating the anionic quinonoid base (A^-), with an even greater bathochromic shift (~50–60 nm total) and a visible color closer to blue **(Figure 6).** These proton dissociation steps result in increasingly delocalized electronic structures, but also make the anthocyanin molecule more reactive and less stable, especially toward oxidation **(Costa et al., 2015; Dangles & Fenger, 2018; Trouillas et al., 2016).**

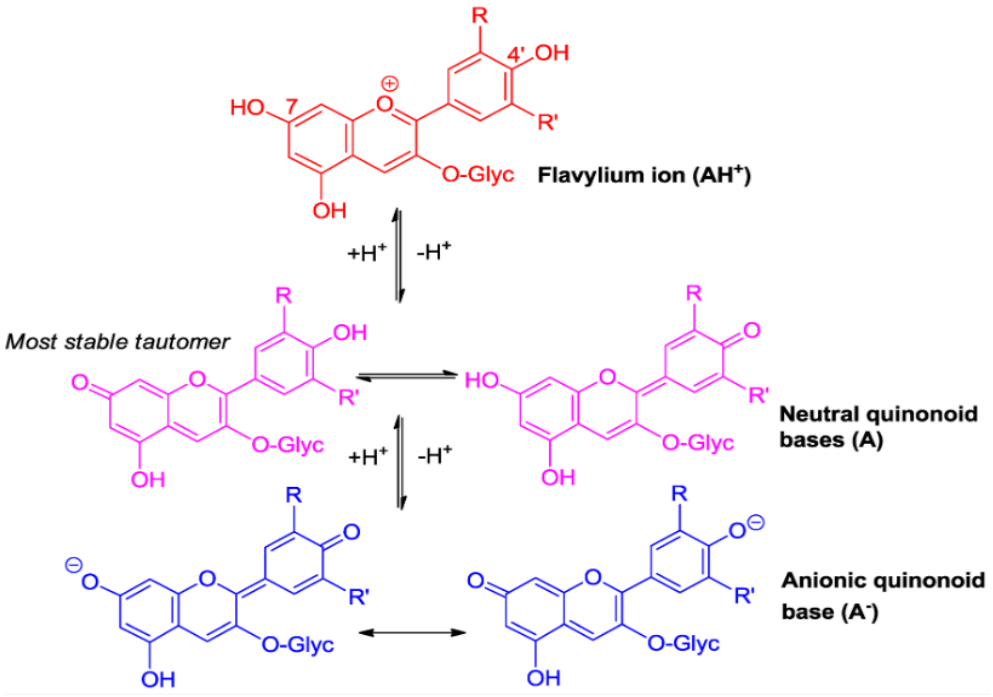

Figure 6. Deprotonation and conversion of flavylium cation into quinonoid bases **(Dangles & Fenger, 2018).**

ii. Water addition and subsequent reactions

In parallel with proton loss, the flavylium cation is subject to nucleophilic attack by water at the C2 position, forming a colorless hemiketal epimers (B) in fast cycle-chain equilibrium with a cis-chalcone tautomer (C_{cis}), itself in slow equilibrium with the *trans*-chalcone (C_{trans}) **(Figure 7).** The corresponding thermodynamic constants are respectively noted K_h, K_t and K_i. The overall hydration equilibrium connecting the flavylium ion and the mixture of colorless forms at equilibrium can be caraterisad by K'_h and is expressed by Eq. (1) **(Cruz et al., 2022; Maria Moloney et al., 2018; Oliveira et al., 2019)**:

$$K'_h = K_h[1 + K_t(1 + K_i)] \quad (1)$$

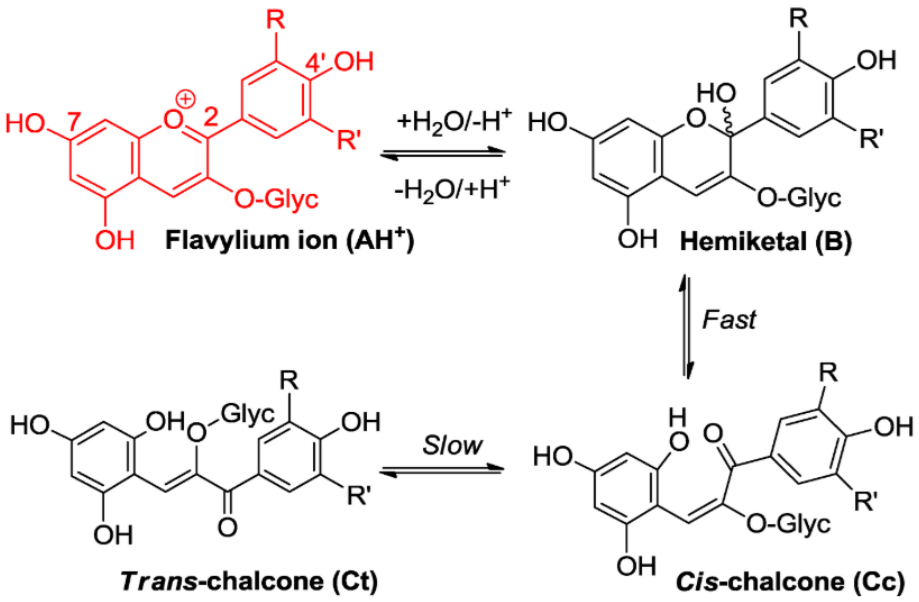

Figure 7. Reaction of flavylium ions at C2 with O-centered nucleophiles leading to hydration and chalcone formation **(Dangles & Fenger, 2018).**

In natural anthocyanins, K_t and K_i values are typically below 1, with chalcones contributing less than 20% to colorless forms . The pK'_h value (indicator of color stability) generally lies between 2–3, while pK_a is close to 4. Among the competing fates of the flavylium ion—proton loss versus hydration—the latter is thermodynamically favored but slower, yielding hemiketals as the main colorless forms (thermodynamic products) and quinonoid bases as kinetic products (Luís Cruz et al., 2015; Pina, 2014). The half-life of the colored species is strongly pH-dependent, from seconds at pH 3 to minutes at pH 5–6, due to the decreasing proportion of electrophilic flavylium ion with increasing pH. Equilibrium constants are determined through spectrophotometric monitoring over defined pH ranges (e.g., pH jump, reverse pH jump, stopped-flow) combined with equilibrium modeling, enabling estimation of K_a and K'_h. Kinetic assays further quantify hydration and dehydration rates. This methodology is equally applicable in the presence of copigments or metal ions, allowing comprehensive assessment of stability and transformation pathways across anthocyanin sources **(Mendoza & Pina, 2021)**.

4.2. Irreversible transformation of anthocyanins

Although anthocyanins exhibit a dynamic and reversible multistate equilibrium in aqueous solution, they are also prone to various irreversible degradation reactions that impair their color

stability **(Oancea et al., 2018; Sousa et al., 2022)**. These transformations, often triggered by environmental or technological stresses such as heat, light, oxygen, or pH changes, lead to permanent color loss, the formation of low-molecular-weight degradation products, or the generation of brown polymeric pigments **(Feitosa et al., 2025)**.

Heat accelerates the breakdown of the flavylium cation and promotes C-ring opening, yielding electron-rich intermediates that are highly susceptible to autoxidation. In acidic media, hydration to chalcones followed by glycosidic bond hydrolysis generates reactive enol structures, whereas at neutral pH, anionic base forms undergo direct oxidation despite minimal hydration. These processes ultimately lead to the formation of degradation products such as phloroglucinaldehyde and p-hydroxybenzoic acid, changes that are often accompanied by non-enzymatic browning and a significant loss of visible color **(Chen et al., 2023; Dangles & Fenger, 2018; Patras et al., 2010).**

Autoxidation, driven by molecular oxygen and catalyzed by transition metals (e.g., Fe^{2+}, Cu^{2+}), oxidizes anthocyanins into quinones and radicals, with susceptibility influenced by medium redox properties, complexing agents, and pH. At neutral pH, oxidation targets anionic base forms despite minimal hydration. Hydrogen peroxide, generated early in autoxidation, further degrades pigments through monooxygenation, via hemiketal attack in acidic conditions or anionic base forms at pH 7, contributing to irreversible color loss **(Fenger et al., 2019; Lopes et al., 2007; Satake & Yanase, 2018).**

Acylated anthocyanins, while extending the pH range of the colored forms, do not necessarily improve storage stability. Diacylated forms, such as those found in red cabbage **(Fenger et al., 2019),** show greater resistance to hydration and heat-induced degradation through intramolecular copigmentation, however, it does not always prevent irreversible autoxidation **(Fenger, et al., 2021a).**

Additional irreversible pathways include condensation or copolymerization with carbonyl compounds or flavanols, producing stable but spectrally altered pigments, advantageous for color stabilization in wine aging but undesirable in most foods **(Torres-Rochera et al., 2024)**, as well as photodegradation, enzymatic oxidation, extreme pH, and interactions with proteins or lipids **(Enaru et al., 2021; Dong et al., 2022)**. Ascorbic acid, although widely recognized as an antioxidant, may paradoxically accelerate degradation through radical-mediated cleavage of the

pyrylium ring and condensation reactions, especially during mechanical treatments **(Farr & Giusti, 2018)**. These combined observations highlight the critical need for precise control of pH, temperature, oxygen exposure, and matrix composition to preserve anthocyanin integrity and maximize their application as natural colorants.

4.3. Influence of substituent on color and chemical stability

Beyond the basic flavylium skeleton, the number and position of hydroxyl (OH) and methoxyl (OCH_3) groups on rings A and B modulate spectral characteristics, reactivity, solubility, and resistance to thermal, enzymatic, or oxidative degradation **(Morata et al., 2019)**. These structural modifications help explain the differences in behavior observed between anthocyanins from different plant sources. An increase in the number of hydroxyl groups generally causes a bathochromic shift (toward longer wavelengths), resulting in a deeper color **(Wallace & Giusti, 2019)**. For example, pelargonidin (four –OH groups) absorbs at 520 nm, cyanidin (five –OH groups) at 535 nm, and delphinidin (six –OH groups) at 545 nm, showing a progressive shift toward violet–blue hues **(He & Giusti, 2010)**. However, these more hydroxylated anthocyanins are also less stable, as they are more susceptible to oxidation. Conversely, the presence of methoxyl groups (e.g., in malvidin or peonidin) tends to stabilize the molecule and shift the color toward reddish–purple, while increasing resistance to oxidation. This phenomenon is explained by the substituents' ability to modulate the electron density of the aromatic ring, which affects the electronic transitions responsible for the visible color **(Cai et al., 2022; Oliveira et al., 2019)**.

The nature of the substituents at position 3 of the flavylium cation has a marked influence on stability **(Sigurdson et al., 2018)**. It is well established that glycosylation at this position enhances resistance to degradation, with anthocyanins (glycosylated forms) showing greater stability than their aglycone counterparts, anthocyanidins **(Farr et al., 2019; Sigurdson et al., 2018)**. Even more stable are 3-deoxyanthocyanidins, which lack the hydroxyl group at C3, suggesting that the absence of reactive functionalities at this position contributes to improved structural stability during storage and processing **(Dangles, 2024)**. Although less extensively studied, 3-deoxyanthocyanidins have been associated with enhanced stability not only because of reduced degradation but also due to a broader pH range in which the flavylium cation remains predominant. For example, studies on sorghum-based matrices containing luteolinidin and apigeninidin have shown stable color retention

for up to 120 days under storage, further supporting their potential as robust natural colorants **(Akogou et al., 2018; Bitard et al., 2023)**.

Glycosylation, generally in position 3 and/or 5 of the C ring, is a universal modification in natural anthocyanins. Sugars (glucose, galactose, arabinose, etc.) play several roles: they increase water solubility, facilitating integration into food matrices; they reduce the reactivity of the flavylium nucleus by stabilizing its structure through electronic and steric effects; and they enable the formation of more stable acyl derivatives, a common structural feature in certain plants (e.g., purple sweet potato, red radish). Moreover, the nature of the sugar moieties (monosaccharide or disaccharide) and their binding position act synergistically to modulate the spectral properties and enhance the overall chemical stability of anthocyanins **(Farr et al., 2019; Zhao et al., 2014).**

4.4. Anthocyanins stabilization via supramolecular interactions

Copigmentation refers to a set of non-covalent interactions that enhance and stabilize the colour of anthocyanins, particularly under pH conditions where the red flavylium cation is no longer predominant **(Di Meo et al., 2012; Trouillas et al., 2016**). In plant vacuoles, where the pH is moderately acidic, anthocyanins often coexist as the red flavylium cation (AH^+) and the less stable quinoidal base (A), which can display blue to purple hues. To preserve pigmentation, plants have evolved stabilization mechanisms that rely on the spatial association of the chromophore with other molecular groups **(Figure 8).** These include **(Baranac et al., 1997; Cao et al., 2023; Moloney et al., 2018; Zhang et al., 2020)**:

- Intermolecular copigmentation: non-covalent association with separate copigment molecules;
- Intramolecular copigmentation; folding of acylated glycosidic chains toward the chromophore;
- Self-association – stacking between anthocyanin molecules themselves;
- Metal chelation – coordination with metal ions via hydroxyl groups.

These interactions can induce bathochromic (red shift) and hyperchromic (absorbance-enhancing) effects, resulting in more vivid and persistent coloration. Their efficiency is influenced by structural parameters such as hydroxylation/methoxylation patterns, the type and position of sugar moieties, and the presence of acyl chains. Overall, copigmentation is a key factor in the long-

term stability and color performance of anthocyanins in both plant tissues and formulated products **(Eiro & Heinonen, 2002; Figueiredo et al., 1996; Malaj et al., 2013)**.

4.4.1 Inter- and intramolecular copigmentation

Among the various modes of copigmentation, the inter- and intramolecular types have been the most extensively studied for their role in both natural and applied systems **(Fei et al., 2021; Malien-Aubert et al., 2001; Quan et al., 2019)**. Intermolecular copigmentation involves π–π stacking, possibly strengthened by hydrogen bonding, between anthocyanins (in either the flavylium or quinoidal form) and external copigments such as flavones, flavonols, or hydroxycinnamic acid derivatives. This association shields the chromophore from nucleophilic attack and hydration, while producing marked hyperchromic and bathochromic shifts. The extent of stabilization depends on the structural compatibility between anthocyanin and copigment, their relative concentrations, and environmental conditions such as pH and temperature **(Kanha et al., 2019; Nave et al., 2010; Pangestu et al., 2020; Limón et al., 2013)**.

Intramolecular copigmentation is characteristic of acylated anthocyanins, in which aromatic or aliphatic acyl groups attached to glycosidic chains fold toward the chromophore. This close proximity allows internal π–π stacking and hydrogen bonding, producing compact, ordered structures that greatly enhance thermal and oxidative resistance. Polyacylated anthocyanins, such as those found in red cabbage, are particularly effective, showing superior stability across a wide pH range **(Moloney et al., 2018; Yang et al., 2022; Zhao et al., 2017)**.

While both mechanisms improve anthocyanin stability, they can also compete for the same binding sites, suggesting a structural trade-off between maximizing intramolecular folding and enabling external copigment binding. Understanding this balance is key for designing anthocyanin-based colorants with optimal performance in specific food and beverage matrices **(Pina et al., 2012; Trouillas et al., 2016).**

4.4.2 Self-association

In addition to inter- and intramolecular copigmentation, anthocyanins can stabilize their color through self-association, a mechanism involving the spontaneous aggregation of anthocyanin molecules into left-handed helical stacks that limit water accessibility and thus improve color stability and intensity **(Fernandes et al., 2015).** This phenomenon becomes particularly relevant at higher pigment concentrations, typically above 0.1 mM, and is strongly influenced by structural

features such as the degree of B-ring methoxylation and hydroxylation. Notably, self-association is more pronounced in the quinoidal base forms of anthocyanins, which predominate under mildly acidic to neutral pH conditions **(Leydet et al., 2012; Qian et al., 2017).**

Studies on red cabbage anthocyanins have demonstrated that self-association contributes to color retention under mildly alkaline conditions, where the quinonoid base predominates **(Moloney et al., 2018).** Furthermore, acylated anthocyanins may benefit from dual stabilization via both intramolecular stacking of acyl moieties and self-association of the chromophores, providing enhanced resistance to degradation **(Fernandes et al., 2015).** However, the interplay between self-association and intermolecular copigmentation appears to be competitive. **González-Manzano et al. (2009)** suggested that excess external copigments may disrupt anthocyanin self-stacking, as later supported by **Qian et al. (2017)**, who found that certain phenolic acids accelerated pigment degradation at high temperatures, likely by interfering with self-association. Interestingly, in young red wines, the self-association of malvidin-3-O-glucoside has been shown to contribute more significantly to color stabilization than external copigmentation **(Lambert et al., 2011)**. Conversely, in some systems, intramolecular copigmentation, notably in mono- and diacylated anthocyanins, has demonstrated superior color enhancement compared to self-association **(Dangles et al., 1993a; Malien-Aubert et al., 2001).** Together, these observations underscore the importance of molecular organization, pH, and concentration in governing the efficiency of anthocyanin self-association and its role within the broader network of copigmentation phenomena.

4.4.3 Metal anthocyanin binding

The complexation of anthocyanins with metal ions represents a key mechanism for modulating both color expression and stability. This process relies on the coordination of specific bivalent or trivalent metal ions—most notably Fe^{3+}, Al^{3+}, Cu^{2+}, and Mg^{2+}—with anthocyanins bearing ortho-positioned hydroxyl groups on the B-ring, such as delphinidin and cyanidin derivatives **(Fenger, et al., 2021b; Mora-Soumille et al., 2013)**. Coordination occurs through the oxygen atoms of the hydroxyl groups and adjacent double bonds, yielding metal–anthocyanin complexes that typically exhibit a bathochromic shift (blue–violet hue), hyperchromia (increased color intensity), and enhanced resistance to pH, light, and thermal degradation **(Sigurdson et al., 2017; Sigurdson & Giusti, 2014).**

Among the commonly studied ions, Fe^{3+} and Al^{3+} generate intensely colored, highly stable bluish complexes; Cu^{2+} produces vivid colors but may accelerate anthocyanin oxidation; Mg^{2+} and Ca^{2+} form weaker yet food-relevant complexes; whereas Sn^{2+} and Pb^{2+}, though capable of binding, are toxic and irrelevant for edible applications. The outcome of complexation is strongly governed by the metal's valence state, ionic radius, and concentration **(Sigurdson et al., 2016)**. The formation of metal complexation is influenced by pH: complexation is favored in slightly acidic to near-neutral environments (pH 4–6), where hydroxyl groups are partially deprotonated. However, competing chelators, such as citric acid or EDTA, can significantly reduce binding efficiency **(Dangles, 2024; Ratanapoompinyo et al., 2017)**.

In plants, this mechanism underlies much of the chromatic diversity of flowers and fruits, including rare blue hues, and is responsible for the stability of certain metalloprotein pigments, such as those found in *Commelina* species. In food systems, it offers opportunities to modulate hue or enhance color intensity, though its application is limited by metal toxicity, complex interactions with the food matrix, and destabilization from pH or concentration fluctuations **(Fedenko et al., 2022; Mendoza et al., 2018; Shiono et al., 2008; Yoshida et al., 2009).**

4.4.4 Interaction with polymers and encapsulation

The association of anthocyanins with food-grade polymers is a widely explored strategy to enhance pigment stability, control release kinetics, and improve bioavailability in complex matrices **(Feitosa et al., 2023)**. Proteins, such as whey protein, caseinate, gelatin, and soy protein isolate, bind anthocyanins through van der Waals interactions between aromatic rings and non-polar domains, complemented by hydrogen bonding between pigment hydroxyl groups and protein carbonyl or amine groups **(Ren et al., 2021; Song et al., 2022).** These protein–anthocyanin assemblies may occur as poorly soluble microparticles, as in the case of casein, which markedly restricts release under gastric conditions, or as soluble microgels, as in whey protein systems, which delay diffusion and protect against thermal, oxidative, and photolytic degradation **(Liao et al., 2021)**. The affinity and protective effect of these complexes depend strongly on protein type, concentration, and conformational changes during digestion **(Jiang & Zhang, 2023)**. Similarly, polysaccharides, including pectin, chitosan, alginate, starch derivatives, cellulose, and maltodextrin, stabilize anthocyanins primarily via hydrogen bonding and electrostatic attraction **(Ćorković et al., 2021; Sarabandi et al., 2019, 2018)**.

Cationic chitosan readily forms nanoparticles with anthocyanins through weak ionic and hydrogen bonds, conferring resistance to oxidation, ascorbic acid, and neutral pH. Cyclodextrins bind anthocyanins through inclusion into hydrophobic cavities and hydrogen bonding, while anionic pectins and alginates can entrap pigments within hydrogel networks, mitigating degradation under adverse conditions **(Fernandes et al., 2018; Guo et al., 2018).**

Hybrid protein–polysaccharide systems combine covalent linkages, such as Maillard-type conjugation, with electrostatic assembly of oppositely charged biopolymers to yield highly ordered structures with improved encapsulation efficiency and controlled release **(Gonçalves et al., 2018; Yang et al., 2020)**. Examples include whey protein–pectin and gum arabic–maltodextrin matrices, which enhance pigment retention during processing, extend gastric residence time, and promote targeted intestinal release **(Song et al., 2022)**. Encapsulation techniques, such as spray-drying, nano- and microencapsulation, and hydrogel or double emulsion formation, act as physical barriers, reducing pigment exposure to oxygen, light, and pro-oxidant metal ions **(Ćorković et al., 2021; Feitosa et al., 2023; Tarone et al., 2020).** Hydrogels and double emulsions further lower water activity and limit ion mobility, slowing autoxidation and thermal breakdown, while enabling controlled release under gastrointestinal conditions **(Xue et al., 2024).** These polymer-based delivery systems thus represent a versatile approach to overcoming the physicochemical challenges faced by anthocyanins in food processing and digestion.

4.5. Anthocyanins in food systems: Applications and processing challenges

In recent years, the global anthocyanin market was valued at over US$500 million in 2018 and is projected to reach US$735.9 million by 2026, with a compound annual growth rate of 4.6% **(Transparency Market Research, 2019)**[7]**.** Anthocyanins are gaining increasing attention as natural food colorants. For example, purple sweet potato anthocyanins are considered safe, non-toxic, odorless, and vividly colored, with additional advantages of high yield, low cost, and improved resistance to light and heat **(Zhou et al., 2019)**. Beyond their role as colorants, anthocyanins are also applied in functional foods, nutraceuticals, pharmaceuticals, and smart

[7] https://www.transparencymarketresearch.com/anthocyanin-market.html

packaging, owing to their antioxidant and health-promoting properties as well as their pH-dependent color variation **(Abdel-Aal et al., 2018; Echegaray et al., 2023; He & Giusti, 2010)**.

Nevertheless, their stability during processing is governed by a delicate interplay between their release from the food matrix and their subsequent degradation, a dynamic strongly influenced by both the structural characteristics of the matrix and the intensity of the treatment applied **(Cordeiro et al., 2021; Kim et al., 2021; Rytel et al., 2021)**. Processing can thus be viewed as a disguised extraction process, where physical and thermal disruptions promote anthocyanin liberation **(Zhu et al., 2019)**, though often at the cost of molecular degradation **(Nie et al., 2017)**. In weakly interacting matrices or under severe processing conditions, degradation tends to dominate, resulting in substantial pigment loss **(Chen et al., 2018; Gérard et al., 2019)**. Conversely, strongly interacting matrices exposed to mild processing may initially favor anthocyanin release, generating a transient phase of enhanced stability before degradation eventually prevails **(Gérard et al., 2019; Li et al., 2020).**

In addition, interactions between anthocyanins and the food matrix constitute a significant limitation for their accurate quantification. Conventional solvents, such as acidified methanol, may lead to an underestimation of anthocyanin retention, as they are often unable to recover compounds sequestered within complex networks generated during processing, particularly those involving pectin, sugars, or dietary fibers. These associations may exert a dual effect, providing a degree of protection against thermal degradation while concurrently restricting solubilization and analytical recovery. To achieve a more reliable assessment of anthocyanin stability, extraction strategies must therefore be optimized, through approaches such as ultrasound- or microwave-assisted techniques, in accordance with the structural properties of the processed matrix **(Chen et al., 2023)**. Ultimately, a rigorous evaluation necessitates the alignment of processing intensity with adapted extraction protocols, ensuring that apparent losses correspond to genuine degradation rather than methodological artifacts. This complexity underscores the need for advanced models and integrated analytical frameworks to predict anthocyanin behavior across heterogeneous food systems **(Cvjetko Bubalo et al., 2018)**.

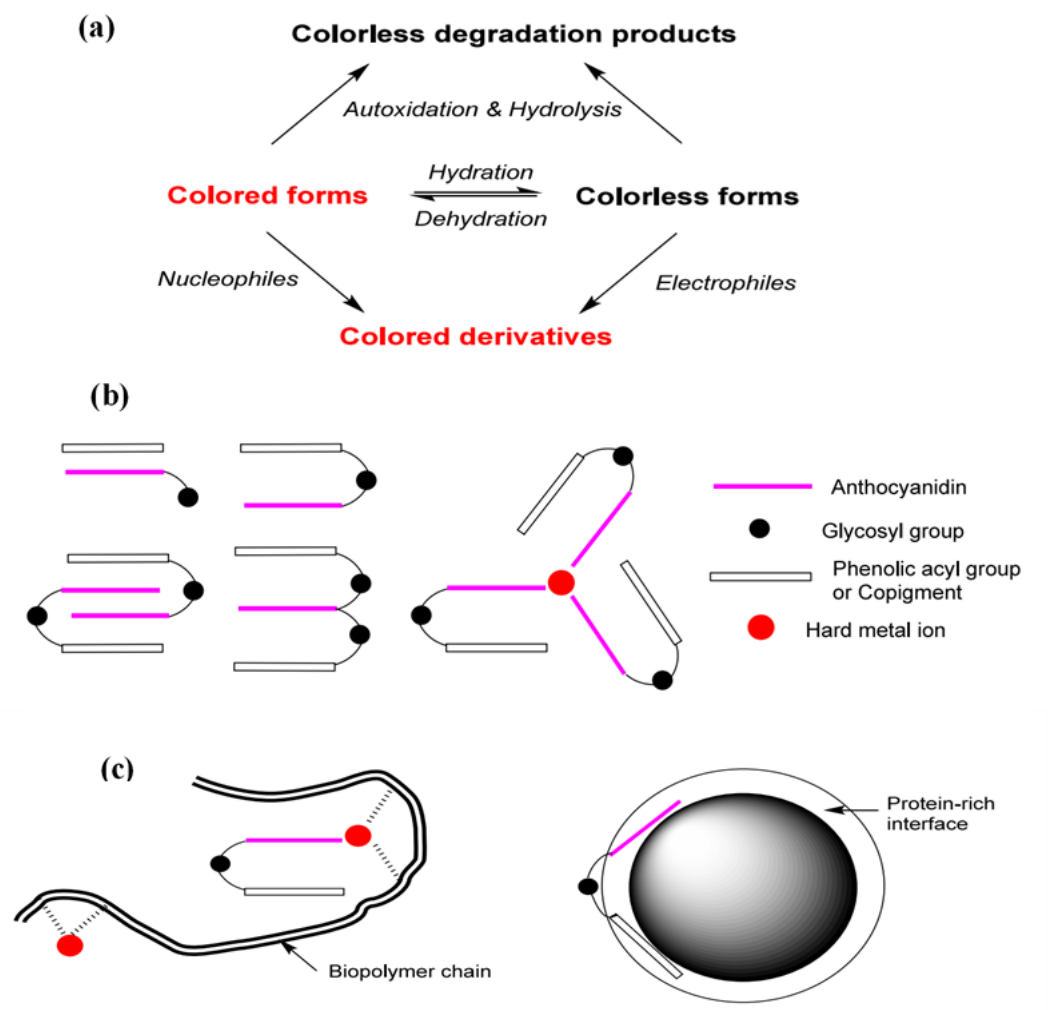

Figure 8. (a) Simplified schemas illustrating the chemical reactivity of anthocyanins. (b–c). Main color-stabilizing mechanisms: inter- and intramolecular copigmentation, self-association, and metal binding (b) and formulations based on gels (left) and emulsions (right) (c) **(Dangles, 2024).**

References

Abdel-Aal, E.-S. M., Hucl, P., & Rabalski, I. (2018). Compositional and antioxidant properties of anthocyanin-rich products prepared from purple wheat. *Food Chemistry*, 254, 13-19. https://doi.org/10.1016/j.foodchem.2018.01.170

Akogou, F. U., Kayodé, A. P., den Besten, H. M., & Linnemann, A. R. (2018). Extraction methods and food uses of a natural red colorant from dye sorghum. *Journal of the Science of Food and Agriculture, 98(1)*, 361-368. https://doi.org/10.1002/jsfa.8479

Albuquerque, T. G., Silva, M. A., Oliveira, M. B. P. P., & Costa, H. S. (2018). Chapter 34—Analysis, Identification, and Quantification of Anthocyanins in Fruit Juices. In G. Rajauria & B. K. Tiwari (Éds.), *Fruit Juices* (p. 693-737). *Academic Press.* https://doi.org/10.1016/B978-0-12-802230-6.00034-5

Alegbe, E. O., & Uthman, T. O. (2024). A review of history, properties, classification, applications and challenges of natural and synthetic dyes. *Heliyon*, *10*(13), e33646. https://doi.org/10.1016/j.heliyon.2024.e33646

Andersen, Ø. M., & Jordheim, M. (2010). Anthocyanins. In Wiley, *Encyclopedia of Life Sciences* (1re éd.). Wiley. https://doi.org/10.1002/9780470015902.a0001909.pub2

Bach Knudsen, K. E., Nørskov, N., Bolvig, A. K., Hedemann, M. S., & Lærke, H. N. (2020). Lignans. In *Dietary Polyphenols* (p. 365-406). John Wiley & Sons, Ltd. https://doi.org/10.1002/9781119563754.ch10

Baranac, J. M., Petranović, N. A., & Dimitrić-Marković, J. M. (1997). Spectrophotometric Study of Anthocyan Copigmentation Reactions. 2. Malvin and the Nonglycosidized Flavone Quercetin. *Journal of Agricultural and Food Chemistry, 45(5)*, 1694-1697. https://doi.org/10.1021/jf9606114

Barciela, P., Perez-Vazquez, A., & Prieto, M. A. (2023). Azo dyes in the food industry : Features, classification, toxicity, alternatives, and regulation. *Food and Chemical Toxicology*, *178*, 113935. https://doi.org/10.1016/j.fct.2023.113935

Basílio, N., & Pina, F. (2016). Chemistry and Photochemistry of Anthocyanins and Related Compounds : A Thermodynamic and Kinetic Approach. *Molecules*, *21*(11), 1502. https://doi.org/10.3390/molecules21111502

Belščak-Cvitanović, A., Durgo, K., Huđek, A., Bačun-Družina, V., & Komes, D. (2018). 1—Overview of polyphenols and their properties. In C. M. Galanakis (Éd.), *Polyphenols : Properties, Recovery, and Applications* (p. 3-44). Woodhead Publishing. https://doi.org/10.1016/B978-0-12-813572-3.00001-4

Belwal, T., Singh, G., Jeandet, P., Pandey, A., Giri, L., Ramola, S., Bhatt, I. D., Venskutonis, P. R., Georgiev, M. I., Clément, C., & Luo, Z. (2020). Anthocyanins, multi-functional natural products of industrial relevance : Recent biotechnological advances. *Biotechnology Advances*, *43*, 107600. https://doi.org/10.1016/j.biotechadv.2020.107600

Benkhaya, S., M'rabet, S., & El Harfi, A. (2020). Classifications, properties, recent synthesis and applications of azo dyes. *Heliyon*, *6*(1), e03271. https://doi.org/10.1016/j.heliyon.2020.e03271

Bitard, H., Laguerre, M., & Dangles, O. (2023). 3-Deoxyanthocyanidins and their derivatives : Modulation of their coloring properties as a function of pH and molecular binding to micelles and biopolymers. *Dyes and Pigments, 213,* 111187. https://doi.org/10.1016/j.dyepig.2023.111187

Cai, D., Li, X., Chen, J., Jiang, X., Ma, X., Sun, J., Tian, L., Vidyarthi, S. K., Xu, J., Pan, Z., & Bai, W. (2022). A comprehensive review on innovative and advanced stabilization approaches of anthocyanin by modifying structure and controlling environmental factors. *Food Chemistry*, 366, 130611. https://doi.org/10.1016/j.foodchem.2021.130611

Cairone, F., Carradori, S., Locatelli, M., Casadei, M. A., & Cesa, S. (2020). Reflectance colorimetry : A mirror for food quality—a mini review. *European Food Research and Technology*, *246*(2), 259-272. https://doi.org/10.1007/s00217-019-03345-6

Cao, Y., Xia, Q., Aniya, Chen, J., & Jin, Z. (2023). Copigmentation effect of flavonols on anthocyanins in black mulberry juice and their interaction mechanism investigation. *Food Chemistry,* 399, 133927. https://doi.org/10.1016/j.foodchem.2022.133927

Chen, W., Karangwa, E., Yu, J., Duhoranimana, E., Xia, S., Feng, B., Zhang, X., & Jia, C. (2018). Coupling effects of preheating time and extraction medium pH on red radish anthocyanin yield, glucosinolate degradation and off-odour removal. *International Journal of Food Science & Technology*, 53(3), 709-718. https://doi.org/10.1111/ijfs.13646

Chen, Y., Belwal, T., Xu, Y., Ma, Q., Li, D., Li, L., Xiao, H., & Luo, Z. (2023). Updated insights into anthocyanin stability behavior from bases to cases : Why and why not anthocyanins lose during food processing. *Critical Reviews in Food Science and Nutrition*, *63*(27), 8639-8671. https://doi.org/10.1080/10408398.2022.2063250

Cheynier, V., Comte, G., Davies, K. M., Lattanzio, V., & Martens, S. (2013). Plant phenolics : Recent advances on their biosynthesis, genetics, and ecophysiology. *Plant Physiology and Biochemistry*, *72*, 1-20. https://doi.org/10.1016/j.plaphy.2013.05.009

Choudhury, A. K. R. (2014). 6—Colour measurement instruments. In A. K. R. Choudhury (Éd.), *Principles of Colour and Appearance Measurement* (p. 221-269). Woodhead Publishing. https://doi.org/10.1533/9780857099242.221

Cordeiro, T., Fernandes, I., Pinho, O., Calhau, C., Mateus, N., & Faria, A. (2021). Anthocyanin content in raspberry and elderberry : The impact of cooking and recipe composition. *International Journal of Gastronomy and Food Science, 24*, 100316. https://doi.org/10.1016/j.ijgfs.2021.100316

Ćorković, I., Pichler, A., Ivić, I., Šimunović, J., & Kopjar, M. (2021). Microencapsulation of Chokeberry Polyphenols and Volatiles : Application of Alginate and Pectin as Wall Materials. *Gels,* 7(4), Article 4. https://doi.org/10.3390/gels7040231

Costa, D., Galvão, A. M., Di Paolo, R. E., Freitas, A. A., Lima, J. C., Quina, F. H., & Maçanita, A. L. (2015). Photochemistry of the hemiketal form of anthocyanins and its potential role in plant protection from UV-B radiation. *Tetrahedron*, *71*(20), 3157-3162. https://doi.org/10.1016/j.tet.2014.06.092

Cruz, L., Basílio, N., Mateus, N., de Freitas, V., & Pina, F. (2022). Natural and Synthetic Flavylium-Based Dyes : The Chemistry Behind the Color. *Chemical Reviews*, *122*(1), 1416-1481. https://doi.org/10.1021/acs.chemrev.1c00399

Cuyckens, F., & Claeys, M. (2004). Mass spectrometry in the structural analysis of flavonoids. *Journal of Mass Spectrometry*, *39*(1), 1-15. https://doi.org/10.1002/jms.585

Cvjetko Bubalo, M., Vidović, S., Radojčić Redovniković, I., & Jokić, S. (2018). New perspective in extraction of plant biologically active compounds by green solvents. *Food and Bioproducts Processing, 109*, 52-73. https://doi.org/10.1016/j.fbp.2018.03.001

Dangles, O. (2024). Anthocyanins as Natural Food Colorings : The Chemistry Behind and Challenges Still Ahead. *Journal of Agricultural and Food Chemistry*, *72*(22), 12356-12372. https://doi.org/10.1021/acs.jafc.4c01050

Dangles, O., & Fenger, J.-A. (2018). The Chemical Reactivity of Anthocyanins and Its Consequences in Food Science and Nutrition. *Molecules*, *23*(8), 1970. https://doi.org/10.3390/molecules23081970

Dangles, O., Saito, N., & Brouillard, R. (1993a). Anthocyanin intramolecular copigment effect. *Phytochemistry*, 34(1), 119-124. https://doi.org/10.1016/S0031-9422(00)90792-1

Dangles, O., Saito, N., & Brouillard, R. (1993b). Kinetic and thermodynamic control of flavylium hydration in the pelargonidin-cinnamic acid complexation. Origin of the extraordinary flower color diversity of Pharbitis nil. *Journal of the American Chemical Society*, *115*(8), 3125-3132. https://doi.org/10.1021/ja00061a011

De Mejia, E. G., Zhang, Q., Penta, K., Eroglu, A., & Lila, M. A. (2020). The Colors of Health : Chemistry, Bioactivity, and Market Demand for Colorful Foods and Natural Food Sources of Colorants. *Annual Review of Food Science and Technology*, *11*(1), 145-182. https://doi.org/10.1146/annurev-food-032519-051729

De Pascual-Teresa, S., Moreno, D. A., & García-Viguera, C. (2010). Flavanols and Anthocyanins in Cardiovascular Health : A Review of Current Evidence. *International Journal of Molecular Sciences*, *11*(4), Article 4. https://doi.org/10.3390/ijms11041679

de Araújo, F. F., de Paulo Farias, D., Neri-Numa, I. A., & Pastore, G. M. (2021). Polyphenols and their applications : An approach in food chemistry and innovation potential. *Food Chemistry*, *338*, 127535. https://doi.org/10.1016/j.foodchem.2020.127535

Di Meo, F., Sancho Garcia, J. C., Dangles, O., & Trouillas, P. (2012). Highlights on Anthocyanin Pigmentation and Copigmentation : A Matter of Flavonoid π-Stacking Complexation To Be

Described by DFT-D. *Journal of Chemical Theory and Computation*, *8*(6), 2034-2043. https://doi.org/10.1021/ct300276p

Dias, M. C., Pinto, D. C. G. A., & Silva, A. M. S. (2021). Plant Flavonoids : Chemical Characteristics and Biological Activity. *Molecules*, *26*(17), 5377. https://doi.org/10.3390/molecules26175377

Dikshit, R., & Tallapragada, P. (2018). Comparative Study of Natural and Artificial Flavoring Agents and Dyes. In *Natural and Artificial Flavoring Agents and Food Dyes* (p. 83-111). Elsevier. https://doi.org/10.1016/B978-0-12-811518-3.00003-X

Dimitrova, M., Corsalini, M., Kazakova, R., Vlahova, A., Barile, G., Dell'Olio, F., Tomova, Z., Kazakov, S., & Capodiferro, S. (2022). Color stability determination of CAD/CAM milled and 3D printed acrylic resins for denture bases : A narrative review. *Journal of Composites Science*, *6*(7), 201.

Durazzo, A., Carocho, M., Heleno, S., Lillian, B., Eliana, B. S., Antonello, S., & Massimo, L. (2022). Food dyes and health : Literature quantitative research analysis. *Measurement: Food*, *7*, 100050. https://doi.org/10.1016/j.meafoo.2022.100050

Durazzo, A., Lucarini, M., Souto, E. B., Cicala, C., Caiazzo, E., Izzo, A. A., Novellino, E., & Santini, A. (2019). Polyphenols : A concise overview on the chemistry, occurrence, and human health. *Phytotherapy Research: PTR*, *33*(9), 2221-2243. https://doi.org/10.1002/ptr.6419

Dutta, K., & Nath, R. (2023). Application of Colorimetry in Food Industries. In *Advances in Colorimetry*. Intech Open. https://doi.org/10.5772/intechopen.112099

Echegaray, N., Guzel, N., Kumar, M., Guzel, M., Hassoun, A., & Lorenzo, J. M. (2023). Recent advancements in natural colorants and their application as coloring in food and in intelligent food packaging. *Food Chemistry*, 404, 134453. https://doi.org/10.1016/j.foodchem.2022.134453

EFSA Panel on Food Additives and Nutrient Sources added to Food (ANS). (2013). Scientific Opinion on the re-evaluation of anthocyanins (E 163) as a food additive. *EFSA Journal*, *11*(4), 3145. https://doi.org/10.2903/j.efsa.2013.3145

Eiro, M. J., & Heinonen, M. (2002). Anthocyanin Color Behavior and Stability during Storage : Effect of Intermolecular Copigmentation. *Journal of Agricultural and Food Chemistry*, 50(25), 7461-7466. https://doi.org/10.1021/jf0258306

El Rayess, Y., Nehme, N., Azzi-Achkouty, S., & Julien, S. G. (2024). Wine Phenolic Compounds : Chemistry, Functionality and Health Benefits. *Antioxidants*, *13*(11), 1312. https://doi.org/10.3390/antiox13111312

Enaru, B., Drețcanu, G., Pop, T. D., Stănilă, A., & Diaconeasa, Z. (2021). Anthocyanins : Factors Affecting Their Stability and Degradation. *Antioxidants*, 10(12), 1967. https://doi.org/10.3390/antiox10121967

Farr, J. E., & Giusti, M. M. (2018). Investigating the Interaction of Ascorbic Acid with Anthocyanins and Pyranoanthocyanins. Molecules, 23(4), Article 4. https://doi.org/10.3390/molecules23040744

Farr, J. E., Sigurdson, G. T., & Giusti, M. M. (2019). Stereochemistry and glycosidic linkages of C3-glycosylations affected the reactivity of cyanidin derivatives. *Food Chemistry,* 278, 443-451. https://doi.org/10.1016/j.foodchem.2018.11.076

Fedenko, V. S., Landi, M., & Shemet, S. A. (2022). Metallophenolomics : A Novel Integrated Approach to Study Complexation of Plant Phenolics with Metal/Metalloid Ions. *International Journal of Molecular Sciences*, 23(19), 11370. https://doi.org/10.3390/ijms231911370

Fei, P., Zeng, F., Zheng, S., Chen, Q., Hu, Y., & Cai, J. (2021). Acylation of blueberry anthocyanins with maleic acid : Improvement of the stability and its application potential in intelligent color indicator packing materials. *Dyes and Pigments*, 184, 108852. https://doi.org/10.1016/j.dyepig.2020.108852

Feitosa, B. F., Decker, B. L. A., Brito, E. S. de, Rodrigues, S., & Mariutti, L. R. B. (2023). Microencapsulation of anthocyanins as natural dye extracted from fruits – A systematic review. *Food Chemistry*, *424*, 136361. https://doi.org/10.1016/j.foodchem.2023.136361

Feitosa, B. F., Decker, B. L. A., de Brito, E. S., Marques, M. C., Rodrigues, S., & Mariutti, L. R. B. (2025). Anthocyanins stability theory – Evidence summary on the effects of

microencapsulation. *Food and Bioproducts Processing*, *153*, 77-86. https://doi.org/10.1016/j.fbp.2025.06.001

Fenger, J.-A., Moloney, M., Robbins, R. J., Collins, T. M., & Dangles, O. (2019). The influence of acylation, metal binding and natural antioxidants on the thermal stability of red cabbage anthocyanins in neutral solution. *Food & Function, 10(10),* Article 10. https://doi.org/10.1039/C9FO01884K

Fenger, J.-A., Roux, H., Robbins, R. J., Collins, T. M., & Dangles, O. (2021a). The influence of phenolic acyl groups on the color of purple sweet potato anthocyanins and their metal complexes. *Dyes and Pigments, 185,* 108792. https://doi.org/10.1016/j.dyepig.2020.108792

Fenger, J.-A., Sigurdson, G. T., Robbins, R. J., Collins, T. M., Giusti, M. M., & Dangles, O. (2021b). Acylated Anthocyanins from Red Cabbage and Purple Sweet Potato Can Bind Metal Ions and Produce Stable Blue Colors. *International Journal of Molecular Sciences, 22(9),* 4551. https://doi.org/10.3390/ijms22094551

Fernandes, A., Brás, N. F., Mateus, N., & Freitas, V. de. (2015). A study of anthocyanin self-association by NMR spectroscopy. *New Journal of Chemistry, 39(4*), 2602-2611. https://doi.org/10.1039/C4NJ02339K

Fernandes, A., Rocha, M. A. A., Santos, L. M. N. B. F., Brás, J., Oliveira, J., Mateus, N., & de Freitas, V. (2018). Blackberry anthocyanins : β-Cyclodextrin fortification for thermal and gastrointestinal stabilization. *Food Chemistry, 245*, 426-431. https://doi.org/10.1016/j.foodchem.2017.10.109

Figueiredo, P., Elhabiri, M., Toki, K., Saito, N., Dangles, O., & Brouillard, R. (1996). New aspects of anthocyanin complexation. Intramolecular copigmentation as a means for colour loss? *Phytochemistry, 41(1),* 301-308.

García-Salas, P., Gómez-Caravaca, A. M., Morales-Soto, A., Segura-Carretero, A., & Fernández-Gutiérrez, A. (2014). Identification and quantification of phenolic compounds in diverse cultivars of eggplant grown in different seasons by high-performance liquid chromatography coupled to diode array detector and electrospray-quadrupole-time of

flight-mass spectrometry. *Food Research International, 57*, 114-122. https://doi.org/10.1016/j.foodres.2014.01.032

Gérard, V., Ay, E., Morlet-Savary, F., Graff, B., Galopin, C., Ogren, T., Mutilangi, W., & Lalevée, J. (2019). Thermal and Photochemical Stability of Anthocyanins from Black Carrot, Grape Juice, and Purple Sweet Potato in Model Beverages in the Presence of Ascorbic Acid. *Journal of Agricultural and Food Chemistry, 67(19)*, 5647-5660. https://doi.org/10.1021/acs.jafc.9b01672

Gonçalves, F. J., Fernandes, P. A. R., Wessel, D. F., Cardoso, S. M., Rocha, S. M., & Coimbra, M. A. (2018). Interaction of wine mannoproteins and arabinogalactans with anthocyanins. *Food Chemistry, 243,* 1-10. https://doi.org/10.1016/j.foodchem.2017.09.097

Gonzalezmanzano, S., Duenas, M., Rivasgonzalo, J., Escribanobailon, M., & Santosbuelga, C. (2009). Studies on the copigmentation between anthocyanins and flavan-3-ols and their influence in the colour expression of red wine. *Food Chemistry, 114(2*), 649-656. https://doi.org/10.1016/j.foodchem.2008.10.002

Guo, J., Giusti, M. M., & Kaletunç, G. (2018). Encapsulation of purple corn and blueberry extracts in alginate-pectin hydrogel particles : Impact of processing and storage parameters on encapsulation efficiency. *Food Research International, 107*, 414-422. https://doi.org/10.1016/j.foodres.2018.02.035

Gürses, A., Açıkyıldız, M., Güneş, K., & Gürses, M. S. (2016). Classification of Dye and Pigments. In A. Gürses, M. Açıkyıldız, K. Güneş, & M. S. Gürses, *Dyes and Pigments* (p. 31-45). Springer International Publishing. https://doi.org/10.1007/978-3-319-33892-7_3

Hasanuzzaman, M., Bhuyan, M. H. M. B., Zulfiqar, F., Raza, A., Mohsin, S. M., Mahmud, J. A., Fujita, M., & Fotopoulos, V. (2020). Reactive Oxygen Species and Antioxidant Defense in Plants under Abiotic Stress : Revisiting the Crucial Role of a Universal Defense Regulator. *Antioxidants*, *9*(8), 681. https://doi.org/10.3390/antiox9080681

He, J., & Giusti, M. M. (2010). Anthocyanins : Natural colorants with health-promoting properties. *Annual Review of Food Science and Technology, 1,* 163-187. https://doi.org/10.1146/annurev.food.080708.100754

Jiang, M., & Zhang, Y. (2023). Biopolymer-based encapsulation of anthocyanins as reinforced natural colorants for food applications. *Journal of Agriculture and Food Research,* 11, 100488. https://doi.org/10.1016/j.jafr.2022.100488

Jingjing Dong, Sidong Li, Sidong Li, Jie Zhang, Jie Zhang, Ake Liu, Ake Liu, Jia-Lin Ren, & Jiahong Ren. (2022). Thermal degradation of cyanidin-3-O-glucoside : Mechanism and toxicity of products. *Food Chemistry,* 370, 131018. https://doi.org/10.1016/j.foodchem.2021.131018

Kanha, N., Surawang, S., Pitchakarn, P., Regenstein, J. M., & Laokuldilok, T. (2019). Copigmentation of cyanidin 3-O-glucoside with phenolics : Thermodynamic data and thermal stability. Food Bioscience, 30, 100419. https://doi.org/10.1016/j.fbio.2019.100419

Kim, A.-N., Lee, K.-Y., Kim, B. G., Cha, S. W., Jeong, E. J., Kerr, W. L., & Choi, S.-G. (2021). Thermal processing under oxygen–free condition of blueberry puree : Effect on anthocyanin, ascorbic acid, antioxidant activity, and enzyme activities. *Food Chemistry, 342*, 128345. https://doi.org/10.1016/j.foodchem.2020.128345

Kola-Ajibade, I. R., Grace, A., & Olusola, A. O. (2021). Effects of Azo Dye Adulterated Palm Oil on the Expression of Inflammatory, Functional, Antioxidant Markers and Body Weights in Albino Rats. *Journal of Toxicology and Risk Assessment*, *7*(1), 041. https://doi.org/10.23937/2572-4061.1510041

Krga, I., & Milenkovic, D. (2019). Anthocyanins : From Sources and Bioavailability to Cardiovascular-Health Benefits and Molecular Mechanisms of Action. *Journal of Agricultural and Food Chemistry*, *67*(7), 1771-1783. https://doi.org/10.1021/acs.jafc.8b06737

Lambert, S. G., Asenstorfer, R. E., Williamson, N. M., Iland, P. G., & Jones, G. P. (2011). Copigmentation between malvidin-3-glucoside and some wine constituents and its importance to colour expression in red wine. *Food Chemistry,* 125(1), 106-115. https://doi.org/10.1016/j.foodchem.2010.08.045

Lehto, S., Buchweitz, M., Klimm, A., Straßburger, R., Bechtold, C., & Ulberth, F. (2017). Comparison of food colour regulations in the EU and the US : A review of current provisions. *Food Additives & Contaminants. Part A, Chemistry, Analysis, Control,*

Exposure & Risk Assessment, *34*(3), 335-355. https://doi.org/10.1080/19440049.2016.1274431

Leydet, Y., Gavara, R., Petrov, V., Diniz, A. M., Jorge Parola, A., Lima, J. C., & Pina, F. (2012). The effect of self-aggregation on the determination of the kinetic and thermodynamic constants of the network of chemical reactions in 3-glucoside anthocyanins. *Phytochemistry, 83*, 125-135. https://doi.org/10.1016/j.phytochem.2012.06.022

Li, X., Zhang, L., Peng, Z., Zhao, Y., Wu, K., Zhou, N., Yan, Y., Ramaswamy, H. S., Sun, J., & Bai, W. (2020). The impact of ultrasonic treatment on blueberry wine anthocyanin color and its In-vitro anti-oxidant capacity. *Food Chemistry, 333,* 127455. https://doi.org/10.1016/j.foodchem.2020.127455

Liao, M., Ma, L., Miao, S., Hu, X., Liao, X., Chen, F., & Ji, J. (2021). The in-vitro digestion behaviors of milk proteins acting as wall materials in spray-dried microparticles : Effects on the release of loaded blueberry anthocyanins. *Food Hydrocolloids, 115*, 106620. https://doi.org/10.1016/j.foodhyd.2021.106620

Limón, P. M., Raquel Gavara, Gavara, R., Fernando Piña, & Pina, F. (2013). Thermodynamics and kinetics of cyanidin 3-glucoside and caffeine copigments. *Journal of Agricultural and Food Chemistry, 61(22),* 5245-5251. https://doi.org/10.1021/jf4006643

Lopes, P., Richard, T., Saucier, C., Teissedre, P.-L., Monti, J.-P., & Glories, Y. (2007). Anthocyanone A : A Quinone Methide Derivative Resulting from Malvidin 3-O-Glucoside Degradation. Journal of Agricultural and *Food Chemistry, 55(7),* 2698-2704. https://doi.org/10.1021/jf062875o

Lourenço Neto, M., Agra, K. L., Suassuna Filho, J., & Jorge, F. E. (2018). TDDFT calculations and photoacoustic spectroscopy experiments used to identify phenolic acid functional biomolecules in Brazilian tropical fruits *in natura*. *Spectrochimica Acta Part A: Molecular and Biomolecular Spectroscopy*, *193*, 249-257. https://doi.org/10.1016/j.saa.2017.12.036

Malaj, N., De Simone, B. C., Quartarolo, A. D., & Russo, N. (2013). Spectrophotometric study of the copigmentation of malvidin 3-O-glucoside with p-coumaric, vanillic and syringic acids. *Food Chemistry, 141(4),* Article 4. https://doi.org/10.1016/j.foodchem.2013.06.017

Malien-Aubert, C., Dangles, O., & Amiot, M. J. (2001). Color Stability of Commercial Anthocyanin-Based Extracts in Relation to the Phenolic Composition. Protective Effects by Intra- and Intermolecular Copigmentation. *Journal of Agricultural and Food Chemistry, 49(1),* 170-176. https://doi.org/10.1021/jf000791o

Martins, N., Roriz, C. L., Morales, P., Barros, L., & Ferreira, I. C. F. R. (2016). Food colorants : Challenges, opportunities and current desires of agro-industries to ensure consumer expectations and regulatory practices. *Trends in Food Science & Technology*, *52*, 1-15. https://doi.org/10.1016/j.tifs.2016.03.009

Medini, F., Fellah, H., Ksouri, R., & Abdelly, C. (2014). Total phenolic, flavonoid and tannin contents and antioxidant and antimicrobial activities of organic extracts of shoots of the plant Limonium delicatulum. *Journal of Taibah University for Science*, *8*(3), 216-224. https://doi.org/10.1016/j.jtusci.2014.01.003

Mendoza, J., & Pina, F. (2021). Achieving Complexity at the Bottom Through the Flavylium Cation-Based Multistate. In *Recent Advances in Polyphenol Research* (p. 1-23). John Wiley & Sons, Ltd. https://doi.org/10.1002/9781119545958.ch1

Mendoza, J., Basílio, N., de Freitas, V., & Pina, F. (2019). New Procedure To Calculate All Equilibrium Constants in Flavylium Compounds : Application to the Copigmentation of Anthocyanins. *ACS Omega*, *4*(7), 12058-12070. https://doi.org/10.1021/acsomega.9b01066

Mendoza, J., Basílio, N., Pina, F., Kondo, T., & Yoshida, K. (2018). Rationalizing the Color in Heavenly Blue Anthocyanin : A Complete Kinetic and Thermodynamic Study. *The Journal of Physical Chemistry B, 122(19*), Article 19. https://doi.org/10.1021/acs.jpcb.8b01136

Miller, M. D., Steinmaus, C., Golub, M. S., Castorina, R., Thilakartne, R., Bradman, A., & Marty, M. A. (2022). Potential impacts of synthetic food dyes on activity and attention in children : A review of the human and animal evidence. *Environmental Health*, *21*(1), 45. https://doi.org/10.1186/s12940-022-00849-9

Moloney, M., Rebecca J. Robbins, Robbins, R. J., Tom M. Collins, Collins, T. M., Tadao Kondo, Kondo, T., Kumi Yoshida, Yoshida, K., Olivier Dangles, Olivier Dangles, Dangles, O., & Olivier Dangles. (2018). Red cabbage anthocyanins : The influence of d-glucose acylation

by hydroxycinnamic acids on their structural transformations in acidic to mildly alkaline conditions and on the resulting color. *Dyes and Pigments*, *158*, 342-352. https://doi.org/10.1016/j.dyepig.2018.05.057

Mora-Soumille, N., Al Bittar, S., Rosa, M., & Dangles, O. (2013). Analogs of anthocyanins with a 3′,4′-dihydroxy substitution : Synthesis and investigation of their acid–base, hydration, metal binding and hydrogen-donating properties in aqueous solution. *Dyes and Pigments, 96(1)*, 7-15. https://doi.org/10.1016/j.dyepig.2012.07.006

Morata, A., López, C., Tesfaye, W., González, C., & Escott, C. (2019). 12—Anthocyanins as Natural Pigments in Beverages. In A. M. Grumezescu & A. M. Holban (Éds.), *Value-Added Ingredients and Enrichments of Beverages* (p. 383-428). Academic Press. https://doi.org/10.1016/B978-0-12-816687-1.00012-6

Nave, F., Petrov, V., Pina, F., Teixeira, N., Mateus, N., & de Freitas, V. (2010). Thermodynamic and Kinetic Properties of a Red Wine Pigment : Catechin-(4,8)-malvidin-3-O-glucoside. *The Journal of Physical Chemistry B*, 114(42), 13487-13496. https://doi.org/10.1021/jp104749f

Nie, Q., Feng, L., Hu, J., Wang, S., Chen, H., Huang, X., Nie, S., Xiong, T., & Xie, M. (2017). Effect of fermentation and sterilization on anthocyanins in blueberry. *Journal of the Science of Food and Agriculture, 97(5)*, 1459-1466. https://doi.org/10.1002/jsfa.7885

Novais, C., Molina, A. K., Abreu, R. M. V., Santo-Buelga, C., Ferreira, I. C. F. R., Pereira, C., & Barros, L. (2022). Natural Food Colorants and Preservatives : A Review, a Demand, and a Challenge. *Journal of Agricultural and Food Chemistry*, *70*(9), 2789-2805. https://doi.org/10.1021/acs.jafc.1c07533

Oancea, A.-M., Cristina Onofrei, Onofrei, C., Mihaela Turturică, Mihaela Turturică, Turturica, M., Gabriela Bahrim, Bahrim, G., Gabriela Râpeanu, Râpeanu, G., Nicoleta Stănciuc, Stănciuc, N., & Stanciuc, N. (2018). The kinetics of thermal degradation of polyphenolic compounds from elderberry (Sambucus nigra L.) extract. *Food Science and Technology International*, *24*(4), 361-369. https://doi.org/10.1177/1082013218756139

Oliveira, H., Basílio, N., Pina, F., Fernandes, I., de Freitas, V., & Mateus, N. (2019). Purple-fleshed sweet potato acylated anthocyanins : Equilibrium network and photophysical properties. *Food Chemistry*, *288*, 386-394. https://doi.org/10.1016/j.foodchem.2019.02.132

Olszowy, M. (2019). What is responsible for antioxidant properties of polyphenolic compounds from plants? *Plant Physiology and Biochemistry*, *144*, 135-143. https://doi.org/10.1016/j.plaphy.2019.09.039

Pangestu, N. P., Gonzalo Miyagusuku-Cruzado, Miyagusuku-Cruzado, G., M. Mónica Giusti, & Giusti, M. M. (2020). Copigmentation with Chlorogenic and Ferulic Acid Affected Color and Anthocyanin Stability in Model Beverages Colored with Sambucus peruviana , Sambucus nigra , and Daucus carota during Storage. *Foods, 9(10),* 1476. https://doi.org/10.3390/foods9101476

Pathare, P. B., Opara, U. L., & Al-Said, F. A.-J. (2013). Colour Measurement and Analysis in Fresh and Processed Foods : A Review. *Food and Bioprocess Technology*, *6*(1), 36-60. https://doi.org/10.1007/s11947-012-0867-9

Patras, A., Brunton, Nigel. P., O'Donnell, C., & Tiwari, B. K. (2010). Effect of thermal processing on anthocyanin stability in foods; mechanisms and kinetics of degradation. *Trends in Food Science & Technology*, *21*(1), Article 1. https://doi.org/10.1016/j.tifs.2009.07.004

Pina, F. (2014). Chemical Applications of Anthocyanins and Related Compounds. A Source of Bioinspiration. *Journal of Agricultural and Food Chemistry*, *62*(29), 6885-6897. https://doi.org/10.1021/jf404869m

Pina, F., Melo, M. J., Laia, C. A. T., Parola, A. J., & Lima, J. C. (2012). Chemistry and applications of flavylium compounds : A handful of colours. *Chem. Soc. Rev.*, *41*(2), 869-908. https://doi.org/10.1039/C1CS15126F

Pridmore, R. W. (2011). Complementary colors theory of color vision : Physiology, color mixture, color constancy and color perception. *Color Research & Application*, *36*(6), 394-412. https://doi.org/10.1002/col.20611

Qian, B.-J., Liu, J.-H., Zhao, S.-J., Cai, J.-X., & Jing, P. (2017). The effects of gallic/ferulic/caffeic acids on colour intensification and anthocyanin stability. *Food Chemistry, 228*, 526-532. https://doi.org/10.1016/j.foodchem.2017.01.120

Quan, W., Wei He, He, W., Mei Lü, Lu, M., Bo Yuan, Yuan, B., Maomao Zeng, Zeng, M., Daming Gao, Gao, D.-M., Fang Qin, Qin, F., Jie Chen, Chen, J., Zhiyong He, & He, Z. (2019). Anthocyanin composition and storage degradation kinetics of anthocyanins-based natural food colourant from purple-fleshed sweet potato. *International Journal of Food Science and Technology, 54(8)*, 2529-2539. https://doi.org/10.1111/ijfs.14163

Quideau, S., Deffieux, D., Douat-Casassus, C., & Pouységu, L. (2011). Plant Polyphenols : Chemical Properties, Biological Activities, and Synthesis. *Angewandte Chemie International Edition*, *50*(3), 586-621. https://doi.org/10.1002/anie.201000044

Ratanapoompinyo, J., Nguyen, L. T., Devkota, L., & Shrestha, P. (2017). The effects of selected metal ions on the stability of red cabbage anthocyanins and total phenolic compounds subjected to encapsulation process. *Journal of Food Processing and Preservation, 41(6),* e13234. https://doi.org/10.1111/jfpp.13234

Ren, S., Jiménez-Flores, R., & Giusti, M. M. (2021). The interactions between anthocyanin and whey protein : A review. *Comprehensive Reviews in Food Science and Food Safety, 20(6),* 5992-6011. https://doi.org/10.1111/1541-4337.12854

Rodriguez-Amaya, D. B. (2019). Update on natural food pigments—A mini-review on carotenoids, anthocyanins, and betalains. *Food Research International*, *124*, 200-205. https://doi.org/10.1016/j.foodres.2018.05.028

Rytel, E., Tajner-Czopek, A., Kita, A., Tkaczyńska, A., Kucharska, A. Z., & Sokół-Łętowska, A. (2021). The Influence of the Production Process on the Anthocyanin Content and Composition in Dried Potato Cubes, Chips, and French Fries Made from Red-Fleshed Potatoes. *Applied Sciences, 11(3),* 1104. https://doi.org/10.3390/app11031104

Šamec, D., Karalija, E., Šola, I., Vujčić Bok, V., & Salopek-Sondi, B. (2021). The Role of Polyphenols in Abiotic Stress Response : The Influence of Molecular Structure. *Plants*, *10*(1), 118. https://doi.org/10.3390/plants10010118

Sarabandi, K., Jafari, S. M., Mahoonak, A. S., & Mohammadi, A. (2019). Application of gum Arabic and maltodextrin for encapsulation of eggplant peel extract as a natural antioxidant and color source. *International Journal of Biological Macromolecules, 140*, 59-68. https://doi.org/10.1016/j.ijbiomac.2019.08.133

Sarabandi, Kh., Peighambardoust, S. H., Sadeghi Mahoonak, A. R., & Samaei, S. P. (2018). Effect of different carriers on microstructure and physical characteristics of spray dried apple juice concentrate. *Journal of Food Science and Technology, 55(8),* Article 8. https://doi.org/10.1007/s13197-018-3235-6

Satake, R., & Yanase, E. (2018). Mechanistic studies of hydrogen-peroxide-mediated anthocyanin oxidation. Tetrahedron, 74(42), 6187-6191. https://doi.org/10.1016/j.tet.2018.09.012

Shamey, R. (Éd.). (2023). Cone Fundamentals, Stockman-Sharpe. In *Encyclopedia of Color Science and Technology* (p. 683-683). Springer International Publishing. https://doi.org/10.1007/978-3-030-89862-5_300189

Shen, N., Wang, T., Gan, Q., Liu, S., Wang, L., & Jin, B. (2022). Plant flavonoids : Classification, distribution, biosynthesis, and antioxidant activity. *Food Chemistry*, *383*, 132531. https://doi.org/10.1016/j.foodchem.2022.132531

Shiono, M., Matsugaki, N., & Takeda, K. (2008). Structure of commelinin, a blue complex pigment from the blue flowers of Commelina communis. *Proceedings of the Japan Academy*, Series B, 84(10), 452-456. https://doi.org/10.2183/pjab.84.452

Sigurdson, G. T., & Giusti, M. M. (2014). Bathochromic and Hyperchromic Effects of Aluminum Salt Complexation by Anthocyanins from Edible Sources for Blue Color Development. *Journal of Agricultural and Food Chemistry, 62(29*), 6955-6965. https://doi.org/10.1021/jf405145r

Sigurdson, G. T., Robbins, R. J., Collins, T. M., & Giusti, M. M. (2018). Impact of location, type, and number of glycosidic substitutions on the color expression of o-dihydroxylated anthocyanidins. *Food Chemistry, 268,* 416-423. https://doi.org/10.1016/j.foodchem.2018.06.079

Sigurdson, G. T., Robbins, R. J., Collins, T. M., & Giusti, M. M. (2017). Spectral and colorimetric characteristics of metal chelates of acylated cyanidin derivatives. *Food Chemistry, 221,* 1088-1095. https://doi.org/10.1016/j.foodchem.2016.11.052

Sigurdson, G. T., Robbins, R. J., Collins, T. M., & Giusti, M. M. (2016). Evaluating the role of metal ions in the bathochromic and hyperchromic responses of cyanidin derivatives in

acidic and alkaline pH. *Food Chemistry, 208,* 26-34. https://doi.org/10.1016/j.foodchem.2016.03.109

Singh, T., Pandey, V. K., Dash, K. K., Zanwar, S., & Singh, R. (2023a). Natural bio-colorant and pigments : Sources and applications in food processing. *Journal of Agriculture and Food Research*, *12*, 100628. https://doi.org/10.1016/j.jafr.2023.100628

Singla, R. K., Dubey, A. K., Garg, A., Sharma, R. K., Fiorino, M., Ameen, S. M., Haddad, M. A., & Al-Hiary, M. (2019). Natural Polyphenols : Chemical Classification, Definition of Classes, Subcategories, and Structures. *Journal of AOAC International*, *102*(5), 1397-1400. https://doi.org/10.5740/jaoacint.19-0133

Snarska, J., Jakimiuk, K., Strawa, J. W., Tomczyk, T. M., Tomczykowa, M., Piwowarski, J. P., & Tomczyk, M. (2024). A Comprehensive Review of Pedunculagin : Sources, Chemistry, Biological and Pharmacological Insights. *International Journal of Molecular Sciences*, *25*(21), 11511. https://doi.org/10.3390/ijms252111511

Song, J., Yu, Y., Chen, M., Ren, Z., Chen, L., Fu, C., Ma, Z. feei, & Li, Z. (2022). Advancement of Protein- and Polysaccharide-Based Biopolymers for Anthocyanin Encapsulation. *Frontiers in Nutrition*, *9*. https://doi.org/10.3389/fnut.2022.938829

Sousa, D., Basílio, N., Oliveira, J., De Freitas, V., & Pina, F. (2022). A New Insight into the Degradation of Anthocyanins : Reversible versus the Irreversible Chemical Processes. *Journal of Agricultural and Food Chemistry*, *70*(2), 656-668. https://doi.org/10.1021/acs.jafc.1c06521

Stich, E. (2016). Food Color and Coloring Food. In *Handbook on Natural Pigments in Food and Beverages* (p. 3-27). Elsevier. https://doi.org/10.1016/B978-0-08-100371-8.00001-4

Tarone, A. G., Cazarin, C. B. B., & Marostica Junior, M. R. (2020). Anthocyanins : New techniques and challenges in microencapsulation. Food Research International, 133, 109092. https://doi.org/10.1016/j.foodres.2020.109092

Tilley, R. J. D. (2020). *Colour and the Optical Properties of Materials*. John Wiley & Sons.

Torres-Rochera, B., Manjón, E., Brás, N. F., Escribano-Bailón, M. T., & García-Estévez, I. (2024). Supramolecular Study of the Interactions between Malvidin-3-O-Glucoside and Wine Phenolic Compounds : Influence on Color. *Journal of Agricultural and Food Chemistry, 72(4),* 1894-1901. https://doi.org/10.1021/acs.jafc.2c08502

Trouillas, P., Sancho-García, J. C., De Freitas, V., Gierschner, J., Otyepka, M., & Dangles, O. (2016). Stabilizing and Modulating Color by Copigmentation : Insights from Theory and Experiment. Chemical Reviews, 116(9), Article 9. https://doi.org/10.1021/acs.chemrev.5b00507

Verma, M. L., Sharma, S., Saini, R., Rani, V., & Kushwaha, R. (2020). Chapter 3 - Bioflavonoids : Synthesis, functions and biotechnological applications. In M. L. Verma & A. K. Chandel (Éds.), *Biotechnological Production of Bioactive Compounds* (p. 69-105). Elsevier. https://doi.org/10.1016/B978-0-444-64323-0.00003-5

Wallace, T. C., & Giusti, M. M. (2015). Anthocyanins. *Advances in Nutrition*, *6*(5), 620-622. https://doi.org/10.3945/an.115.009233

Wallace, T. C., & Giusti, M. M. (2019). Anthocyanins—Nature's Bold, Beautiful, and Health-Promoting Colors. *Foods, 8*(11), 550. https://doi.org/10.3390/foods8110550

Xue, H., Zhao, J., Wang, Y., Shi, Z., Xie, K., Liao, X., & Tan, J. (2024). Factors affecting the stability of anthocyanins and strategies for improving their stability : A review. *Food Chemistry: X, 24,* 101883. https://doi.org/10.1016/j.fochx.2024.101883

Yadav, S., Tiwari, K. S., Gupta, C., Tiwari, M. K., Khan, A., & Sonkar, S. P. (2023). A brief review on natural dyes, pigments : Recent advances and future perspectives. *Results in Chemistry*, *5*, 100733. https://doi.org/10.1016/j.rechem.2022.100733

Yang Lin, Cong Li, Cong Liu, Ping Shao, Ping Shao, Ligang Jiang, Liyu Jiang, Bilian Chen, Bilian Chen, Mohamed A. Farag, & Mohamed A. Farag. (2022). Enzymatic acylation of cyanidin-3-O-glucoside in raspberry anthocyanins for intelligent packaging : Improvement of stability, lipophilicity and functional properties. *Current research in food science*. 5, 2219-2227. https://doi.org/10.1016/j.crfs.2022.11.008

Yang, W., Deng, C., Xu, L., Jin, W., Zeng, J., Li, B., & Gao, Y. (2020). Protein-neutral polysaccharide nano- and micro-biopolymer complexes fabricated by lactoferrin and oat β-

glucan : Structural characteristics and molecular interaction mechanisms. *Food Research International, 132*, 109111. https://doi.org/10.1016/j.foodres.2020.109111

Yoshida, K., Mori, M., & Kondo, T. (2009). Blue flower color development by anthocyanins : From chemical structure to cell physiology. *Natural Product Reports, 26(7)*, 884. https://doi.org/10.1039/b800165k

Zagoskina, N. V., Zubova, M. Y., Nechaeva, T. L., Kazantseva, V. V., Goncharuk, E. A., Katanskaya, V. M., Baranova, E. N., & Aksenova, M. A. (2023). Polyphenols in Plants : Structure, Biosynthesis, Abiotic Stress Regulation, and Practical Applications (Review). *International Journal of Molecular Sciences*, *24*(18), 13874. https://doi.org/10.3390/ijms241813874

Zand, A., Enkhbilguun, S., Macharia, J. M., Budán, F., Gyöngyi, Z., & Varjas, T. (2023). Tartrazine Modifies the Activity of DNMT and HDAC Genes-Is This a Link between Cancer and Neurological Disorders? *Nutrients*, *15*(13), 2946. https://doi.org/10.3390/nu15132946

Zeng, Y., Guo, D., Li, X., Cai, D., Sun, J., & Bai, W. (2022). Progress in research on the structure and properties of pyranoanthocyanins. *FOOD SCIENCE*, *43(13)*: 199-209. https://www.spkx.net.cn/EN/Y2022/V43/I13/199

Zhang, B., Wang, Q., Zhou, P.-P., Li, N.-N., & Han, S.-Y. (2020). Copigmentation evidence of oenin with phenolic compounds : A comparative study of spectrographic, thermodynamic and theoretical data. *Food Chemistry*, *313*, 126163. https://doi.org/10.1016/j.foodchem.2020.126163

Zhang, Y., Deng, Z., Li, H., Zheng, L., Liu, R., & Zhang, B. (2020). Degradation Kinetics of Anthocyanins from Purple Eggplant in a Fortified Food Model System during Microwave and Frying Treatments. Journal of Agricultural and Food Chemistry, 68(42), 11817-11828. https://doi.org/10.1021/acs.jafc.0c05224

Zhao, C. L., Chen, Z. J., Bai, X. S., Ding, C., Long, T. J., Wei, F. G., & Miao, K. R. (2014). Structure–activity relationships of anthocyanidin glycosylation. *Molecular Diversity, 18(3),* 687-700. https://doi.org/10.1007/s11030-014-9520-z

Zhao, C.-L., Yu, Y.-Q., Chen, Z.-J., Wen, G.-S., Wei, F.-G., Zheng, Q., Wang, C.-D., & Xiao, X.-L. (2017). Stability-increasing effects of anthocyanin glycosyl acylation. *Food Chemistry, 214,* 119-128. https://doi.org/10.1016/j.foodchem.2016.07.073

Zhou, X., Gao, Q., Praticò, G., Chen, J., & Dragsted, L. O. (2019). Biomarkers of tuber intake. Genes & Nutrition, 14(1), 9. https://doi.org/10.1186/s12263-019-0631-0

Zhu, N., Zhu, Y., Yu, N., Wei, Y., Zhang, J., Hou, Y., & Sun, A. (2019). Evaluation of microbial, physicochemical parameters and flavor of blueberry juice after microchip-pulsed electric field. *Food Chemistry, 274*, 146-155. https://doi.org/10.1016/j.foodchem.2018.08.092

Zollinger, H. (2003). Color Chemistry: Syntheses, Properties, and Applications of Organic Dyes and Pigments. *Angewandte Chemie International Edition.* John Wiley & Sons. https://doi.org/10.1002/anie.200385122

Chapter II. Material & methods

1. Materials

1.1. Selection of plant materials

Three plant materials, eggplant (*Solanum melongena L.*), blood orange (*Citrus sinensis (L.) Osbeck*), and pomegranate (*Punica granatum*) were selected for their richness in non-acylated anthocyanins, the predominant but moderately stable forms in nature **(Figure 9)** Their botanical and structural diversity, in anthocyanin types and polyphenol profiles, allows comparative evaluation of the color and chemical stability of anthocyanin-rich extracts and their coloring efficiency in food applications.

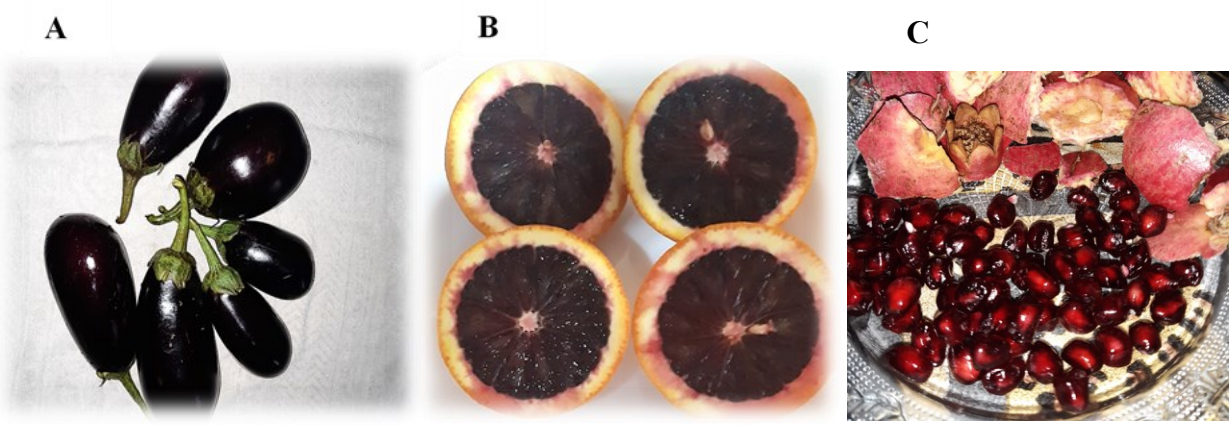

Figure 9. Plant materials used in this study: A) eggplant (*Solanum melongena L.),* B) blood orange (*Citrus sinensis (L.) Osbeck*), and C) pomegranate (*Punica granatum L.*).

1.2. Chemical reagents

Sodium acetate, hydrochloric acid, phosphoric acid, sodium hydroxide, potassium chloride, citric acid monohydrate, formic acid, and aluminum chloride hexahydrate, calcium chloride, were purchased from Biochem Chemopharma (France). Methanol, acetonitrile and ethyl acetate were supplied by Honeywell Riedel-de-Haën (France). Boric acid, Folin–Ciocalteu reagent, sodium carbonate (Na_2CO_3), gallic acid standard (≥98%), and 2,2-diphenyl-1-picrylhydrazyl (DPPH) were obtained from Sigma–Aldrich (Steinhaus, Germany). Solvents and reagents were all of analytical grade (≥ 97%).

A universal buffer of Theorell and Stenhagen was prepared by mixing 2.25 mL of phosphoric acid (85% w/w), 7.00 g of monohydrated citric acid, 3.54 g of boric acid, 343 mL of a 1 M NaOH solution, and deionized water to a total volume of 1 L. All aqueous solutions were prepared from deionized or distilled water.

2. Methods

2.1. Sample preparation

Eggplant (*Solanum melongena L.*), blood orange (*Citrus sinensis (L.) Osbeck*), and pomegranate (*Punica granatum*) were collected from different localities of Bejaia (Algeria), then washed by distilled water. Fresh eggplants were purchased from local market in March 2020 and peeled using a sharp knife. The whole peel (EPP) was dried at 40°C into a ventilated oven (Memmert). Blood orange juice (BOJ) was collected and either directly used for the analyses, or freeze-dried after mixing with the pulp in a blender (Christ Alpha 1-4 LD plus). The dried sample was ground in a grinder (IKA A11 Basic, Germany), sieved to particle size < 250 nm, then stored in a deep-freezer at -18ºC for subsequent analyses. The arils from pomegranate were mechanically extracted by squeezing the arils. The juice (PGJ) obtained was centrifuged during 30 min at 9000 rpm at 4°C.

2.1.1 Bioactive compound extraction

The application of ultrasound-assisted extraction to plant or food matrices represents an emerging technology capable of enhancing extraction yields and/or accelerating mass transfer kinetics. These improvements are primarily attributed to acoustic cavitation bubbles generated near the surface of the plant material, which expand during the rarefaction cycle. When these bubbles reach a critical size, they collapse and release large amounts of energy. The resulting microjets are directed toward the plant surface, disrupting cell walls and thereby facilitating the release of bioactive compounds from the plant material into the extraction medium **(Achat et al., 2012).**

The extraction was carried out according to the procedure of Dranca & Oroian **(2017)**. with slight modifications. Five grams of powdered samples (eggplant peel and blood orange) were extracted in amber flasks with 50 mL of MeOH/H_2O (7:3, v/v) containing 0.1% HCl for anthocyanin extraction (pH 1.6), and without acidification for total phenolic compound analysis.

The mixtures were kept in an ultrasonic bath (42 kHz, Bransonic) for 50 min at 50°C, then centrifuged at 4600 rpm for 15 min. The supernatants were collected and the remaining residues re-extracted using the same procedure. The collected extracts were gathered, then filtered (Whatman paper filter nº 4) prior to their analysis for total anthocyanin and total polyphenol contents. For anthocyanin purification, MeOH was evaporated at 40°C and the remaining aqueous solutions were diluted to a known volume with 0.01% aqueous HCl (v/v).

Figure 10. (A, B) Extraction from powdered samples: **(A)** blood orange juice and **(B)** eggplant peel; **(C)** pomegranate juice obtained mechanically by squeezing the arils.

2.1.2 Anthocyanin purification.

Purification of anthocyanin-rich extracts is often necessary because the solvent systems commonly used for extraction are not selective for these pigments. As a result, a variety of accompanying compounds are co-extracted and concentrated in the colored extracts, which can interfere with both anthocyanin stability and analytical accuracy **(Jackman & Smith, 1996)**. Solid-phase extraction **(Figure 11)** is therefore frequently employed to improve extract purity. This method uses mini-columns packed with C18-bonded silica, which retain anthocyanins through interactions between their aromatic rings and the hydrophobic stationary phase, while allowing highly polar components of the plant matrix, such as sugars and organic acids, to pass through. A subsequent washing step with ethyl acetate removes other phenolic compounds that are less strongly retained than anthocyanins. This selective retention and washing process yields extracts enriched in anthocyanins, better suited for stability testing and detailed analytical studies (**Durst & Wrolstad, 2001**).

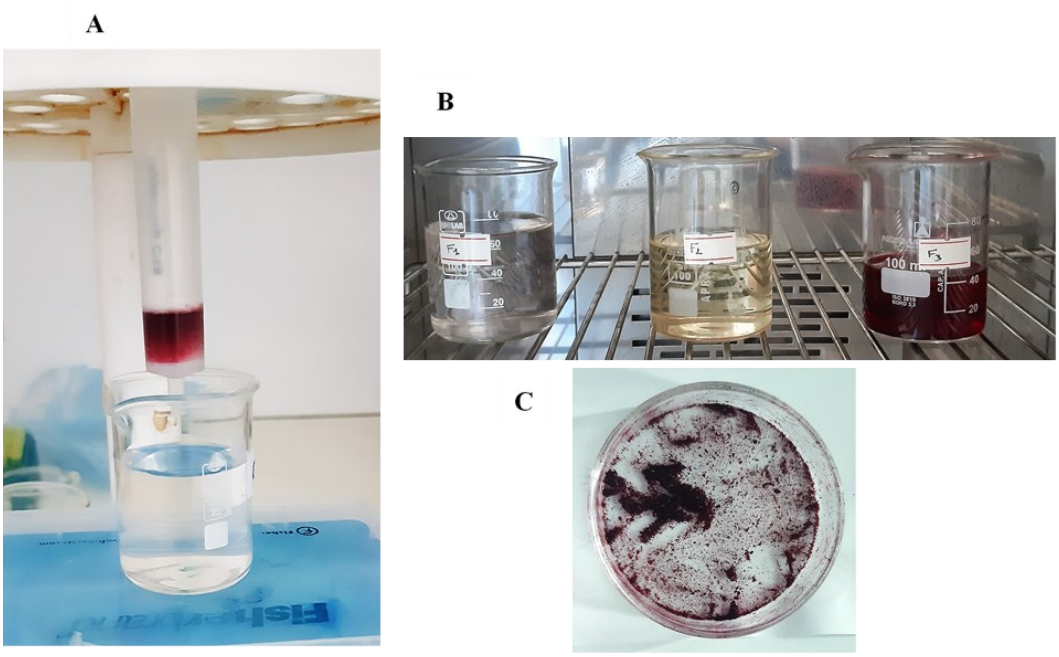

Figure 11. (A) Solid-phase (C18) purification of anthocyanins; (B) fractions obtained during purification: F1, water-soluble compounds such as sugars and organic acids; F2, colorless phenolic compounds other than anthocyanins; F3, the anthocyanin fraction; (C) dried anthocyanin-rich extract.

The aqueous extracts of eggplant and blood orange **(Section, 2.1.1)** and the pomegranate juice (pH 3.4) were purified using a Sep-Pak C18 cartridge (Thermos Fisher Scientific, USA) previously activated with HPLC-grade MeOH followed by 0.01% aqueous HCl. ACNs and other polyphenols were adsorbed onto the column, whereas sugars, acids, and other water-soluble compounds were removed by washing the column with 18 mL of 0.01% aqueous HCl. The column was further washed with 18 mL of EtOAc to partially remove colorless non-ACN phenols. ACNs from the extract were collected by washing the column with 0.01% HCl in MeOH. The ACN-rich extract was dried at 30°C.

2.2. Assessment of total polyphenols, anthocyanins, and radical scavenging activity

2.2.1 Polyphenolic content

The total polyphenol content (TPC) in each liquid extract was determined using the Folin–Ciocalteu method. This method relies on the oxidation of phenolic compounds in an alkaline

medium by the yellow molybdotungstophosphoric heteropolyanion reagent. The reaction produces a blue complex, known as molybdotungstophosphate blue, which can then be quantified by colorimetric measurement. The intensity and maximum absorption of this blue pigment are influenced not only by the qualitative and quantitative composition of the phenolic mixture but also by the pH of the solution. In practice, the alkaline conditions required for the reaction are usually established by the addition of sodium carbonate **(Cicco et al., 2009)**.

The procedure of Dranca & Oroian. **(2017)** was followed with some modifications, using gallic acid (GA) as the standard. Briefly, 200 µL of sample were mixed with 1,000 µL of Folin reagent, previously diluted in distilled water at a ratio of 1:10 (v/v). The mixture was shaken for 3 min, followed by the addition of 800 µL of sodium carbonate solution (7.5% w/v) and vigorous mixing. The reaction mixture was then allowed to stand in the dark for 30 min, after which the absorbance was measured at 750 nm. The TPC was calculated from the GA calibration curve **(see Appendix 1)**: TPC (mg/mL) = 0.0096x + 0.0166 (R^2 = 0.9988). The results were expressed as milligrams of GA equivalent per 100 g of dried powder for eggplant peel and blood orange, and as mg GAE / L for the juices (BOJ and PGJ).

2.2.2 Anthocyanin content

The total ACN content was determined using the pH differential method, which relies on the reversible structural transformations of anthocyanins with pH, producing distinct absorbance spectra. At pH 1.0, anthocyanins predominantly exist in the colored flavylium cation form, whereas at pH 4.5 they are mainly in the colorless hemiketal form. Measuring absorbance at these two pH values enables accurate quantification of total anthocyanins, even in the presence of polymerized or degraded pigments and other interfering compounds **(Giusti & Wrolstad, 2001)**. The acidified extracts of eggplant and blood orange (**see 2.1.1**) and the pomegranate & blood orange juices were diluted in pH 1 (0.1 M HCl) and pH 4.5 (0.4 M sodium acetate) solutions with the appropriate dilution factor for each sample. The solutions were allowed to equilibrate for 15 min in the dark. The visible absorbance of samples was measured (vs. a blank cell filled with distilled water) at the wavelength of maximal absorption (λmax = 520 nm) and at 700 nm to correct for possible haze contamination. Measurements were performed in triplicates using a Shimadzu UV-visible spectrophotometer (UV-1800, Biotech Engineering Management, UK).

The total ACN content (TAC) was calculated as cyanidin 3-O-glucoside (C3G) or delphinidin 3-O-glucoside (D3G) equivalent by the following Eq. 1:

$$\text{TAC (mg/L)} = \frac{\triangle A\ M\ DF\ 1000}{\varepsilon L} \quad (1)$$

With $\triangle A = (A_{520} - A_{700})$ at pH 1.0 – $(A_{520} - A_{700})$ at pH 4.5;

M (molecular mass) = 449.2 g/mol (C3G) or 465.2 g/mol (D3G);

ε = molar absorption coefficient at λmax (26900 and 29000 M^{-1} cm^{-1} for C3G and D3G, respectively), L = optical pathlength (1 cm), DF = dilution factor. The equation was applied to both powdered and liquid matrices. For powdered samples, results were expressed in mg/100g, by adjusting the calculation with the sample mass (g) and total extract volume (mL).

2.2.3 DPPH• scavenging assay of crude and fractionated extracts

The free radical scavenging capacity of the extracts was evaluated using the 1,1-diphenyl-2-picrylhydrazyl (DPPH•) assay, a rapid and widely used screening method to estimate the potential free radical quenching ability of phenolic compounds. DPPH• is a stable free radical with a deep violet color, showing a maximum absorption at 517 nm due to electron delocalization within the molecule. When a compound capable of donating a hydrogen atom or electron is present, DPPH• is reduced to the pale-yellow hydrazine form (DPPH–H), resulting in a decrease in absorbance **(Gulcin, 2020)**. The assay was performed following the procedure described by **Xu and Chen (2013)** with slight modifications: 0.1 mL of extract was mixed with 1.9 mL of DPPH• solution (0.2 mM) and incubated in the dark for 1 h. The absorbance was measured at 517 nm against a control (100%). The scavenging capacity was expressed as IC_{50} (mg/mL), representing the concentration of extract required to quench 50% of the DPPH• radicals, calculated using the equation:

$$IC50 = \frac{(A\ of\ control - A\ of sample) \times 100}{A\ of control}$$

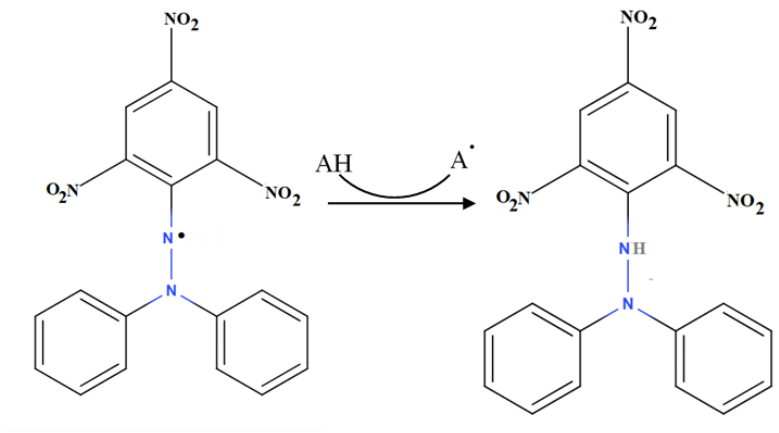

Figure 12. DPPH• radical scavenging mechanism by an antioxidant (AH) **(Gulcin, 2020)**.

2.3. Anthocyanin rich-extract composition

2.3.1 HPLC analysis

The samples (extracts in 0.1M HCl) were analyzed by HPLC (Merck Hitachi Elite Lachrom) on a reversed-phase C18 column (Agilent Poroshell 120, 250 × 4.6 mm inner diameter, pore size of 2.7 µm) thermostated at 25°C (Merck Hitachi Column Oven L-2300). The detection was carried out at 520 and 280 nm using a diode-array detector (DAD, Merck Hitachi L-2455). The binary solvent system used was composed of solvent A (1% formic acid in water) and solvent B (1% formic acid in 30% acetonitrile). The gradient was as follows: 0-20% B over 5 min, 20-85% B over 70 min at a flow rate of 0.4 mL/min. The chromatographic column was washed with 100% B for 10 min and then stabilized with the initial conditions for another 10 min.

From the peak areas in the chromatogram at 520 nm the ACN composition in each extract was determined and an average molecular mass for the ACN pool was calculated, from which an apparent molar absorption coefficient at the wavelength of maximal visible absorption was estimated (Beer's plot). This value was used to estimate a) the overall ACN concentration in the acidic solutions (pH 1, 100% flavylium) used in the physicochemical experiments, and b) the ACN content in the purified extracts **(see annex 2)**.

2.3.2 HPLC-DAD-ESI-MS

The samples were analyzed on a Finnigan Surveyor series liquid chromatograph coupled with a diode array detector and a LCQ DECA XP MAXXL mass detector (Finnigan Corp., San Jose, CA, USA). The quadrupole ion trap was equipped with an electrospray ionization (ESI) interface. Separation was carried out on a reversed-phase column (4.6 × 250 mm Poroshell 120 EC-C18 2.7µm) thermostated at 25°C using the same elution conditions as for the HPLC analysis (see above). The electrospray, capillary and tube lens voltages were 3.5 kV, 11 V, and 120 V, respectively. The capillary temperature was set at 300°C. N_2 was used as both the sheath and auxiliary gas. Mass spectra were recorded in positive and negative ion modes in the *m/z* range 110-2000, according to three scans: a full mass scan (MS), a zoom scan of the most intense ion in the first scan (MS^2), and a MS-MS scan of the most intense ion (MS^3).

2.4. Thermodynamics of water addition and proton transfer

The reversible transformations of ACNs in mildly acidic solution (pH 1 – 6) are recalled on **Figure 13.** They consist a) in a fast proton transfer between the red flavylium ion (AH^+) and the purple neutral base (A, mixture of tautomers), and b) in water addition to AH^+, yielding hemiketal B, in fast tautomeric equilibrium with cis-chalcone Cc, itself slowly isomerizing into trans-chalcone Ct. The last three species are all colorless. Color loss by hydration was studied by UV-visible spectroscopy using the pH jump technique **(Pina, 2014)**. This approach involves the rapid addition of a base to solutions previously equilibrated in the flavylium cation form of anthocyanins. Concentrated stock solutions of extracts (9.15, 10.0 and 16.67 mg/mL for the, pomegranate, eggplant and blood orange extracts, resp.) were prepared in 0.1 M HCl (pH 1, 100% AH^+). At time zero of the kinetic experiments, a small volume of stock solution was rapidly added to a volume of universal buffer (dilution by a factor 1:90, final pH ranging from 2.5 to 6) placed in the quartz cell of a Shimadzu UV-visible spectrophotometer (UV-1800) and the UV-Vis spectra were recorded from 250 to 800 nm until the hydration equilibrium (a mixture of colored and colorless forms) was reached. The pH was measured with a Hanna edge pH-meter.

The initial and final absorbance values (A_0, A_f) at the flavylium's λ_{max}, as well as the apparent first-order rate constant of hydration (k_{obs}), were collected. The k_{obs} values were calculated for each pH using Eq. 2 and the Origin Pro software.

$$A(t) = (A_0 - A_f)\, exp(-k_{obs}t) + A_f \qquad (2)$$

A_f: absorbance at pseudo-equilibrium (all forms, except the slowly accumulating trans-chalcone), A_0: initial absorbance (just after the pH-jump), $A(t)$: absorbance at time t.

From the pH dependence of k_{obs} **(Pina, 2014):** the rate constants of hydration / tautomerization (k_h, $AH^+ \rightarrow B + Cc$) and the reverse reaction (k_{-h}, $B + Cc \rightarrow AH^+$), as well as the acidity constant (K_a, $AH^+ \rightarrow A$ equilibrium) can be estimated using Eq. 3 and the Scientist software (Micromath).

$$k_{obs} = \frac{[H^+]}{[H^+]+K_a} k_h + k_{-h}[H^+] \quad (3)$$

From the pH dependence of A_f, acidity constant $K\hat{}a$, connecting the flavylium ion and all neutral forms except Ct, can be determined. The curve-fitting was carried out using Eq. 4 and the Solver function of Microsoft Excel.

$$A_f = A_0 \frac{1+r_a 10^{(pH-pK_a)}}{1+10^{(pH-pK\hat{}a)}} \quad (4)$$

With A_0 = absorbance of a solution of pure flavylium ion at λ_{max},

$K\hat{}_a = [H^+]\frac{[A]+[B]+[Cc]}{[AH^+]}, K_a = [H^+]\frac{[A]}{[AH^+]}$, $r_a = \varepsilon(A)/\varepsilon(AH^+)$ at the flavylium's λ_{max}.

When the spectral measurements are repeated a few hours later, full equilibrium is reached (including Ct), and the corresponding global acidity constant is:

$K'_a = [H^+]\frac{[A]+[B]+[Cc]+[Ct]}{[AH^+]}$.

The pK'_a value can be determined from Eq.4 with A_{eq} (absorbance at complete equilibrium) replacing A_f, pK'_a and replacing $pK\hat{}_a$. The percentage of residual color was also evaluated as $RC\% = 100 \times A_{eq}/A_0$. Finally, thermodynamic constants of hydration at pseudo-equilibrium and full equilibrium can be deduced from the following relationships:

$K_h\hat{} = \frac{k_h}{k_{-h}} = [H^+]\frac{[B]+[Cc]}{[AH^+]} = K\hat{}_a - K_a, K'_h = [H^+]\frac{[B]+[Cc]+[Ct]}{[AH^+]} = K'_a - K_a$.

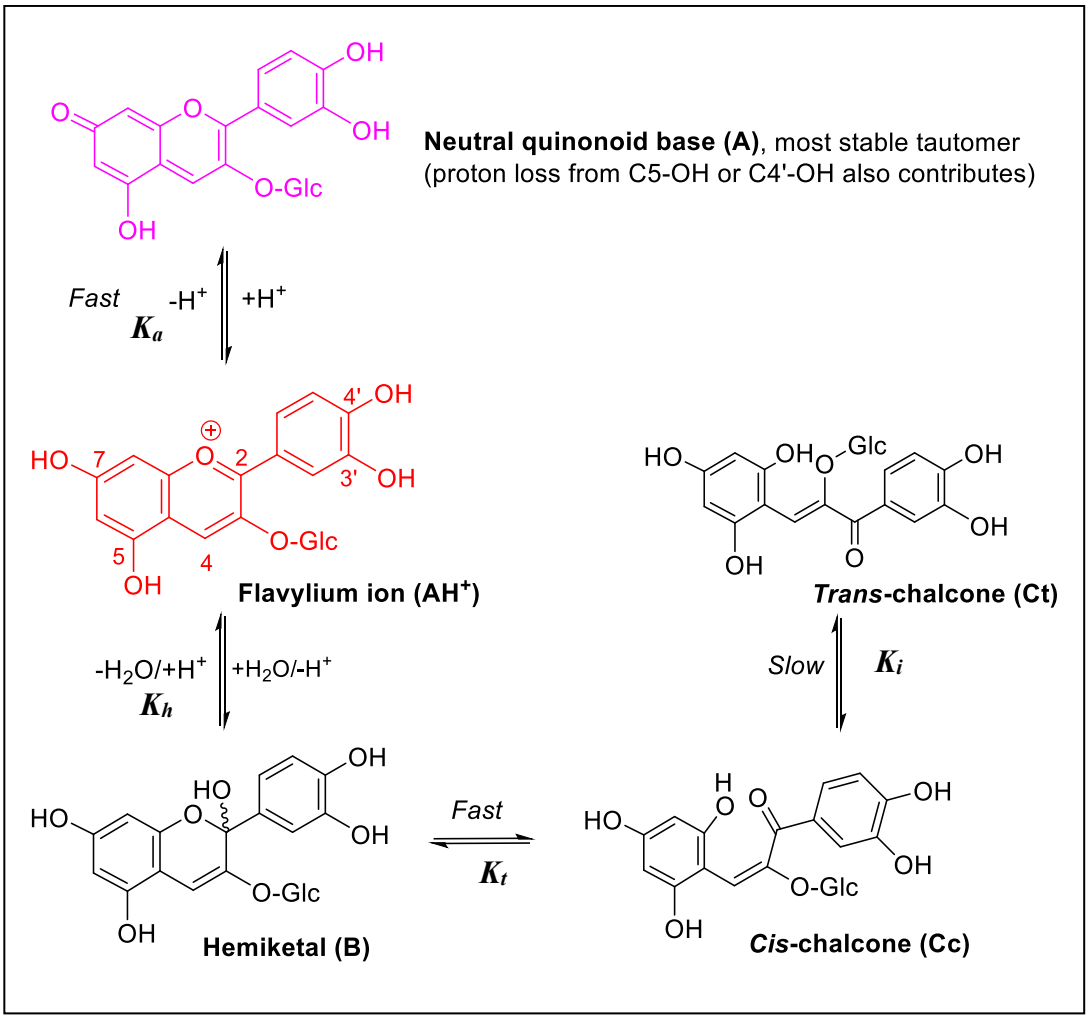

Figure 13. The reversible transformations of ACNs in mildly acidic solution (pH 1 – 6)

2.5. Metal binding experiment

Metal-ACN binding experiment was performed according a previously reported method with some modifications **(Fenger et al., 2021a)**. To 2.67 mL of a pH 5 buffer solution (0.01 M acetate), 30 µL of ACN stock solution were rapidly added and placed in the spectrometer cell. After a few minutes (pseudo-equilibrium), 30 µL of a fresh solution of Al^{3+} (in 0.1M HCl) were added. The metal/ACN ratios in solution were 0.5, 1 and 2 equivalents. Spectra were recorded every 0.5 s over 5 min. The binding was relatively fast and accompanied by the development of a large visible band in the range 550–600 nm characteristic of the metal-ACN complex.

At $t = 0$ (Al^{3+} addition), $A = A_{eq}$ (pseudo-equilibrium). Then, A(t) at λ_{max} of complex increases to a final value A_f (complexation equilibrium). The percentage of color regeneration is expressed as 100xA_f/A_{eq} at λ_{max} of the complex.

2.6. Thermal degradation

Thermal degradation was carried out at pH 5 and 50°C in a thermostated water bath according to a previously reported method **(Fenger et al., 2019)** with some modifications. Concentrated solutions of extracts (19.1 mg/mL, 32.8 mg/mL and 36.1 mg/mL for the pomegranate, eggplant and blood orange extracts, resp.) were prepared in 0.1 M HCl. At time zero, aliquots of 0.5 mL were added to 20 mL of buffer solution (10 mM acetate, pH 5), with or without added metal ion, and placed in a ventilated oven at 50°C under magnetic stirring. Two daily samplings were performed. Samples were cooled down and their UV-vis spectra recorded, giving $A_{(t, pH\ 5)}$. Then, samples were acidified to pH 1 by 6M HCl (negligible dilution), and stored in the dark at room temperature till the next day in order to convert all the non-degraded ACN forms (colored and colorless) into the flavylium cation for titration. The corresponding absorbance is noted $A_{(t, pH\ 1)}$. Control experiments (no degradation) were also performed. To 2 mL acetate buffer, 50 µL of stock solution were added and the absorbance at λ_{max}, $A_{(0, pH\ 5)}$, immediately recorded (mostly, a solution of neutral base). The same experiments were repeated with 2 mL 0.1 M HCl to obtain $A_{(0, pH\ 1)}$. The fractions of residual color and residual pigments were calculated as:

$X_{color} = A_{(t, pH\ 5)} / A_{(0, pH\ 5)}$ and $X_{pigment} = A_{(t, pH\ 1)} / A_{(0, pH\ 1)}$. Both were plotted vs. time.

All absorbance values were approximately corrected for light scattering (which gradually took place after prolonged heating, $t > 48$h), by subtracting the absorbance at 800 nm.

2.7. Encapsulation technique

Encapsulation by ionic gelation (ionotropic gelation) is a simple and low-cost technique widely used in food, pharmaceutical, and medical applications. It involves dripping or atomizing a polymeric (hydrocolloid) solution containing the active compound into a calcium chloride solution, where ionic crosslinking occurs, forming hydrogel beads. The method is mild, solvent-free, and does not require elevated temperature or specialized equipment, and the resulting gel matrix allows the entrapment and controlled release of bioactive compounds in response to external stimuli such as pH **(Gadziński et al., 2022; Guerra-Valle et al., 2022).**

2.7.1 Preparation of solutions

- **Alginate solutions**

Sodium alginate (NaAlg, low viscosity, from Büchi. Sigma-Aldrich, Darmstadt, Germany) was dispersed in distilled water (2%, i.e. 20 g/L) and left for several hours for complete dissolution. Alginate-pectin solutions were prepared similarly with additional 1% (i.e. 10 g/L) pectin from Citrus Pectin, degree of esterification >50%. The pH values of these solutions are 8.0 and 4.2, respectively.

- **Preparation of the $CaCl_2$ bath**

Acetate buffers (10 mM) were prepared at pH 4 or 5, and calcium chloride (2%, i.e., 20 g/L) was added to the buffer solution. For the encapsulation of metal–anthocyanin complexes, the $CaCl_2$ bath was further supplemented with $AlCl_3$ (2 equiv. vs. ACN concentration in extracts).

2.7.2 Alginate bead preparation

Ionic gelation technique **(Sampaio et al., 2019)** was used to encapsulate anthocyanins-rich extracts using two polysaccharides (PS), Alginate and Pectin (Ca^{2+}-dependent gelation properties). 50 µmol of extract ACNs are dissolved in the PS solutions: 10 g of sodium alginate 2% (w/v) and 10 g sodium alginate 2% (w/v) – pectin 1% (w/v). The solution was kept under stirring until homogenized, then allowed to stand for approximately 15 min to eliminate air bubbles. The pH of the solutions was near neutral (readjusted, when necessary, with a few drops of 0.1M NaOH or HCl), so that water addition to anthocyanins (color loss) is very slow. The mixture (ACNs + polymer) was dripped using a 22G gauge syringe, over a 2% (w/v) $CaCl_2$ bath (10 mL), with the needle tip positioned ≈ 3cm above the bath surface. Once formed, the colored beads were left to harden under magnetic stirring for 30 min. The liquid was then drained, and the beads were washed with distilled water to remove excess calcium.

2.7.3 Determination of encapsulation efficiency

Process performance was evaluated by the encapsulation efficiency (EE), which was calculated using two approaches:

Method 1: Acidic dissociation of encapsulated anthocyanins.

Anthocyanins entrapped in the beads were released by acidic dissociation in 0.1 M HCl (pH 1). A sample of beads of known mass (m) was immersed in a volume V of HCl solution and stirred regularly until complete decolorization of the beads, indicating full release of anthocyanins into the medium as the red flavylium cation (from visual appreciation). The visible absorbance of the solution was then measured at λ_{max}, $A = \varepsilon c$

-The mole fraction of anthocyanins released from the beads was calculated as:

$n_B = CV \times \frac{m_B}{m}$, where m_B is the total mass of beads.

-The encapsulation yield (%) was expressed as:

$EE\ (\%) = 100 \times \frac{n_B}{n_{tot}}$, with n_{tot} the total mole number of anthocyanins initially added to the NaAlg solution.

Method 2: Quantification of non-encapsulated anthocyanins in the $CaCl_2$ bath.

After bead recovery by filtration, the filtrate together with the washing fractions was acidified to pH 1 using 6 M HCl (to minimize dilution). The total volume was adjusted to V. The solution was left until complete recovery of the red color (reversion to flavylium form), and the visible absorbance was measured at λmax, $A = \varepsilon c$

Mole number of non-encapsulated anthocyanins in the filtrate: $n_F = CV$.

Encapsulation yield (%):

$EE(\%) = 100 \times \frac{n_{tot} - n_F}{n_{tot}}$.

If dilution was required after acidification, the dilution factor was taken into account in the calculations.

2.7.4 Moisture content determination

The moisture content of the samples was determined by oven drying (Memmert) at 105 °C until constant weight, following the AOAC official method 971.28 (2000). Each sample (initial mass = m_0) was placed in a ventilated oven and periodically weighed until a stable final mass (mf) was obtained. The moisture content (MC) was then calculated using the formula:

$$MC(\%) = 100 \times \frac{m_0 - m_f}{m_0}$$

2.7.5 Thermal treatment of beads

Thermal treatment was carried out at 50 °C by placing 3 g of beads in hermetically sealed 5 mL hemostasis tubes and incubating them in an oven. Samples were collected after 24 and 48 h. To quantify the residual pigment, bead samples (250 mg) were dissociated in 5 mL of 0.1 M HCl, and the absorbance of the released colorants was measured at λ_{max}. The residual pigment content was calculated as described in **Section 2.7.3**. **Method 1.**

2.7.6 Colorimetric data

Our perception of the color of an object depends on the characteristics of the light source, the optical properties of the object, and the response of the human eye. Colorimetry is a psychophysical discipline that quantifies color using objective numerical systems. In the color industry, color is commonly expressed in the CIE L*a*b* space, where L* represents lightness (0 = black, 100 = white), and a* and b* represent chromatic coordinates: green (–a*) to red (+a*) and blue (–b*) to yellow (+b*), respectively **(Shamey, 2023)**. From these values, chroma (C*) and hue angle (H°) can also be derived.

Color measurements were performed with a PCE-XXM 30 colorimeter (PCE Deutschland GmbH, Meschede, Germany) with a light beam diameter of 8 mm, programmed in the CIE-Lab system with standard illuminant D65 and a 10° standard observer. For bead samples, measurements were taken after filtration, and the beads were transferred into 24-well TC-treated plates. The stability of encapsulated anthocyanins was assessed by monitoring colorimetric parameters after 48 h of heating. Measurements were carried out in quadruplicate, and the instrument was calibrated with a white calibration plate before use.

Although chroma (C*) and hue angle (H°) values were directly obtained from the instrument, they are typically calculated as:

$$C^* = \sqrt{a^{*2} + b^{*2}}$$

$$H^0 = \tan^{-1}\left({}^{b^*}/_{a^*}\right)$$

The total color difference (ΔE*) between samples and controls was calculated as:

$$\Delta E^* = \sqrt{\Delta L^{*2} + \Delta a^{*2} + \Delta b^{*2}}$$

Hue angle values typically correspond to 0° (red), 90° (yellow), 180° (green), and 270° (blue). ΔE* values are interpreted as: not noticeable (0–0.5), slightly noticeable (0.5–1.5), noticeable (1.5–3.0), visible (3.0–6.0), and significant (> 6.0) **(Cserhalmi et al., 2006).**

2.8. Application of anthocyanins extract in hard candy matrix

2.8.1 Hard candy preparation

Hard candies were prepared following a standardized cooking process in which sucrose and glucose syrup acted as the main structuring agents of the matrix **(Ozel et al., 2024)**. Granulated sucrose (54%), glucose syrup (43%), and water (6.3%) were first manually homogenized at room temperature to obtain a uniform mixture. The mixture was then heated to approximately 145 °C, monitored with a calibrated probe thermometer (Testo 905-T1, Germany), without stirring to prevent caramelization. When the mixture reached 145 °C, the candy mass was allowed to cool. At 115–121 °C, citric acid (0.15%), anthocyanin-rich extracts, or Allura Red (0.02%) were incorporated and mixed manually until homogeneous. The 0.02% level corresponds to the legally permitted maximum for Allura Red. The final mixture was poured into silicone molds and cooled at ambient temperature for 15–20 min. Solidified candies were removed from the molds, wrapped in cellophane film, and stored at 4°C until analysis. For each extract, two types of hard candies were prepared: (i) candies containing 0.02% anthocyanins, and (ii) candies containing 0.02% anthocyanins and 0.15% citric acid.

2.8.2 Hard candy characterization

- Moisture content was determined as previously described in Section 2.7.4.
- pH was measured using a pH meter (Hanna Edge) after dissolving 1 g of hard candy in 10 mL of distilled water.
- Colorimetric parameters were determined following the procedure described in Section 2.7.6

2.8.3 Sensory acceptability.

Acceptability test was conducted to assess only the visual appearance of the hard candies. A total of 100 candy consumers, recruited among university students and staff, participated in the study, with no restrictions on age or gender (18–60 years). The samples were assessed for glossiness, color, overall visual acceptability, perception of artificial color, and purchase intention (yes or no). Product appreciation was measured using a 9-point hedonic scale (9 = like extremely, and 1 = dislike extremely). In addition, three open-ended questions were included to gain deeper insights into consumer perceptions (see **Appendix 9**). Sensory profiles were illustrated using radar plots, and product characterization was based on the identification of discriminant descriptors. External preference mapping (PREFMAP) was applied to relate sensory attributes to overall acceptability.

The samples were presented simultaneously, each identified by a random one-digit number for non-acidified candies, and a letter for acidified ones, to minimize any bias related to formulation. Each sample consisted of a single candy unit, displayed in an individual Petri dish on a white background.

3. Statistical Analyses.

The experiments were performed in duplicate or triplicate and the final results were expressed as mean values and standard deviation (SD). All statistical data were processed using Origin Pro software, and statistical significance was determined by applying Analysis of Variance (ANOVA). and Tukey's Test at the 5% level of significance ($p < 0.05$).

The treatment of the sensorial analysis data was determined by XLSTAT 2025 (Addinsoft, Paris, France, 2025).

References

Achat, S., Tomao, V., Madani, K., Chibane, M., Elmaataoui, M., Dangles, O., & Chemat, F. (2012). Direct enrichment of olive oil in oleuropein by ultrasound-assisted maceration at laboratory and pilot plant scale. *Ultrasonics Sonochemistry*, 19(4), 777-786. https://doi.org/10.1016/j.ultsonch.2011.12.006

Cicco, N., Lanorte, M. T., Paraggio, M., Viggiano, M., & Lattanzio, V. (2009). A reproducible, rapid and inexpensive Folin–Ciocalteu micro-method in determining phenolics of plant methanol extracts. *Microchemical Journal*, *91*(1), 107-110. https://doi.org/10.1016/j.microc.2008.08.011

Cserhalmi, Zs., Sass-Kiss, Á., Tóth-Markus, M., & Lechner, N. (2006). Study of pulsed electric field treated citrus juices. *Innovative Food Science & Emerging Technologies*, *7*(1), 49-54. https://doi.org/10.1016/j.ifset.2005.07.001

Dranca, F., & Oroian, M. (2017). Total Monomeric Anthocyanin, Total Phenolic Content and Antioxidant Activity of Extracts from Eggplant (*S olanum Melongena* L.) Peel Using Ultrasonic Treatments : Eggplant antioxidants extraction. *Journal of Food Process Engineering*, *40*(1), Article 1. https://doi.org/10.1111/jfpe.12312

Durst, R. W., & Wrolstad, R. E. (2001). Separation and Characterization of Anthocyanins by HPLC. *Current Protocols in Food Analytical Chemistry*, *00*(1), Article 1. https://doi.org/10.1002/0471142913.faf0103s00

Fenger, J.-A., Moloney, M., Robbins, R. J., Collins, T. M., & Dangles, O. (2019). The influence of acylation, metal binding and natural antioxidants on the thermal stability of red cabbage anthocyanins in neutral solution. Food & Function, 10(10), Article 10. https://doi.org/10.1039/C9FO01884K

Fenger, J.-A., Roux, H., Robbins, R. J., Collins, T. M., & Dangles, O. (2021). The influence of phenolic acyl groups on the color of purple sweet potato anthocyanins and their metal complexes. *Dyes and Pigments*, *185*, 108792. https://doi.org/10.1016/j.dyepig.2020.108792

Gadziński, P., Froelich, A., Jadach, B., Wojtyłko, M., Tatarek, A., Białek, A., Krysztofiak, J., Gackowski, M., Otto, F., & Osmałek, T. (2022). Ionotropic Gelation and Chemical Crosslinking as Methods for Fabrication of Modified-Release Gellan Gum-Based Drug Delivery Systems. Pharmaceutics, 15(1), 108. https://doi.org/10.3390/pharmaceutics15010108

Giusti, M. M., & Wrolstad, R. E. (2001). Characterization and Measurement of Anthocyanins by UV-Visible Spectroscopy. *Current Protocols in Food Analytical Chemistry*, *00*(1), F1.2.1-F1.2.13. https://doi.org/10.1002/0471142913.faf0102s00

Guerra-Valle, M., Petzold, G., & Orellana-Palma, P. (2022). Optimization of Encapsulation by Ionic Gelation Technique of Cryoconcentrated Solution : A Response Surface Methodology and Evaluation of Physicochemical Characteristics Study. *Polymers*, *14*(5), 1031. https://doi.org/10.3390/polym14051031

Gulcin, İ. (2020). Antioxidants and antioxidant methods : An updated overview. *Archives of Toxicology*, *94*(3), 651-715. https://doi.org/10.1007/s00204-020-02689-3

Jackman, R. L., & Smith, J. L. (1996). Anthocyanins and betalains. In G. A. F. Hendry & J. D. Houghton (Éds.), *Natural Food Colorants* (p. 244-309). Springer US. https://doi.org/10.1007/978-1-4615-2155-6_8

Ozel, B., Kuzu, S., Marangoz, M. A., Dogdu, S., Morris, R. H., & Oztop, M. H. (2024). Hard Candy Production and Quality Parameters : A review. *Open Research Europe*, *4*, 60. https://doi.org/10.12688/openreseurope.16792.1

Pina, F. (2014). Chemical Applications of Anthocyanins and Related Compounds. A Source of Bioinspiration. *Journal of Agricultural and Food Chemistry*, *62*(29), 6885-6897. https://doi.org/10.1021/jf404869m

Sampaio, G. L. A., Pacheco, S., Ribeiro, A. P. O., Galdeano, M. C., & Gomes, F. S. (2019). Encapsulation of a lycopene-rich watermelon concentrate in alginate and pectin beads : Characterization and stability. *LWT*, *116*, 108589. https://doi.org/10.1016/j.lwt.2019.108589

Shamey, R. (Éd.). (2023). Cone Fundamentals, Stockman-Sharpe. In *Encyclopedia of Color Science and Technology* (p. 683-683). Springer International Publishing. https://doi.org/10.1007/978-3-030-89862-5_300189

Xu, B., & Chen, X. (2013). Comparative Studies on Free Radical Scavenging Capacities and Total Phenolic Contents of Whole and Dehulled Adlay (*coix Lacryma-Jobi Var. Ma-Yuen*) as Affected by Thermal Processing Methods. *Journal of Food Processing and Preservation*, *37*(5), 630-636. https://doi.org/10.1111/j.1745-4549.2012.00683.x

Chapter III. Results and discussion

1. Composition and Characterization of Anthocyanin-Rich Extracts

In this section, anthocyanin-rich extracts from pomegranate juice (PGJ), blood orange juice (BOJ), and eggplant peel (EPP) were prepared and structurally characterized. HPLC-UV/MS analyses provided detailed profiles of anthocyanins and other polyphenolic constituents, providing a diversified basis to study pigment–copigment interactions and their influence on anthocyanin physicochemistry.

1.1. Anthocyanin and total polyphenol contents in extracts

The TPC and TAC of the three crude extracts (before fractionation on C18 silica gel) are reported in **Table 1**. The three investigated plant are a noticeable in terms of their contents of secondary metabolites, including anthocyanins. And The results are in agreement with those reported in the literature. For comparison, high TAC (227.6 mg/100 g, extraction in MeOH, 45 kHz, 50°C for 50 min) and TPC (7.84 g/100 g, extraction in 2-propanol, 45 kHz, 60°C for 40 min) in eggplant peel were also reported in the literature **(Dranca & Oroian, 2017)**. Extraction of pomegranate juice under different pressure values (pneumatic press) yielded TPC values of 694 to 1076 mg/g fresh weight, and TAC values of 274 to 552 mg/L **(Catania et al., 2020)**. In a study of six Spanish pomegranate cultivars, TAC was found in the range 72 - 200 mg/L of juice **(Legua et al., 2012)**. As for the most representative cultivars of blood orange in the Mediterranean basin, TPC values between 117.3 and 241.9 mg GAE/100g of fresh weight were estimated. The highest TAC was found in Moro (133.1 mg/L), followed by Sanguinelli (45.6 mg/L) **(Legua et al., 2022)**. Another study reversed this ranking with TAC values of 101.1 and 90.1 mg/L for Sanguinelli and Moro, respectively, the other varieties analyzed being much less rich in ACNs (TAC between 4.7 and 23.8 mg/L) **(Forner-Giner et al., 2023)**

After purification on C18 silica gel, the ACN content in the extracts was strongly enhanced, up to a factor *ca*. 100 for BOJ **(Table 1).**

Table 1. Total anthocyanin and total polyphenol contents in the extracts with DPPH IC_{50} values. For EPP, ref = delphinidin 3-O-Glc, for PGJ and BOJ, ref = cyanidin 3-O-Glc. GA: gallic acid.

Crude extract	Eggplant peel	Pomegranate juice	Blood orange juice
TAC (mg ref / 100g)	297.4 ± 2.9	-	72.9 ± 2.9 d)
TAC (mg ref / L)	-	251.4 ± 3.6	124.4 ± 5.5
TPC (mg GA / 100g)	2640 ± 82	-	1455 ± 26 d)
TPC (mg GA / L)	-	2017 ± 21	1364 ± 15
DPPH IC_{50} (mg/mL)	0.091 ± 0.003	0.40 ± 0.01	0.94 ± 0.02 (0.54 ± 0.01e)
Purified extract	Eggplant peel	Pomegranate juice	Blood orange juice
M (g mol^{-1}) a)	626	523	495
ε_{app} (M^{-1} cm^{-1}) b)	4980	4910	2330
TAC (g ref / 100g) c)	12.8	15.7	7.9
DPPH IC_{50} (µg/mL)	6.64 ± 0.08	3.8 ± 0.06	27.36 ± 1.30

a) Mean molecular mass deduced from composition (HPLC analysis).

b) Apparent molar absorption coefficient at λ_{max}(visible) and pH 1 (pure flavylium). From Beer's law assuming 100% ACN content in extract **(see appendix 2).**

c) Comparison with a pure reference sample. TAC (g ACN / g extract) = $\frac{\varepsilon_{app}\, M_{Ref}}{\varepsilon_{ref}\, M}$

d) Lyophilized powder from a mixture of juice and pulp

e) IC_{50} of Lyophilized powder from a mixture of juice and pulp.

1.2. Identification of major pigments and copigments

After fractionation on C18 silica gel, ACNs and other polyphenols were identified using HPLC-DAD-MS by comparison with the literature. The corresponding data are presented in **Table 2 & Table 3 and Figure 14 (see also appendix 3).**

1.2.1. Eggplant peel. Based on comparison of retention time and LC-MS fragmentation pattern with published data **(Kacjan Maršić et al., 2014; Zhang et al., 2020),** four anthocyanins were identified in eggplant peel **(Figure 14, Table 2 & Appendix 3)** Peaks 3 and 4 were identified as delphinidin-3-O-glucoside (D3G) and delphinidin 3-O-rutinoside (D3R). Peaks 1 and 2 had the same molecular ion (*m/z* 773). Mass fragmentation indicated that peak 1 is a delphinidin diglycoside bearing one hexose and one rutinose. Despite the absence of fragments for peak 2, both peaks were tentatively identified as delphinidin 3-O-rutinoside-5-O-galactoside (peak 1) and delphinidin 3-O-rutinoside-5-O-glucoside (peak 2) from their retention times. Delphinidin 3-O-rutinoside was the predominant ACN in eggplant peel with a peak area of 85.5% of total ACNs identified. Although delphinidin 3-O-(*p*-coumaroyl)rutinoside-5-glucoside **(Ichiyanagi et al., 2005)** and the *cis* and *trans* isomers of delphinidin 3-O-(*p*-coumaroyl)glucoside **(Zhang et al., 2020)** were previously reported to be the major ACN in eggplant, we did not detect the corresponding peaks in LC-MS analysis. Petunidin 3-O-rutinoside, malvidin 3-O-rutinoside-5-O-glucoside and cyanidin 3-O-rutinoside were also detected in eggplant peel extracts **(Ferarsa et al., 2018)**. These discrepancies are possibly due to differences in varietal and growth conditions **(García-Salas et al., 2014).**

The copigments identified in eggplant peel extracts were diamide derivatives of triamine spermidine following acylation by caffeic and dihydrocaffeic acids **(Table 3 & Appendix 3).** The main mass fragmentations observed consisted in the cleavage of a) the C-N bond of caffeoylamides with release of caffeoyl- and dihydrocaffeoyl-spermidines (*m/z* 308 & 310, resp.), while the dihydro homologs were not cleaved, and b) the central amine group with release of caffeoyl- and dihydrocaffeoyl-allylamines (*m/z* 220 & 222, resp.), in agreement with the literature.**(Sun et al., 2015)** Asymmetry in the latter cleavage allowed discriminating the two regioisomers (peaks 2 and 3 in **Table 3**).

1.2.2. Pomegranate juice. The ACN profile consists in mono- and di-O-glucosides of delphinidin and cyanidin, and in pelargonidin 3-O-glucoside **(Table 2, Figure 14, Appendix 3)** in agreement with the literature **(Mena et al., 2012).** The most abundant anthocyanin is cyanidin 3-O-glucoside (C3G, peak 4), representing 42% of the total ACN peak area, followed by cyanidin 3,5-O-diglucoside (C3,5DG, peak 2, 38%). Minor ACNs include delphinidin 3,5-O-diglucoside (6.9%, peak 1), delphinidin 3-O-glucoside (7.9%, peak 3), and pelargonidin 3-O-glucoside (5.1%, peak 5). Additionally, Fisher et *al* **(2011)**. reported the presence of a cyanidin pentoside–hexoside and a cyanidin pentoside, while pelargonidin 3,5-O-diglucoside was documented by Mena et *al*. **(2012)** and Santiago et *al*. **(2014)**,though these were not detected in our extract.

Ellagitannins are complex polyphenols (hydrolysable tannins) based on a D-glucose core acylated by galloyl and hexahydroxydiphenoyl (HHDP) units. They are recognized as major phenolic compounds in pomegranate juice **(Díaz-Mula et al., 2019).** In our pomegranate juice extract, ellagitannin 1 was detected with a molecular ion at *m/z* 783 **(Table 3, Appendix 3)** consistent with a D-glucose core acylated by 2 HHDP moieties. Its fragments at *m/z* 301 is characteristic of ellagic acid released after cleavage of a HHDP moiety **(Fischer et al., 2011)**. Ellagitannin 1 was thus identified to pedunculagin I.

1.2.3. Blood orange juice. The extract is the most diversified in terms of ACN distribution with ten compounds identified **(Table 2, Figure 14, Appendix 3)**, seven cyanidin derivatives (peaks 2, 3, 4, 6, 7, 8, and 10), two peonidin (peaks 5 and 9) and one delphinidin derivatives (peaks 1). Compared to the other extracts, blood orange juice is specific in its content in acylated anthocyanins. For instance, peak 7, one of the most abundant BOJ ACNs, showed a molecular ion at *m/z* 535 and a fragment at *m/z* 287 (cyanidin aglycone) corresponding to the loss of a malonylglucoside unit. Although minor ACNs, peaks 6, 8 and 10 (molecular ions at *m/z* 593, 593 and 679, resp. + a common fragment at *m/z* 287), are all cyanidin 3-O-dioxalylglucosides with an additional malonyl residue for peak 10, remarkable for its triacylated single Glc moiety. By contrast, peak 9 bears a unique malonyl residue and was identified to peonidin 3-O-(6”-malonyl)glucoside. Cebadera-Miranda et *al.* **(2019)** reported a similar ACN composition in blood orange juice, but also identified delphinidin 3-O-(6”-malonyl)glucoside and cyanidin 3-O-sophoroside, which were not found in our study. The major BOJ ACNs are cyanidin 3-O-glucoside (C3G, peak 4, 57.1%) and cyanidin 3-O-(6”-malonyl)glucoside (C3MG, peak 7, 28.0%) (**Table 1**, **Appendix 3**.), in agreement with the literature **(Hillebrand et al., 2004; Morales et al., 2021).**

Four flavonoid copigments could be identified in BOJ **(Table 3, Appendix 3)** by comparing with the literature **(Barreca et al., 2011).** Compound 1 was identified as a diglucoside of the flavone apigenin. The absence of the typical fragmentation of O-glycoside (loss of the glycosyl unit) points to a di-C-glucoside with a complex fragmentation pattern, combining the loss of fragments at *m/z* 18 (-H_2O), 90, 120, 210, and 240. The last four fragmentations are consistent with the loss of $(CH_2O)_3$ and $(CH_2O)_4$ fragments, or a combination of them, from the C-glycosyl units. Compound 1 was thus identified as apigenin 6,8-di-C-glucoside (vicenin-2). Compounds 2-4 were identified as O-glycosides of flavanones naringenin and hesperetin. The fragmentation of compound 2 (molecular ion at *m/z* 741) clearly showed the sequential loss of glycosyl units, *i.e.* -Glc (*m/z* 579), -Rha (*m/z* 433), -Glc (*m/z 271*), typical of naringenin-7-O-rutinoside-4'-O-glucoside.

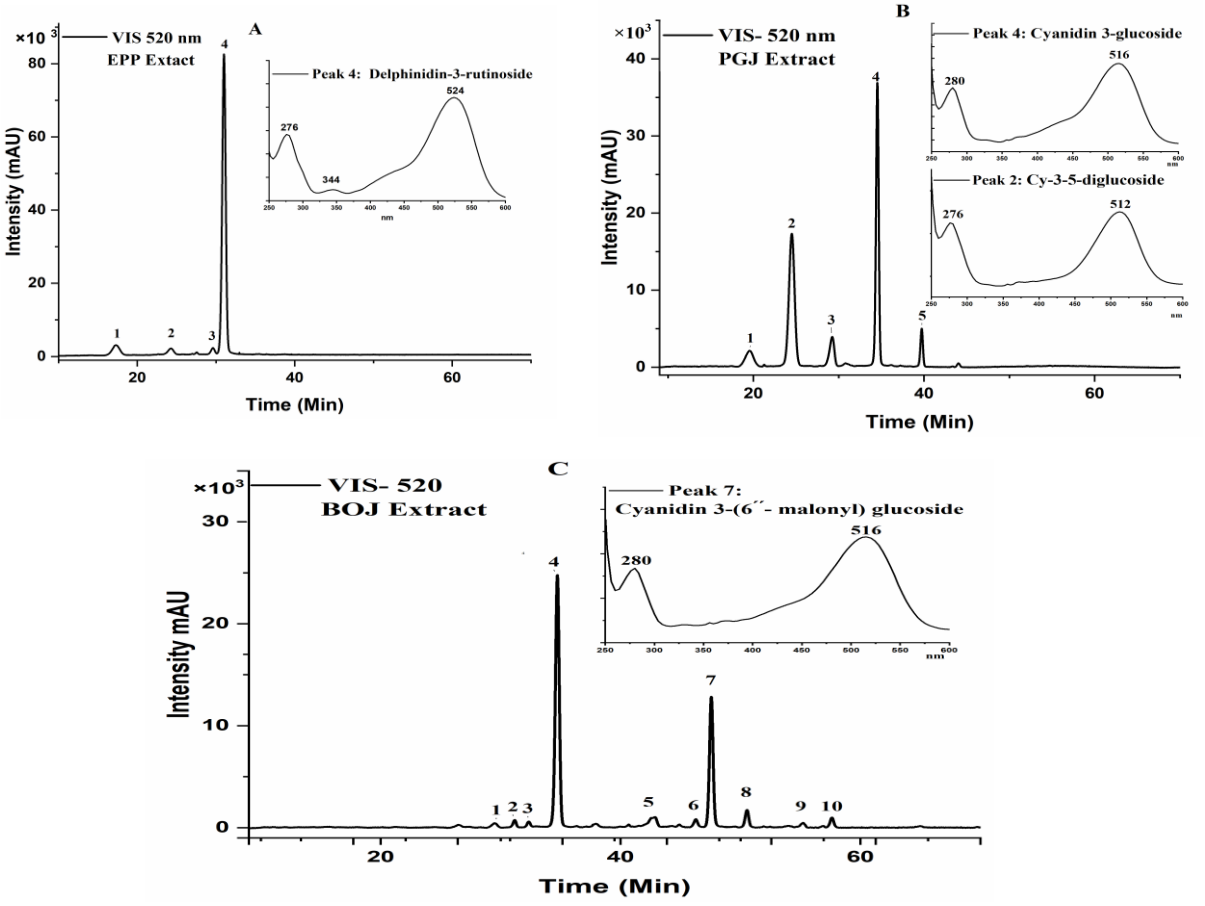

Figure 14. HPLC chromatograms showing the anthocyanin profiles of eggplant peel (A), pomegranate juice (B), and blood orange juice (C). Peak identification is provided in **Table 2**, and MS data for the major anthocyanins of each extract are given in **Appendix 3.**

Table 2. HPLC-DAD-MS Data and Putative Identification of Anthocyanins in the Different Extracts.

Peak	t_R (min)	λ_{max} (nm)	Full MS (*m/z*) a)	MS^2 (*m/z*)	MS^3(*m/z*)	Structure
Eggplant peel						
1	17.3	524, 276	773	611, 303, 465	611 → 303, 465	Delphinidin-3-O-rutinoside-5-O-galactoside
2	24.3	520, 280	773			Delphinidin-3-O-rutinoside-5-O-glucoside
3	29.6	524, 276	465, 303			Delphinidin-3-O-glucoside
4	31.0	524, 276 (344)	611	303, 465	303 → 257, 229, 285	Delphinidin-3-O-rutinoside*
Pomegranate juice						
1	19.6	520	627, 465, 303			Delphinidin-3,5-di-O-glucoside
2	24.5	512, 276	611	449, 287	449 → 287	Cyanidin-3,5-di-O-glucoside*
3	29.3	516, 272	465, 303			Delphinidin-3-O-glucoside
4	34.5	516, 280	449	287	287 → 213, 231, 259, 241, 189, 175, 137, 269, 149	Cyanidin-3-O-glucoside*
5	39.7	504	433, 271			Pelargonidin-3-O-glucoside
Blood orange juice						
1	29.5	528	465, 303			Delphinidin-3-O-glucoside
2	31.2	520	611, 287			Cyanidin-3-O-sophoroside
3	32.3	516	449, 287			Cyanidin-3-O-galactoside
4	34.7	516, 280	449	287	287 → 213, 231, 259, 241, 189, 175, 137, 269, 149, 203	Cyanidin-3-O-glucoside*
5	42.9	520	625, 301, 463			Peonidin-3,5-di-O-glucoside
6	46.3	512	593, 287			Cyanidin-3-O-dioxalylglucoside
7	47.6	516, 280	535	287	287 → 213, 231, 259, 241, 189, 175, 137, 269, 149	Cyanidin-3-O-(6˝-malonyl)glucoside*
8	50.6	520, 280	593, 287			Cyanidin-3-O-dioxaloylglucoside
9	55.2	520	549, 301			Peonidin-3-O-(6˝-malonyl)glucoside
10	57.6	520	679, 287			Cyanidin-3-O-(malonyl, dioxalyl)glucoside

a) Positive ESI, MS fragments are ranked according to decreasing intensity. * major pigment(s)

Table 3. HPLC-DAD-MS Data and Putative Identification of Copigments in the Different Extracts.

Peak	t_R (min)	λ_{max} (nm)	Full MS (*m/z*)	MS^2 (*m/z*)	MS^3 (*m/z*)	Structure
Eggplant peel a)						
1	37.3	280	474	222, 457, 165	222 → 165	N^1,N^8-Di-dihydrocaffeoylspermidine
2	40.6	288, 320	472	220, 310, 455, 163	220→ 163	N^1-Caffeoyl-N^8 -dihydrocaffeoylspermidine
3	42.7	288, 320	472	222, 310, 293, 455, 165	222 →165	N^1-Dihydrocaffeoyl-N^8-caffeoylspermidine
4	45.8	296, 320	470	308, 220, 453, 163, 291, 234	308→ 291, 220, 234	N^1,N^8-Dicaffeoylspermidine
Pomegranate juice b)						
1	24.8	264	783	765, 774, 689, 613	765→ 597, 613, 301, 275, 533, 427, 229	Pedunculagin I
Blood orange juice b)						
1	42.0	272, 336	593	473, 503, 353, 575, 383	473 → 353, 383	Apigenin-6,8-di-C-glucoside
2	45.5	284	777*	433, 741, 271, 579	433 → 271	Naringenin-7-O-rutinoside-4'-O-glucoside
3	66.6	284	579	271	271 → 151, 177, 165	Naringenin-7-O-neohesperidoside
4	72.8	284	609	301	301 → 286, 283, 242, 257, 199, 125	Hesperetin-7-O-neohesperidoside

a) Positive ESI, b) negative ESI. MS fragments are ranked according to decreasing intensity. * Undefined adduct (+36).

1.3. Radical scavenging activity

The reducing capacity of the anthocyanin-rich extracts was assessed through their ability to scavenge the stable radical DPPH (2,2-diphenyl-1-picrylhydrazyl). This assay, based on electron or hydrogen atom transfer to the radical species, is widely used as a rapid indicator of antioxidant capacity. Although it provides useful comparative data, it mainly reflects the reducing power of phenolics and should not be interpreted as a direct measure of antioxidant performance in vivo or in food matrices, where more complex mechanisms are involved **(Dangles et al., 2016; Dangles & Fenger, 2018)**.

Both crude and purified extracts demonstrated a strong capacity to neutralize DPPH radicals, confirming the important antioxidant potential of anthocyanin-rich matrices. Among the crude extracts, eggplant peel (EPP) exhibited the best activity, which can be related to its higher levels of both total anthocyanins (TAC) and total phenolics (TPC). The abundance of these compounds

likely provides more hydroxyl groups available for hydrogen or electron donation, thereby enhancing radical scavenging efficiency. Previous studies have confirmed the high antioxidant potential of these matrices through different methodologies, supporting our observations **(Gil et al., 2000; Riso et al., 2005; Zearah, 2024).**

After purification, the trend reversed: pomegranate juice (PGJ) exhibited the lowest IC_{50}, indicating the highest antioxidant activity, surpassing EPP. This can be attributed to two factors. First, purification enriched anthocyanins more in PGJ than in EPP, amplifying their contribution to antioxidant activity and explaining PGJ's higher efficacy despite the presence of delphinidin derivatives in EPP, which are structurally expected to be more active **(Zhao et al., 2014)**. Second, in crude extracts, interactions with other compounds, such as sugars, organic acids, or amino acids, can mask the intrinsic activity of anthocyanins, as previously reported by **de Oliveira et al. (2017)**, who showed that such interfering agents affect $DPPHEC_{50}$ measurements. By removing some of these compounds through purification, the true antioxidant potential of the anthocyanins becomes more apparent. Overall, the antioxidant activity followed the order: PGJ > EPP > BOJ **(Table 1).**

Overall, Extracts of common plant food were easily prepared, then enriched in anthocyanins. The characterization of the three plant extracts highlighted substantial differences in both anthocyanin composition and accompanying phenolic compounds. This diversity constitutes a valuable basis for exploring anthocyanin physico-chemistry under conditions that more closely reflect natural matrices. By combining pigments with their native copigments, these extracts provide an opportunity to assess not only the intrinsic reactivity of anthocyanins but also the potential role of copigmentation in enhancing their stability.

2. Susceptibility of Anthocyanins to Color Loss: Effect of Hydration, Heat, Metals, and Copigments

In this part, kinetic analyses were carried out and the thermodynamic constants of each extract were determined, thereby providing predictive parameters for estimating color and pigment loss. Since pH 5 represents the critical condition where color fading is most pronounced, complementary experiments were therefore performed to evaluate the influence of mild heat treatment and aluminum complexation on anthocyanin stability at this pH.

2.1. Reversible color loss in the extracts

Several pH jump experiments were conducted and the spectral changes in the visible region were monitored over time. By fitting the decay of the final visible absorbance as a function of pH, the p$K^{\wedge}_a$ value (pseudo-equilibrium connecting the flavylium ion and all neutral forms, except the *trans*-chalcone) was determined. Repeating the titration after a sufficiently long period to ensure complete equilibrium afforded the pK'_a value (including the *trans*-chalcone) **(Figure 15, Table 4).** As expected, the trend observed is pK'_a < p$K^{\wedge}_a$, but the differences are very small. It can thus be stated that the mole fraction of C_t at equilibrium is low (< 15%).

The pK'_a values can be compared with those of the literature for the main ACNs in the extract **(Leydet et al., 2012; Mazza & Brouillard, 1987)** *i.e.* delphinidin 3-O-glucoside for EPP (assuming close behavior to delphinidin 3-O-rutinoside, the actual major EPP ACN), cyanidin 3-O-glucoside and cyanidin 3,5-O-diglucoside for PGJ, and cyanidin 3-O-glucoside for BOJ (assuming close behavior to cyanidin 3-O-(6”-malonyl)glucoside, the other major BOJ ACN).

From **Table 4**, it is clear that the global acidity constant pK'_a mostly reflects the overall formation of the colorless forms ($K'_a >> K_a$, p$K'_a \approx$ pK'_h). and is thus a good measure of the sensitivity of a given extract to color loss through hydration. The pK'_a values indicate that the color of the BOJ and EPP extracts is more stable than that of PGJ, which is fully consistent with PGJ containing a high proportion of anthocyanidin 3,5-O-diglucoside, known to be much more prone to hydration than their 3-O-glucoside counterpart (a likely consequence of the electron-withdrawing effect of the additional Glc, which increases the electrophilic character of the flavylium ion) **(Seco et al., 2024).** This effect is obvious form the pK'_a difference between cyanidin 3,5-O-diglucoside and cyanidin 3-O-glucoside **(Table 4).** It is confirmed by the values of the

hydration rate constant k_h, the one of PGJ being higher by a factor 2-3 than those of BOJ and EPP. While it is satisfying to assign PGJ a pK'_a value that is intermediate between those of its two main ACNs, EPP and BOJ display higher pK'_a values than that of the main pure ACN they contain. This is a manifestation of intermolecular copigmentation within the extracts. Indeed, since hydroxycinnamic acids are recognized as potent ACN copigments **(Trouillas et al., 2016),** N,N-dicaffeoylspermidine amides are likely to interact rather strongly with the EPP anthocyanins and thus contribute to color stability by limiting hydration. This is also true for the flavones and flavanones of BOJ, but probably much less so for PGJ because ellagitannins are rather poor copigments **(Trouillas et al., 2016).**

Because of the competing thermodynamically favored hydration reaction, pK_a values are typically harder to accurately assess, requiring to monitor the apparent rate constant of hydration as a function of pH **(Figure 16).** However, the trend observed is that the extracts pK_a's tend to be higher than that of the main pure ACNs. This again could reflect copigmentation. Indeed, phenolic copigments usually interact more strongly with the flavylium ion than with the neutral base **(Trouillas et al., 2016)**, thus broadening the pH range of flavylium predominance.

From the pK'_a and pK_a values, the speciation diagrams for the colored forms AH^+ and A, and the complete pool of colorless forms B + Cc + Ct were plotted for each extract over the pH range 1-6 **(Figure 17).** They show that above pH 3, PGJ solutions are almost colorless, while EPP, and even more so BOJ, solutions still retain part of their color. This is confirmed by their visual appearance.

Table 4. Kinetic and thermodynamic data for the anthocyanin-rich extracts and a selection of pure anthocyanins for comparison. Major ACNs in extracts: D3R (EPP), C3G + C3,5diG (PGJ), C3G + C3MG (BOJ).

	EPP	**PGJ**	**BOJ**	**D3G⁑**	**C3G⁑**	**C3,5diG***
pK_a 1)	4.0 (± 0.1)	3.7 (± 0.2)	4.4 (± 0.1)	3.8	3.8	3.38
pK'_a 2)	2.75 (± 0.01)^a	2.41 (± 0.02)^b	2.85 (± 0.04)^a	2.6	2.5	2.08
p$K^\wedge_a$ 3)	2.76 (± 0.01)^b	2.47 (± 0.06)^c	2.93 (± 0.02)^a	-	-	-
pK'_h 4)	2.78	2.43	2.86	2.6	2.5	2.10
p$K^\wedge_h$ 5)	2.79 (2.73)	2.50 (2.16)	2.94 (3.13)	(2.5)	(2.5)	(2.23)
k_h (s^{-1})	0.11 (± 0.01)	0.25 (± 0.05)	0.08 (± 0.01)	0.09	0.11	-
k_{-h} (M^{-1} s^{-1})	58 (± 4)	36 (± 19)	106 (± 8)	30	31	-

* From Mazza & Brouillard, 1987. ⁑ From Leydet et al., 2012.

1) From the pH dependence of the hydration reaction, 2) titration at equilibrium, 3) titration at pseudo-equilibrium, 4) $K'_h = K'_a - K_a$, 5) $K^\wedge_h = K^\wedge_a - K_a$, values between parentheses: $K^\wedge_h = k_h/k_{-h}$. Values with letters are the means of two determinations with standard deviations. Different letters in the same line refer to significantly different data ($p < 0.05$). Other standard deviations are from the curve fitting experiments.

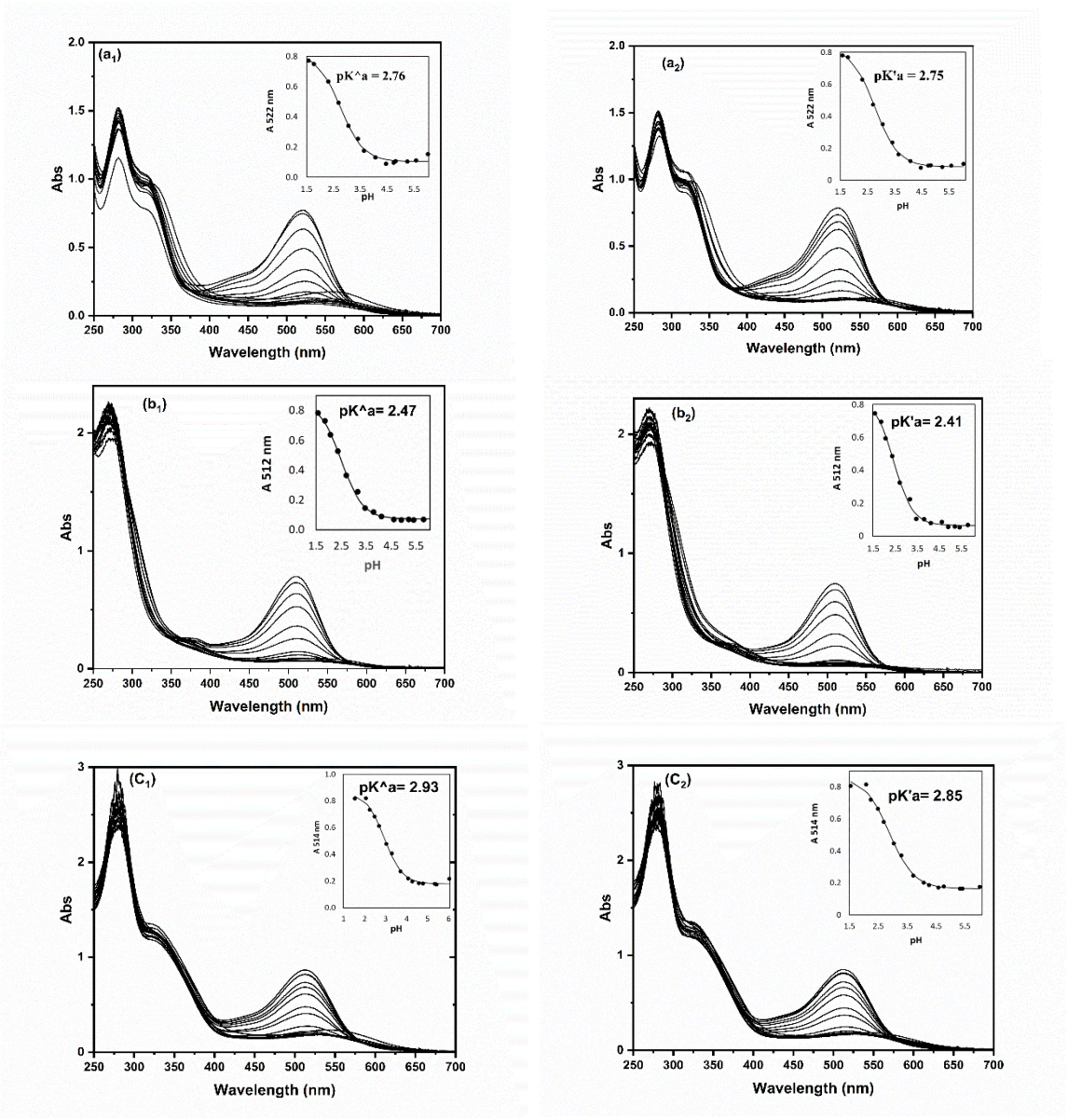

Figure 15. Spectral variations of anthocyanin-rich extracts after several direct pH jump in the range 2-6 at pseudo-equilibrium (left panel) and at equilibrium (right panel). Top: eggplant peel. Middle: pomegranate juice. Down: blood orange juice.

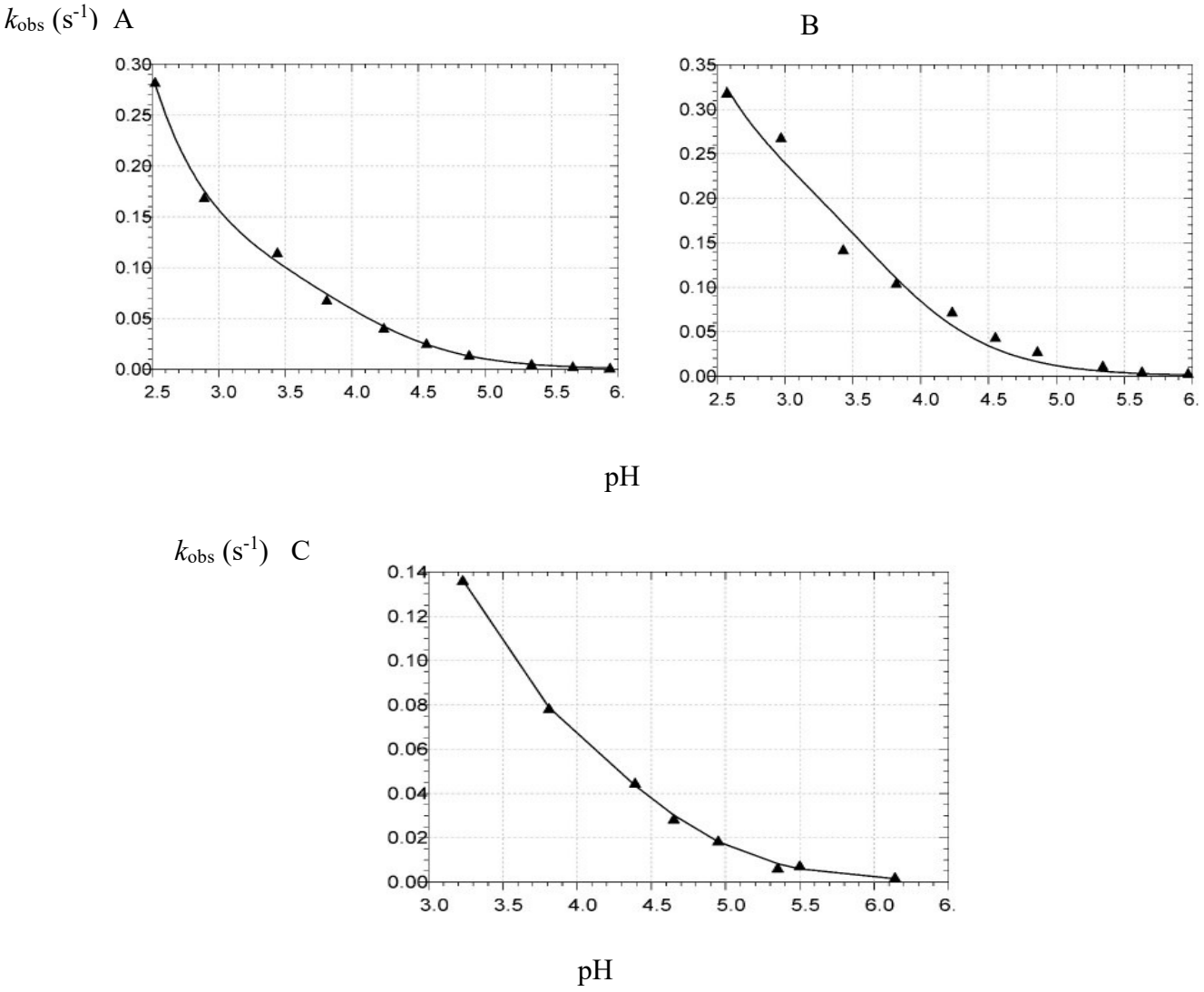

Figure 16. pH dependence of the apparent rate constant of water addition after pH jumps from pH 2 in aqueous solutions of anthocyanin-rich extracts. A: eggplant peel. B: pomegranate juice. C: blood orange juice.

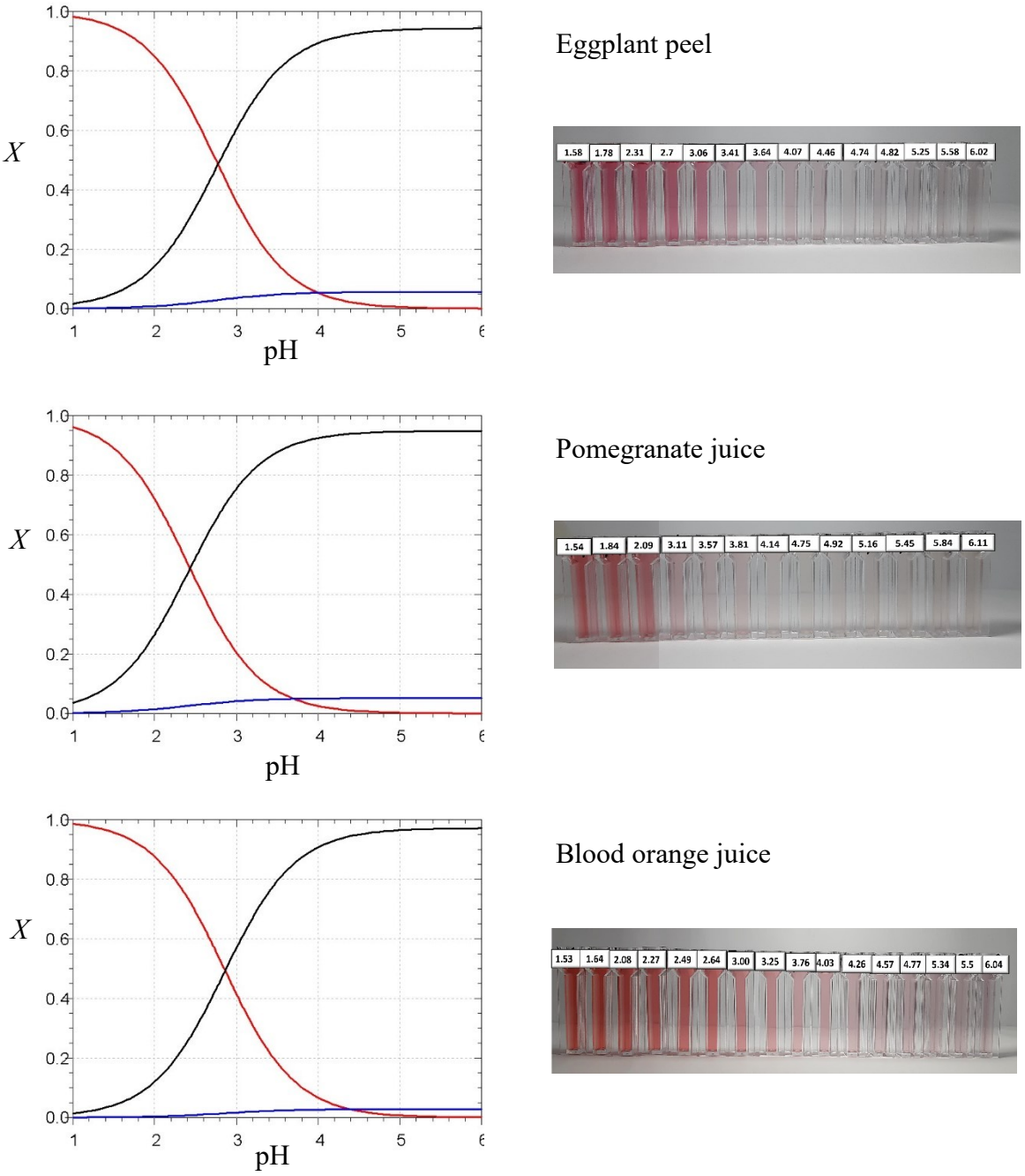

Figure 17. Left: molar fractions of flavylium ion (red), quinonoid base (blue) and the pool of colorless forms (black) as a function of pH. Right: residual color of the equilibrated solutions. Final ACN concentration in the solutions: 0.10, 0.11 and 0.18 mg/mL for the pomegranate, eggplant and blood orange extracts, resp.

2.2. Metal binding

As the main ACNs in the EPP, PGJ and BOJ extracts are cyanidin or delphinidin derivatives, they are expected to bind hard metal ions via their B-ring. Under mildly acidic conditions, this property is selective to the colored forms, as their B-ring protons are much more acidic than those of the colorless forms **(Yang et al., 2024),** and thus more easily displaced by the incoming metal ion. Hence, the hydration equilibrium is reversed to the profit of the colored forms and hyperchromism is observed. Within their metal complexes, ACNs adopt quinonoid structures that are resistant to water addition and also express distinct purple – blue colors **(Fenger et al., 2021b; Trouillas et al., 2016).** Overall, metal – ACN binding is a powerful mechanism to both stabilize and diversify ACN colors.

When Al^{3+} was added to equilibrated solutions of extract at pH 5, rapid bathochromic and hyperchromic shifts were observed **(Table 5).** This is evidence that the colored forms selectively bind Al^{3+}, thus reversing the hydration equilibrium, and that other extract's components, which could potentially compete with ACNs for Al^{3+}, do not prevent metal – ACN binding. While the Al^{3+}-induced bathochromic shifts (compared to free flavylium ion) were approximately the same (*ca*. 50 nm) for the three extracts, the hyperchromic shifts (expressed as color regenerated CR) varied with EPP and BOJ showing much higher CR values than PGJ **(Figure 18).**

The low CR for PGJ can be attributed to the presence of ellagitannins that probably compete with ACNs for Al^{3+}. By contrast, the N,N-dicaffeoylspermidine amides of EPP and BOJ flavonoids probably have less affinity for Al^{3+}. The highest percentage of color regenerated was achieved at a metal/ACN molar ratio of 2 in the three extracts studied. The strong influence of Al^{3+} on the color expressed in EPP is evident **(Figure 19),** as delphinidin glycosides (with their additional OH group in the B-ring), once bound to Al^{3+}, provide a nice blue color, while the Al^{3+} complexes of cyanidin glycosides in PGJ and BOJ remain purple.

Table 5. The potential of Al^{3+} binding for color regeneration from extracts at the hydration equilibrium. A_0: maximal visible absorbance before hydration (t = 0), A_{eq}: maximal visible absorbance at the hydration equilibrium, A_f: maximal visible absorbance after metal binding, RC: residual color at the hydration equilibrium, CR: color regenerated after metal binding. For EPP, A_0 and A_{eq} are measured at 548 nm, while A_f is measured at 572 nm. For PGJ and BOJ, A_0 and A_{eq} are measured at 536 nm, while A_f is measured at 562 nm.

Extract	A_0	A_{eq}	**RC (%)** a)	**Al^{3+} (equiv.)**	A_f	**CR (%)** b)
EPP	0.523 ± 0.035	0.111 ± 0.009	19.2 ± 1.0	2	0.759 ± 0.052	145.1 ± 0.4
	0.514 ± 0.016	0.113 ± 0.001	22.0 ± 0.8	1	0.657 ± 0.007	127.9 ± 2.6
	0.501 ± 0.002	0.119 ± 0.001	23.3 ± 0.2	0.5	0.657 ± 0.003	127.8 ± 0.2
PGJ	0.297 ± 0.006	0.049 ±0.006	16.7 ± 0.4	2	0.322 ± 0.029	108.9 ± 6.8
	0.304 ± 0.010	0.056 ± 0.000	18.4 ± 0.7	1	0.270 ± 0.005	89.1 ± 2.2
	0.304 ± 0.002	0.059 ± 0.003	19.2 ± 1.0	0.5	0.261 ± 0.007	85.8 ± 1.6
BOJ	0.475 ± 0.058	0.160 ± 0.006	34.1 ± 5.6	2	0.669 ± 0.031	141.4 ± 10.9
	0.471 ± 0.006	0.165 ± 0.006	35.1 ± 0.8	1	0.596 ± 0.014	125.1 ± 2.8
	0.521 ± 0.004	0.189 ± 0.005	36.4 ± 1.4	0.5	0.627 ± 0.004	120.5 ± 0.3

a) % RC= $100A_{eq}/A_0$, b) % CR=$100A_f/A_0$. CR values higher than 100% simply reflect ε_{max}(complex) > ε_{max}(free form).

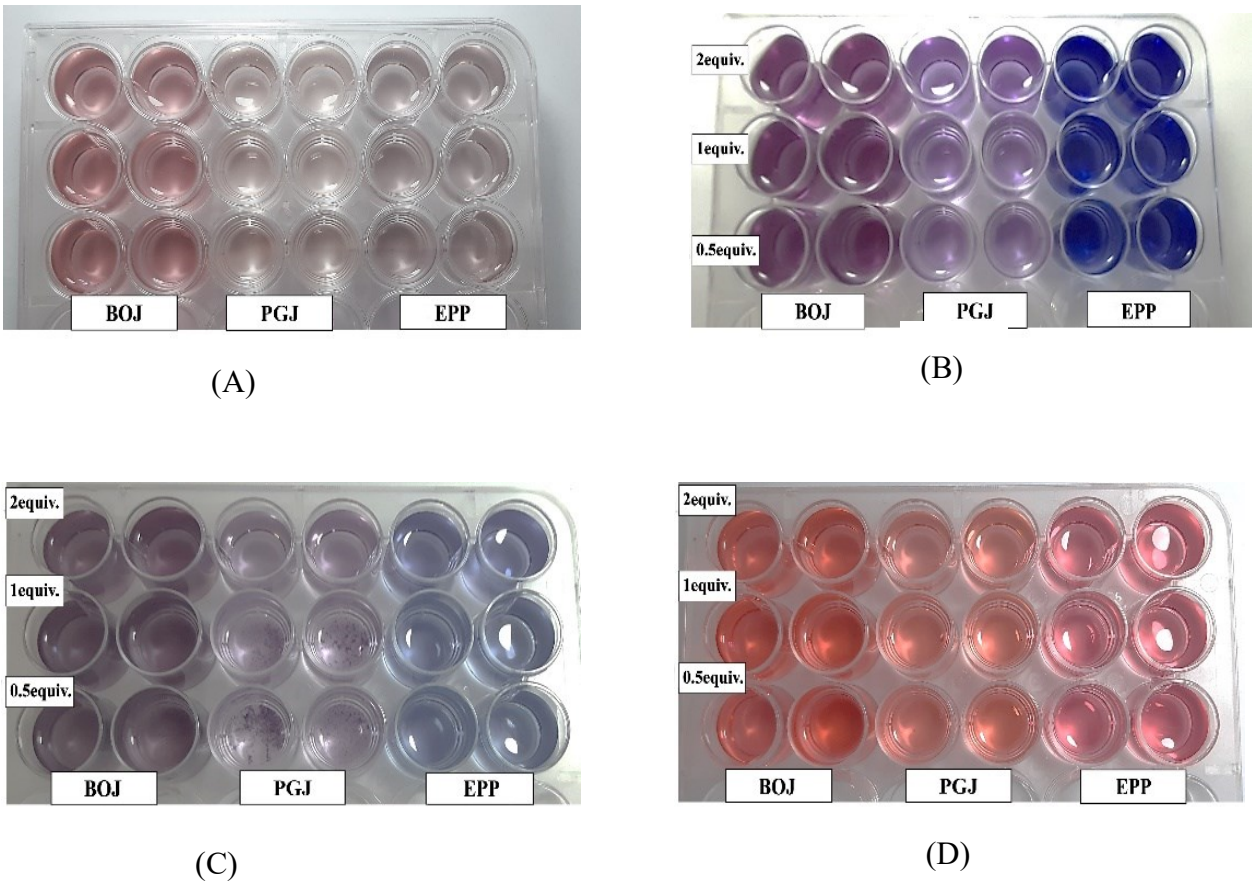

Figure 18. Solutions of anthocyanin-rich extracts. (A) Extracts at the hydration equilibrium (pH 5). (B) Extracts after Al^{3+} binding (pH 5). (C) Extracts supplemented with Al^{3+} after thermal treatment (50°C for 24 h, pH 5). (D) The same after acidification to pH 1.

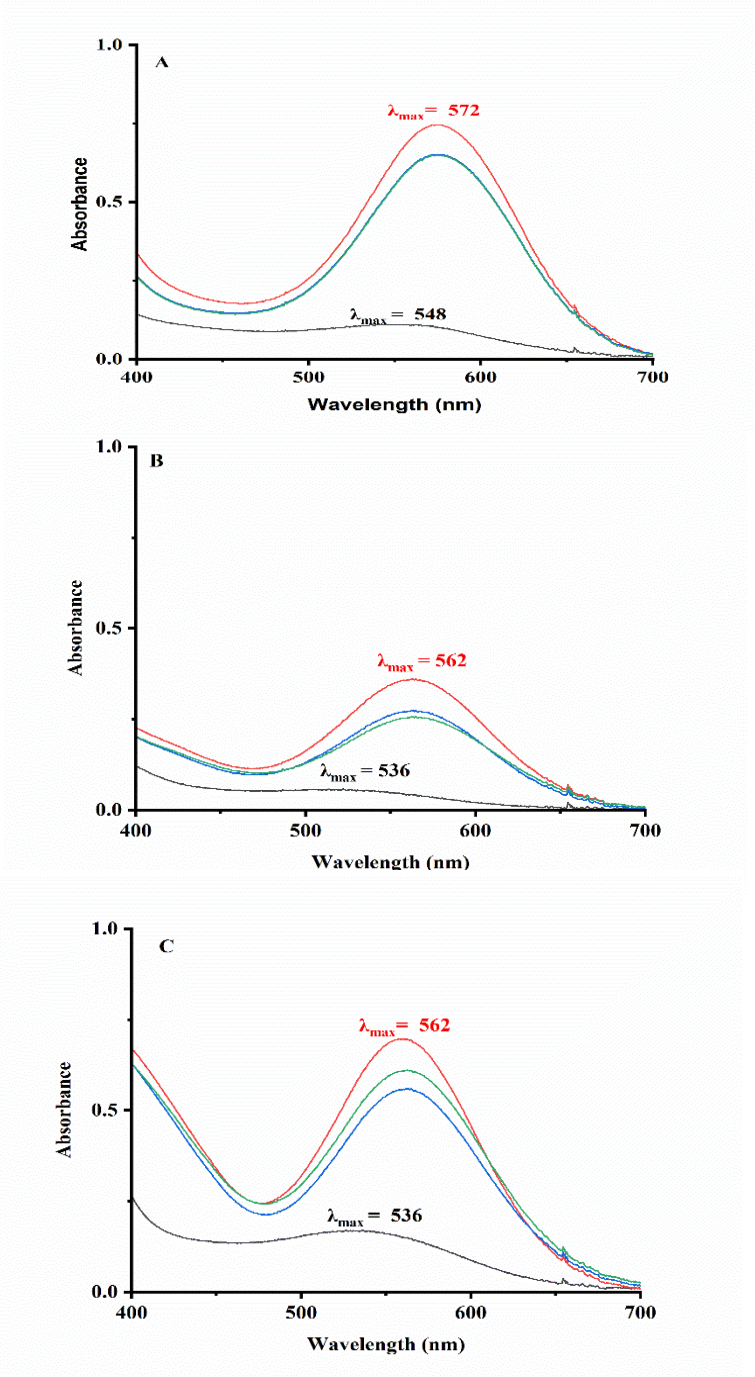

Figure 19. UV-visible spectra of eggplant peel (A), pomegranate juice (B), and blood orange juice (C) anthocyanins recorded at equilibrium at pH 5 (10 mM acetate buffer) for different Al^{3+}/ACN molar ratios: — (0), — (0.5), — (1), — (2).

2.3. Thermal degradation

The stability of the anthocyanin-rich extracts was evaluated at pH 5 and 50°C. Under such conditions, a fast color loss occurred during the first few minutes, mainly due to hydration and subsequent C-ring opening with accumulation of the *trans*-chalcone. Beyond *ca*. 30 min, the color loss was much slower and mainly assigned to degradation by a combination of autoxidation and hydrolysis. The residual color intensity followed the following ranking: BOJ > PGJ > EPP. Over longer heating periods (> 20h), the absorbance measurements gradually became blurred by browning and light scattering featuring precipitation, especially with EPP and PGJ, as evidenced by their higher browning index at 24h **(Table 6).**

No such problems occurred after acidification of samples to pH 1, so as to convert all residual ACN forms to the flavylium ion for the assessment of the total pigment loss **(Fenger et al., 2019)**, which was then plotted *vs*. time to assess the pigments' half-life **(Figure 20)**. Blood orange juice emerged as the most stable one, boasting a half-life ($t_{1/2}$) of *ca*. 90h. Pomegranate juice followed with $t_{1/2}$ = 60h, while eggplant peel showed the lowest stability with $t_{1/2}$ = 18h.

Previous studies have shown that the thermal degradation of purified and non-purified anthocyanins is faster when temperature and pH increase **(Nayak et al., 2011; Patras et al., 2010).** For example, the half-life of purified C3G at pH 3 is *ca*. 126, 81 and 66 min at 50, 70 and 90°C, respectively. However, it is greatly prolonged in the presence of different phenolic copigments in large excess (100 equiv.): 321, 258, and 209 min for ferulic acid, 279, 204, and 150 min for dopamine, and 326, 296, and 261 min for (+)-catechin. **(Kanha et al., 2019)** In our extracts, the favorable effect of intermolecular copigmentation is also manifested. For instance, BOJ, the most stable extract, contain flavonoids, especially flavones, whose flat tricyclic nuclei are particularly suitable to develop strong -stacking interactions with ACNs (Trouillas et al., 2016). Under acidic conditions, the *trans*-chalcone is the most vulnerable ACN form.**(Cruz et al., 2022; Sadilova et al., 2007)** Indeed, the rate-limiting hydrolysis of its 3-O-glycosyl group releases an electron-rich enol group highly sensitive to autoxidation. Hence, strong π-stacking interactions between flavonoids and the ACN colored forms are expected to limit water addition (as evidenced by the significantly higher pK'a value for BOJ, compared to its main ACN C3G, **Table 6**) and subsequent *trans*-chalcone accumulation, thereby also limiting thermal degradation. Cao et al. **(2009)** studied the thermal degradation of cyanidin 3-(6''-malonyl) glucoside (C3MG) and cyanidin 3-glucoside

(C3G), the two main BOJ ACNs, at pH 3.5.During the first hours of heating, HPLC-MS analysis revealed that C3MG was hydrolyzed to C3G, which tended to accumulate, suggesting that its degradation was slower than its formation from C3MG.

Unlike flavones and flavonols, ellagitannins are only modest copigments and their impact on the thermal stability of PGJ ACNs may be negligible. Moreover, PGJ is rich in C3,5DG and anthocyanidin 3,5-O-diglucosides, which are known to be less thermally stable than their 3-O-glucoside homologs, a likely consequence of the former being more sensitive to water addition than the latter **(Seco et al., 2024)**. Indeed, at pH 3.5, the colorless species were the first intermediates in the degradation pathway **(Kanha et al., 2019)**.In addition, bulky ACNs (*e.g.*, di- and triglucosides) form less stable copigmentation complexes than monoglucosides **(Trouillas et al., 2016).**

The faster degradation of EPP anthocyanins might reflect their higher sensitivity to autoxidation due to the presence of caffeoyl derivatives in the extract. Indeed, although the caffeoyl residues of acylated ACNs are effective in slowing down color loss by hydration (intramolecular copigmentation), their redox activity can, on the other hand, accelerate the thermal degradation **(Fenger et al., 2021a)**. This was confirmed by adding caffeic acid to ACN solutions before heating. In this study, new pigments were detected resulting from the coupling between the nucleophilic A-ring of anthocyanins and the electrophilic *o*-quinone derived from the caffeoyl residues or free caffeic acid by autoxidation.

Anthocyanins are largely unstable during thermal processes, such as steaming, boiling, and microwave heating, when temperature reaches 100°C **(Zhang et al., 2020)**. Phenolic acids from B-ring (C2-C3 cleavage) and phloroglucinaldehyde from A-ring (C3-C4 cleavage) were the two main degradation compounds identified **(Sadilova et al., 2007).** Anthocyanins in solid food were more stable than in beverages, showing the importance of water activity in the degradation. A high content in dietary fiber also tends to increase ACN stability. For solid food, steaming was a better way to retain ACNs than boiling, while the opposite was observed with beverages **(Zhang et al., 2020).**

Precipitation occurred in the PGJ and BOJ extracts supplemented with 0.5 or 1 equiv. of Al^{3+}. Hence, the influence of metal binding was quantified with 2 equiv. of Al^{3+}. Overall, color stability during heating at pH 5 was significantly improved, especially with PGJ and BOJ **(Table 6, Figure 5).** This improvement is largely due to the quinonoid structure of the metal complexes, which does

not undergo water addition **(Denish et al., 2021; Fenger, et al., 2021b)** However, with PGJ and EPP, the extent of pigment loss remains high, meaning that the metal complexes remain vulnerable to autoxidation. With BOJ, the metal complexes are more resistant to degradation and the relatively modest color loss observed is thus largely due to the gradual dissociation of the metal complexes with subsequent hydration of the free ACNs.

Table 6. Color loss and pigment loss in solutions of anthocyanin-rich extracts with or without supplementation with Al^{3+} (2 equiv.) after 24h at pH 5 and 50°C.

No added metal ion	X_{color}	**% Color loss**	$X_{pigment}$	**% Pigment loss**	**BI** a)
EPP	0.32 ± 0.02	68 ± 2	0.45 ± 0.02	55 ± 2	1.9 ± 0.10
PGJ	0.41 ± 0.02	59 ± 2	0.76 ± 0.05	24 ± 5	2.13 ± 0.03
BOJ	0.57 ± 0.05	43 ± 5	0.73 ± 0.02	27 ± 2	1.00 ± 0.03
Al^{3+} (2 equiv.)	X_{color}	**% Color loss**	$X_{pigment}$	**% Pigment loss**	**-**
EPP	0.50 ± 0.01	50 ± 1	0.57 ± 0.01	43 ± 1	-
PGJ	0.59 ± 0.01	41 ± 1	0.59 ± 0.01	41 ± 1	-
BOJ	0.67 ± 0.02	33 ± 2	0.84 ± 0.01	16 ± 1	-

a) Browning index, defined as A(420 nm) / A(λ_{max} visible).

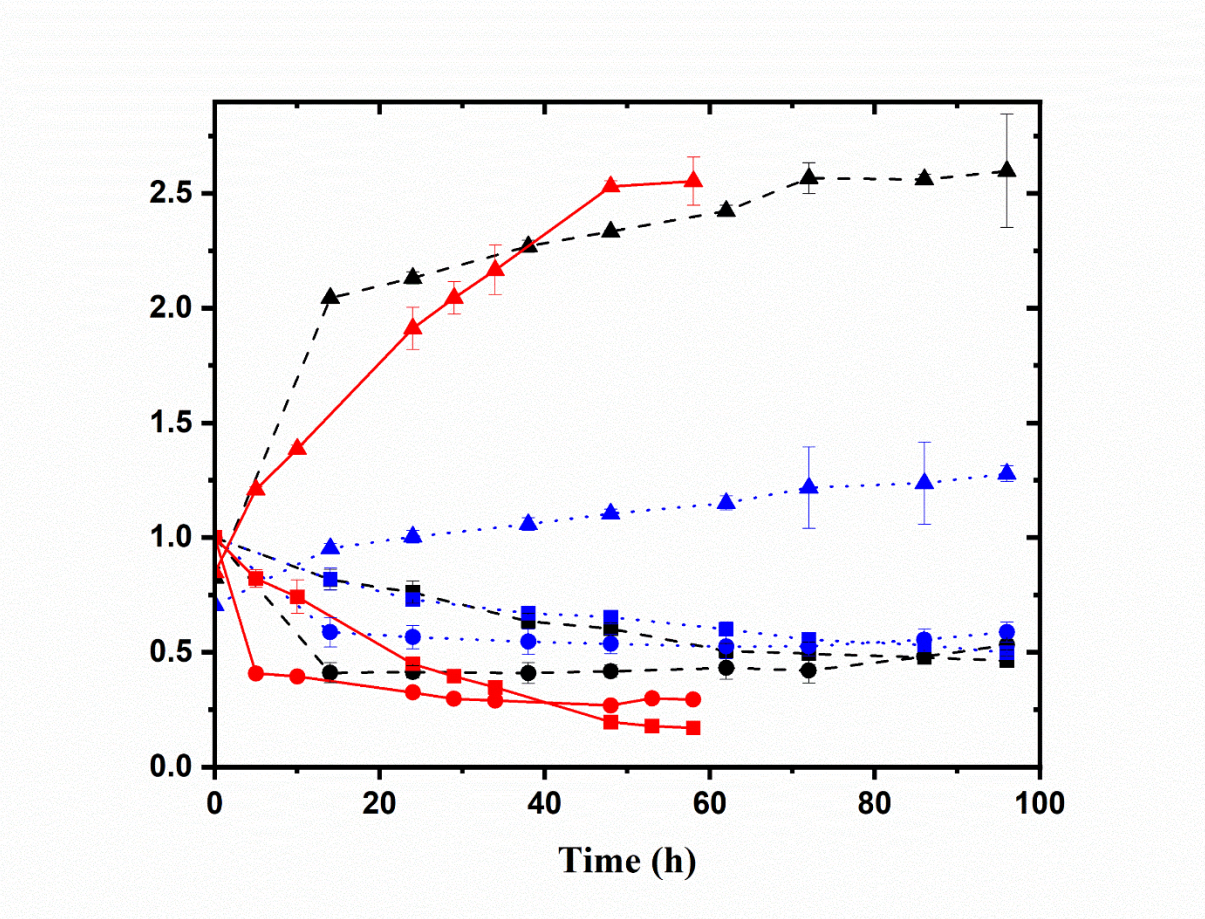

Figure 20. Color loss (●), pigment loss (■), and browning index (▲) in anthocyanin-rich extracts at pH 5 and 50°C as a function of time: — (EPP), - - - (PGJ), ... (BOJ). Error bars represent the standard deviation calculated from duplicate measurements.

Overall, among the three extracts studied, the anthocyanins from blood orange juice appear most promising as food colorings, being less sensitive to water addition and capable of forming stable metal complexes. This improvement may be assigned to the endogenous flavonoids through their capacity to develop π-stacking interactions with ACNs and their metal complexes (intermolecular copigmentation).

3. Stability of Anthocyanin-Rich Extracts via Alginate–Pectin Encapsulation

In order to better approximate food-like environments, the anthocyanin-based extracts obtained in this work were encapsulated within alginate–pectin hydrogel beads, which provided a suitable model system to assess their stability under semi-solid conditions while simultaneously exploring the interactions between the pigments and the encapsulating polymers.

3.1. Encapsulation efficiency of ACNs

Hydrogel beads formation occur when alginate or alginate-pectin droplets containing ACNs comes in contact with the $CaCl_2$ bath solution **(Figure 21).** During gel formation and curing steps, ACNs loss from droplets first and then from particles during the 30 min of the curing process **(Guo et al., 2018)**.

After bead formation, two methods are used to evaluate the encapsulation efficiency. The first method consists of quantifying the anthocyanins retained within the gel matrix by inducing their release through acidic dissociation of the beads in a hydrochloric acid solution (10^{-1} M, pH 1). The second involves estimating anthocyanin loss by analyzing the filtrate collected after the curing step. Method 1, based on the direct analysis of the beads, systematically produced lower encapsulation values than Method 2, which relies on filtrate analysis **(Figure 22).** Method 1 is based on the assumption of complete release of anthocyanins after immersion of the beads in a 0.1 M HCl solution, which is not always verified, especially in the case of beads complexed with metal ions. Indeed, anthocyanin release is slow and can extend over several hours. This behavior is clearly illustrated by the EPP-Al^{3+} beads at pH 5, which remain visibly colored even after 24 hours of immersion in the acidic solution. This behavior is likely due to the protonation of carboxylate groups in acidic media, resulting in the release of Ca^{2+} ions and a modification of the gel network structure, without causing full disintegration of the hydrogel. This also suggests the possible establishment of an equilibrium between the residual anthocyanin concentration within the beads and that in the surrounding release medium, preventing complete release of the pigment.

This partial retention leads to an underestimation of the encapsulation yield, particularly for matrices that are more cross-linked or strengthened by ionic interactions. In this context, Method 2 is considered more reliable, despite being indirect, as it allows for a more representative estimation of the amount of anthocyanins retained in the encapsulating matrix.

The results also indicate a slightly higher encapsulation efficiency in all alginate–pectin formulations, whose structure is more rigid than that of beads made with alginate alone. It has been reported that the addition of other polysaccharides (pectin, cellulose derivatives, and chitosan) to alginate improves the encapsulation of polyphenols by modifying the porous structure of alginate, thereby enabling the entrapment of compounds with lower molecular weight. The combination of alginate and pectin with proteins or cellulose derivatives also enhances polyphenol encapsulation by reducing the effective diffusivity through the alginate hydrogel microstructure, where the additional components act as a solid barrier that hinders the transport of compounds from the beads to the surrounding medium **(Ćorković et al., 2021; Kiaei Pour et al., 2020; Singh et al., 2018).**

This trend was observed at both tested pH levels.

Encapsulation efficiency at pH 5 was generally higher than at pH 4, which can be attributed to the increased ionization of the biopolymers at pH 5. This enhances electrostatic interactions between anthocyanins and the carboxyl groups of the polysaccharides **(Cao et al., 2020; Shi et al., 2024)**. However, exceptions were observed for PGJ-A^G (pH 4: 56.4 % vs. pH 5: 53.1 %) and EPP-A^G (pH 4: 50.0 ± 0.5% vs. pH 5: 42.4 ± 0.4%), where higher efficiencies were recorded at pH 4. Finally, anthocyanins complexed with metal ions showed significantly higher encapsulation yields than non-complexed forms, particularly at pH 5, where quinoidal base forms readily coordinate with metal ions to generate stable complexes **(Cai et al., 2022).** During bead formation, Ca^{2+} crosslinked the polysaccharide network, while Al^{3+} selectively bound anthocyanins, with complexation occurring concomitantly with gelation. This dual interaction stabilized anthocyanin chromophores and reinforced the hydrogel matrix, thereby enhancing pigment retention and limiting losses by diffusion. The highest encapsulation yields were obtained for the pH 5 alginate-pectin-aluminum beads containing EPP (EE = 82.1 ± 0.4%) or PGJ (EE = 74.0 ± 0.2%).

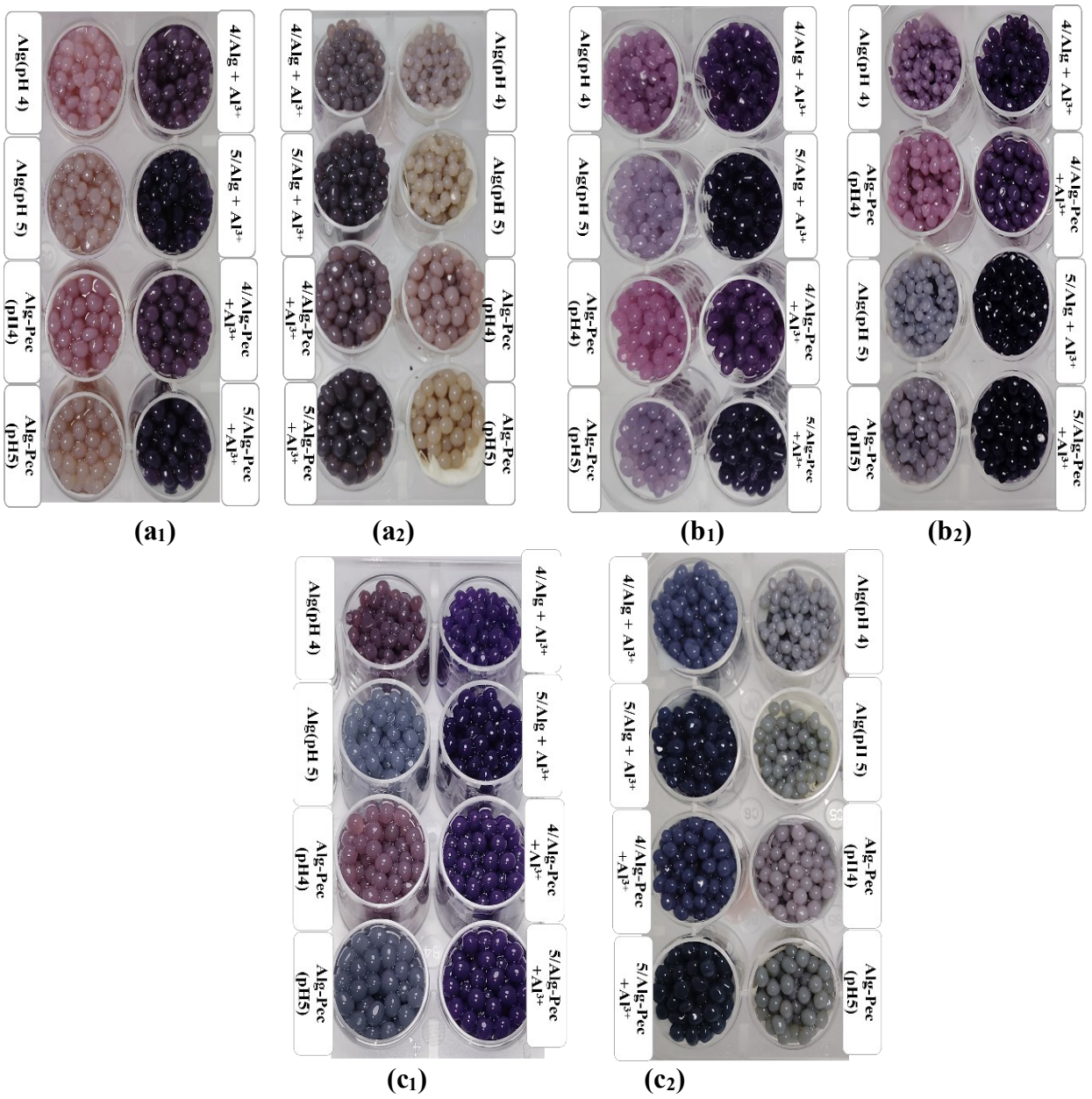

Figure 21. Hydrogel beads using different formulations (pH 4 and 5, ± pectin, ± Al^{3+}): a_1–a_2 with PGJ extract (0 h and 48 h thermal treatment at 50 °C, respectively), b_1–b_2 with BOJ extract, and c_1–c_2 with EPP extract. Alg : alginate, Pec: Pectin.

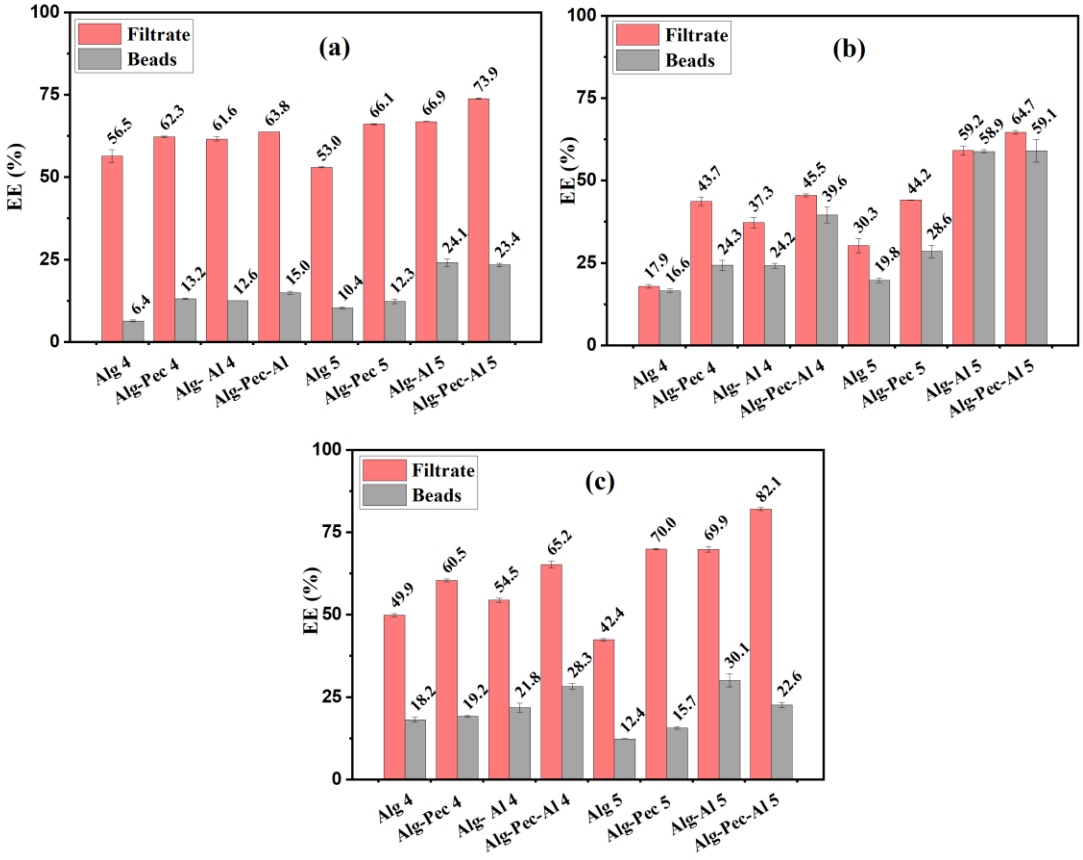

Figure 22. Encapsulation efficiency of anthocyanins determined by two methods: (1) quantification of non-encapsulated anthocyanins in the $CaCl_2$ bath (filtrate, red bars), and (2) acidic dissociation of beads (grey bars). (a) PGJ, (b) BOJ, and (c) EPP extracts. Alg : alginate, Pec: pectin

3.2. Effect of ACN botanical source

At pH 4–5, alginate and alginate–pectin blends carry a net negative charge due to deprotonation of their carboxyl groups (pKa ≈ 3.4–3.6) **(Kopač et al., 2021; Menegatti et al., 2024)**. At pH 4 more than 50% of the carboxyl groups are already ionized, and at pH 5 the percentage of anionic form is at least 95%. Pectin, rich in galacturonic acid, shows a similar pKa, giving the blend an even higher negative charge density **(Said et al., 2023)**. This was proposed to favor electrostatic attraction with anthocyanins under the cationic flavylium form, thereby improving their retention in the gel matrix **(Liudvinaviciute et al., 2020)**.

However, under the moderately acidic pH conditions used in this study (pH 4 or 5), the flavylium form of anthocyanins is not predominant (see diagram distribution determined for each extract on the **section 2.1, Figure 17**). Instead, anthocyanins exist primarily as neutral species such as hemiketals, quinoidal bases, and chalcones, which reduces the extent of strong (ionic) electrostatic interactions with anionic polysaccharides like alginate and pectin. Hence, other non-covalent interactions, including hydrogen bonding and van der Waals interactions, probably play a major role in pigment retention. Additionally, physical entrapment in the gel matrix and copigmentation phenomena may also contribute to anthocyanin stabilization **(Tan et al., 2021)**.

A comparison of EE (%) among the three matrices across the different formulations is presented in **Figure 23**, and the main finding are as follow:

Encapsulation efficiencies were consistently lower for BOJ than for PGJ and EPP. This may be another manifestation of intermolecular copigmentation within the extract. Preferential interactions between BOJ flavones and flavanones on the one hand, and the anthocyanin pigments on the other hand, could have limited their encapsulation, an effect particularly evident in BOJ–alginate formulations at pH 4 and 5, where efficiencies reached only 17.9% and 30.3%, respectively. Such results suggest either retention of ACNs in solution as copigmentation complexes, or competitive encapsulation of phenolic copigments at the expense of anthocyanins. In contrast, in PGJ, the weaker pigment–copigment competition (ellagitannins are modest and bulky copigments) favored pigment–polymer interactions, leading to higher anthocyanin retention. Ćorković et al. **(2021)** reported that, in addition to cyanidin glycosides, phenolic acids (chlorogenic and neochlorogenic acid) and flavonols (quercetin, rutin, hyperoside) were efficiently encapsulated within alginate–pectin hydrogel beads produced from chokeberry juice. The incorporation of pectin into the wall material enhanced the entrapment of specific polyphenols, which was attributed to additional stabilization mechanisms involving hydrogen bonding and van der Waals interactions with the polysaccharide matrix. Such a co-encapsulation not only supports the structural stabilization of anthocyanins through copigmentation but also broadens the functional potential of the beads by retaining a wider spectrum of bioactive compounds.

EPP, exhibited efficiencies comparable to PGJ, most likely due to delphinidin-3-O-rutinoside, whose additional hydroxyl group on the B-ring reinforces hydrogen bonding with alginate–pectin. Indeed, previous studies have demonstrated that anthocyanins with a greater number of hydroxyl

groups on the B-ring (e.g., delphinidin-3-glucoside with a pyrogallol group) form stronger hydrogen bonds with pectin, compared to cyanidin or malvidin derivatives, while methoxy substitutions tend to weaken such interactions **(Fernandes et al., 2014; Koh et al., 2020; Lin et al., 2016).** Moreover, the nature of the glycosidic moiety also influences binding, with glucose or galactose promoting stronger affinity than pentose sugars **(Shi et al., 2024)**.

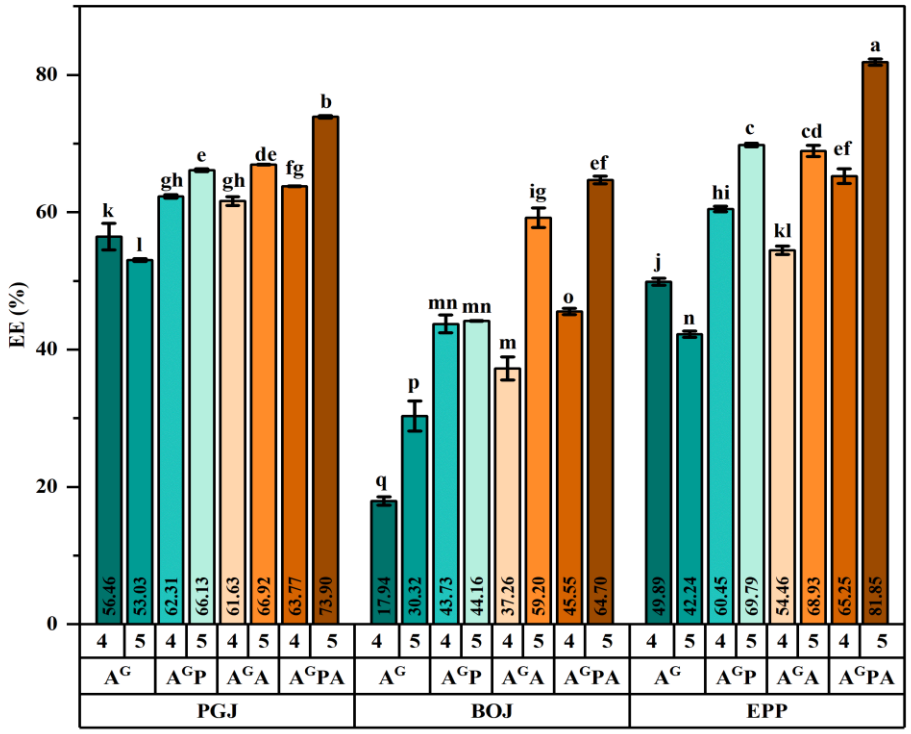

Figure 23. Effect of pH, Al^{3+} and/or pectin on pigment retention determined by method two. Data are presented as mean ± SD. Statistical significance was assessed using three-way ANOVA followed by Tukey's HSD post hoc test ($p < 0.05$). Means not sharing the same letter are significantly different. (A^G: alginate, A^GP: alginate-pectin, A^GA: alginate-Al^{3+}, A^GPA: alginate-pectin-Al^{3+}).

Statistical analysis of encapsulation efficiency (EE %), calculated by the indirect method from filtrate measurements, showed that pH, Al^{3+} and/or pectin had significant effects ($p < 0.05$). In addition, significant three-way interactions were observed, highlighting the decisive role of the combined influence of these factors on EE **(Figure 23).**

3.3. Bead characteristics

Regardless of pH, pectin content and presence of metal ions (Al^{3+}), the water content of the beads was found to range between 93% and 97% **(Appendix 6).** These values are consistent with previous findings reported for anthocyanin-containing microcapsules **(Mohammadalinejhad et al., 2023; Silva et al., 2023)**. This high water content, combined with good encapsulation efficiency, indicates that anthocyanins, entrapped within the gel matrix during bead formation, remain in a highly hydrated environment that promotes their homogeneous dispersion **(Cheng et al., 2023)**. As a result, uniform coloration in purple to bluish tones is observed **(Figure 21).** This high moisture is largely attributed to the intrinsic properties of pectin and alginate, two biopolymers well known for their high water absorption and retention capacity, which contributes to the hydration and structural stability of the gel matrix **(Menegatti et al., 2024)**.

Colorimetric analysis based on CIELAB parameters **(Table 7, Figure 24)** was performed to assess color differences and stability among the formulated beads. At initial conditions (t_0, no heating, lines 1 in **Table 7**), the chromatic attributes of the beads varied significantly, depending on anthocyanin-rich extract, pH and presence of Al^{3+} ions. In terms of CIELAB coordinates, the following points can be highlighted:

- At pH 4, the color differences observed between extracts were clearly linked to their specific anthocyanin profiles. The PGJ-based extract exhibited moderate a* values (11.5–12.2) and slightly positive b* values (3–5), corresponding to a reddish-orange hue ($H^{\circ} \approx 18–23$) of low saturation. The BOJ extract, with higher a* values (12–18) and negative b* values (≈ –10), showed a shift toward a more violet-toned red (h ≈ 320–328). In contrast, the EPP extract displayed more negative b* values (–14.5 to –11) and hue angles around 300°, indicating a bluish-violet coloration.

These results are fully consistent with the anthocyanin profile of each extract and their respective pH-dependent behavior (**See section 2.1**).

Table 7. Colorimetric parameters of gel beads: upper row = before heating, lower row = after heating at 50 °C for 48 h.

matrix	pH	beads	L^*	a^*	b^*	C^*	Hab	ΔE
PGJ	4	A^G	43.2 ± 0.1^{a}	12.2 ± 0.2^{d}	$5.1 \pm 0.3^{b,c}$	$13.2 \pm 0.3^{n,o}$	22.7 ± 0.7^{l}	8.6
			39.9 ± 1.6	7.0 ± 0.9	-1.0 ± 0.02	7.1± 0.5	349.7 ± 4.6	
		A^GP	40.2 ± 1.1^{b}	$11.5 \pm 0.2^{d,e}$	3.5 ± 0.2^{c}	$12.1 \pm 0.7^{h,n,o}$	17.9 ± 1.6^{l}	4.1
			38.1 ± 1.7	8.6 ± 0.2	1.5 ± 0.08	8.8 ± 0.7	9.9 ± 0.7	
		A^GA	23.3 ± 1.1^{f}	8.6 ± 0.5^{f}	-10.1 ± 0.3^{d}	$12.9 \pm 0.3^{n,o}$	310.3 ± 1.2^{c}	8.9
			19.6 ± 0.5	1.6 ± 0.1	-6.0 ± 0.1	6.2 ± 0.1	284.9 ± 1.1	
		A^GPA	$19.0 \pm 0.2^{g,h}$	$7.7 \pm 0.4^{f,g}$	$-10.5 \pm 0.3^{d,e}$	$12.9 \pm 0.6^{n,o}$	$304.1 \pm 3.5^{d,e}$	7.6
			24.3 ± 0.4	5.5 ± 0.4	-5.6 ± 0.1	7.3 ± 0.6	311.7 ± 5.3	
	5	A^G	$42.6 \pm 0.7^{a,b}$	$4.6 \pm 0.4^{i,j}$	$6.3 \pm 0.3^{a,b}$	7.8 ± 0.3^{p}	53.6 ± 0.5^{k}	2.4
			44.1 ± 1.4	3.9 ± 0.3	4.5 ± 0.4	6.0 ± 0.5	49.1 ± 2.6	
		A^GP	36.4 ± 0.1^{c}	$5.8 \pm 0.3^{h,i}$	8.2 ± 0.1^{a}	$10.0 \pm 0.3^{l,o,p}$	54.9 ± 0.6^{k}	2.7
			38.5 ± 0.5	6.3 ± 0.3	9.7 ± 0.3	11.6 ± 0.3	57.0 ± 0.9	
		A^GA	$8.0 \pm 0.5^{j,k}$	4.2 ± 0.2^{j}	$-12.2 \pm 0.6^{e,f,g}$	$12.9 \pm 0.6^{n,o}$	289.4 ± 0.4^{f}	13.9
			18.7 ± 0.4	2.4 ± 0.1	-3.5 ± 0.3	4.2 ± 0.2	304.8 ± 5.2	
		A^GPA	8.8 ± 0.1^{j}	$4.9 \pm 0.4^{i,j}$	$-13.6 \pm 0.1^{g,h,i}$	$14.5 \pm 0.1^{j,k,m,n}$	289.8 ± 1.2^{f}	13.0
			16.0 ± 0.1	1.5 ± 0.1	-3.3 ± 0.1	3.6 ± 0.3	293.8 ± 0.8	
BOJ	4	A^G	28.0 ± 0.3^{e}	12.1 ± 0.2^{d}	-10.0 ± 0.4^{d}	$15.7 \pm 0.4^{i,j,k,m,n}$	320.5 ± 0.7^{b}	8.1
			20.0 ± 0.4	10.8 ± 0.2	-10.6 ± 0.4	15.2 ± 0.6	315.5 ± 0.7	
		A^GP	31.0 ± 0.3^{d}	18.4 ± 0.4^{a}	$-11.3 \pm 0.3^{d,e,f}$	$21.9 \pm 0.1^{c,d}$	328.6 ± 0.1^{a}	6.1
			34.0 ± 0.1	16.6 ± 0.7	-6.3 ± 0.3	17.8± 2.4	339.2 ± 8.3	
		A^GA	$8.2 \pm 0.1^{j,k}$	14.2 ± 0.1^{c}	$-12.7 \pm 0.1^{f,g,h}$	$19.1 \pm 0.3^{d,e,f}$	$318.1 \pm 3.6^{a,b}$	4.2
			9.9 ± 0.6	11.0 ± 0.5	-14.8 ± 0.6	16.7± 1.0	297.8 ± 0.6	
		A^GPA	11.4 ± 0.1^{i}	16.8 ± 0.1^{b}	$-15.7 \pm 0.1^{j,k,l}$	23.0 ± 0.2^{c}	317.1 ± 0.5^{b}	4.7
			14.6 ± 0.6	13.9 ± 1.7	-13.9 ± 0.5	17.7 ± 0.8	308.2 ± 0.2	
	5	A^G	33.3 ± 0.2^{d}	8.4 ± 0.1^{f}	$-11.5 \pm 0.4^{d,e,f}$	$14.2 \pm 0.4^{k,m,n}$	$306.3 \pm 0.7^{c,d,e}$	7.7
			30.0 ± 0.5	2.5 ± 0.1	-8.0 ± 0.1	8.3 ± 0.1	287.4 ± 0.5	
		A^GP	31.9 ± 1.2^{d}	$8.0 \pm 0.2^{f,g}$	$-11.1 \pm 0.2^{d,e,f}$	$13.9 \pm 0.4^{k,m,n}$	$307.2 \pm 1.1^{c,d}$	6.7
			29.9 ± 0.7	3.8 ± 0.1	-6.3 ± 0.3	7.4 ± 0.1	300.5 ± 0.6	
		A^GA	5.3 ± 0.2^{l}	$4.6 \pm 0.3^{i,j}$	-18.1 ± 1.0^{m}	$18.2 \pm 1.4^{e,f,i}$	$284.7 \pm 0.5^{f,g}$	4.4
			2.3 ± 0.1	2.3 ± 0.1	-15.3 ± 1.3	13.2 ± 0.1	279.8 ± 0.1	
		A^GPA	$5.8 \pm 0.2^{k,l}$	0.3 ± 0.0^{l}	$-16.7 \pm 0.1^{k,l,m}$	$16.7 \pm 0.1^{f,g,i,j,k,m}$	269.9 ± 0.8^{i}	3.4
			5.6 ± 0.1	-0.9 ± 0.0	-13.5 ± 0.1	10.4 ± 0.1	265.9 ± 1.7	

Values are mean ± SD. Different letters indicate significant differences according to three-way ANOVA followed by Tukey's HSD ($p < 0.05$).

Table 7. Colorimetric parameters of gel beads: upper row = before heating, lower row = after heating at 50 °C for 48 h.

matrix	pH	beads	L*	a*	b*	C*	Hab	ΔE
EPP	4	A^G	17.8 ±1.3^{h}	10.2 ± 0.4^{e}	-14.5 ± 0.0^{h,i,j}	17.7 ± 0.2^{f,i,j}	305.5±1.0^{c,d,e}	17.3
			27.7 ± 1.1	-1.8 ± 0.1	-6.9 ± 0.1	7.0 ± 0.1	255.4 ± 2.8	
		A^GP	19.9±1.0^{g,h}	6.8 ± 0.3^{g,h}	-11.6±0.0^{d,e,f,g}	13.4 ± 0.2^{g,h,m,n}	300.7 ± 1.0^{e}	17.3
			35.5 ± 0.7	1.7 ± 0.1	-6.4 ± 0.1	6.4 ± 0.4	284.5 ± 3.9	
		A^GA	11.7 ± 0.7^{i}	10.4 ± 0.1^{e}	-28.9 ± 0.6^{p}	30.1 ± 1.0^{b}	287.4 ± 2.9^{f,g}	15.4
			17.1 ± 1.0	-2.3 ± 0.3	-22.0 ± 0.6	22.2 ± 1.8	264.0 ± 2.2	
		A^GPA	13.3 ± 0.5^{i}	11.3±0.4^{d,e}	-31.3 ± 0.1^{q}	34.5 ± 1.6^{a}	290.1 ± 0.8^{f}	16.6
			16.1 ± 1.0	-2.1 ± 0.1	-21.8 ± 0.2	21.9 ± 0.5	264.5 ± 0.3	
	5	A^G	21.3±0.4^{f,g}	-8.1 ± 0.9^{m}	-17.7 ± 1.3^{l,m}	19.5 ± 1.8^{d,e,f,g,h}	245.4 ± 0.4^{j}	17.4
			29.5 ± 2.2	-3.0 ± 0.4	-3.2 ± 0.1	4.0 ± 0.6	229.2 ± 2.8	
		A^GP	20.0±1.3^{g,h}	-7.8 ± 0.3^{m}	-15.1 ± 0.8^{i,j,k}	16.9 ± 1.0^{f,i,j,k,l}	243.1 ± 0.1^{j}	15.6
			28.9 ± 0.3	-3.3 ± 0.1	-3.2 ± 0.1	4.5 ± 0.4	221.9 ± 2.0	
		A^GA	5.2 ± 0.3^{l}	2.6 ± 0.4^{k}	-21.1 ± 1.3^{n}	21.3 ± 0.4^{c,d,e}	277.0 ± 0.8^{h}	8.6
			10.6 ± 0.2	-3.8 ± 0.2	-19.1 ± 1.3	19.4 ± 1.2	259.0 ± 1.0	
		A^GPA	8.3 ± 0.1^{j}	4.6 ± 0.4^{i,j}	-23.5 ± 0.4^{o}	23.9 ± 0.4^{c}	281.0 ±0.7^{g,h}	13.6
			10.9 ± 0.6	-7 ± 0.0	-16.7 ± 1.2	18.2 ± 0.3	247.0 ± 1.8	

- Changing the pH from 4 to 5 generally causes a marked decrease in color saturation (c*) in all extracts, accompanied by a shift of a* to less positive values and b* to more negative values. PGJ lost chromaticity considerably (c* ≈ 6–7), shifting toward a dull yellowish hue ($H^{\circ} \approx 60$), which reflects the reduced color stability of cyanidin-3,5-diglucoside under near-neutral conditions. This behavior is also consistent with the predominance of the colorless hemiketal at this pH, a typical feature of the high sensitivity of cyanidin-3,5-diglucoside to hydration.

In contrast, both BOJ and EPP retained high chromatic intensities, with BOJ showing c* ≈ 14 and a hue angle around 306°, and EPP exhibiting even higher c* values (16–19) with hue angles between 243° and 245°. These characteristics correspond to cooler-toned hues, ranging from purplish to greenish-blue, driven by strongly negative b* values. This consistent shift toward cooler hues in both matrices reflects a bluing phenomenon, resulting from a decrease in the proportion of red flavylium cations and a concomitant increase in the fraction of neutral quinoidal base species.

- The addition of Al^{3+} induced marked hue shifts and enhanced color saturation in all extracts, reflecting the formation of metal–anthocyanin complexes. In PGJ, Al^{3+} complexation caused only modest chroma increases and a shift toward purple to bluish-purple tones, consistent with its weaker binding capacity. BOJ responded with more vivid purple-blue hues and higher chroma,

particularly stabilized at pH 5. The strongest effect was observed in EPP, which reached the highest chroma values and retained deep bluish tones, especially at pH 5, highlighting the strong metal-binding affinity of delphinidin derivatives.

-The presence of pectin may have contributed to limiting the free mobility of pigments or restricting their complexation with Al^{3+}, thereby modulating pigment accessibility and stability. This effect was particularly noticeable in some cases, such as BOJ at pH 5, where color intensity appeared attenuated. However, the impact of pectin remained highly matrix-dependent. Interestingly, the texture of the particles was improved by pectin addition. This phenomenon was observed in previous works **(Azhar et al., 2021; Said et al., 2023; Sandoval-Castilla et al., 2010)** Indeed, gelling agents play a valuable role in conferring creaminess to foods and enabling the transformation of liquid formulations into jelly-like consistencies, all while upholding overall stability. The size and uniformity of microcapsules are important for food formulation, wherein smaller particles of more homogenous size are preferred due to their even distribution within the food matrix. In this work, the size and firmness of the particles were not quantified but simply assessed from visual and tactile perception. Nonetheless, the advantage of pectin incorporation into the beads was clearly discernible.

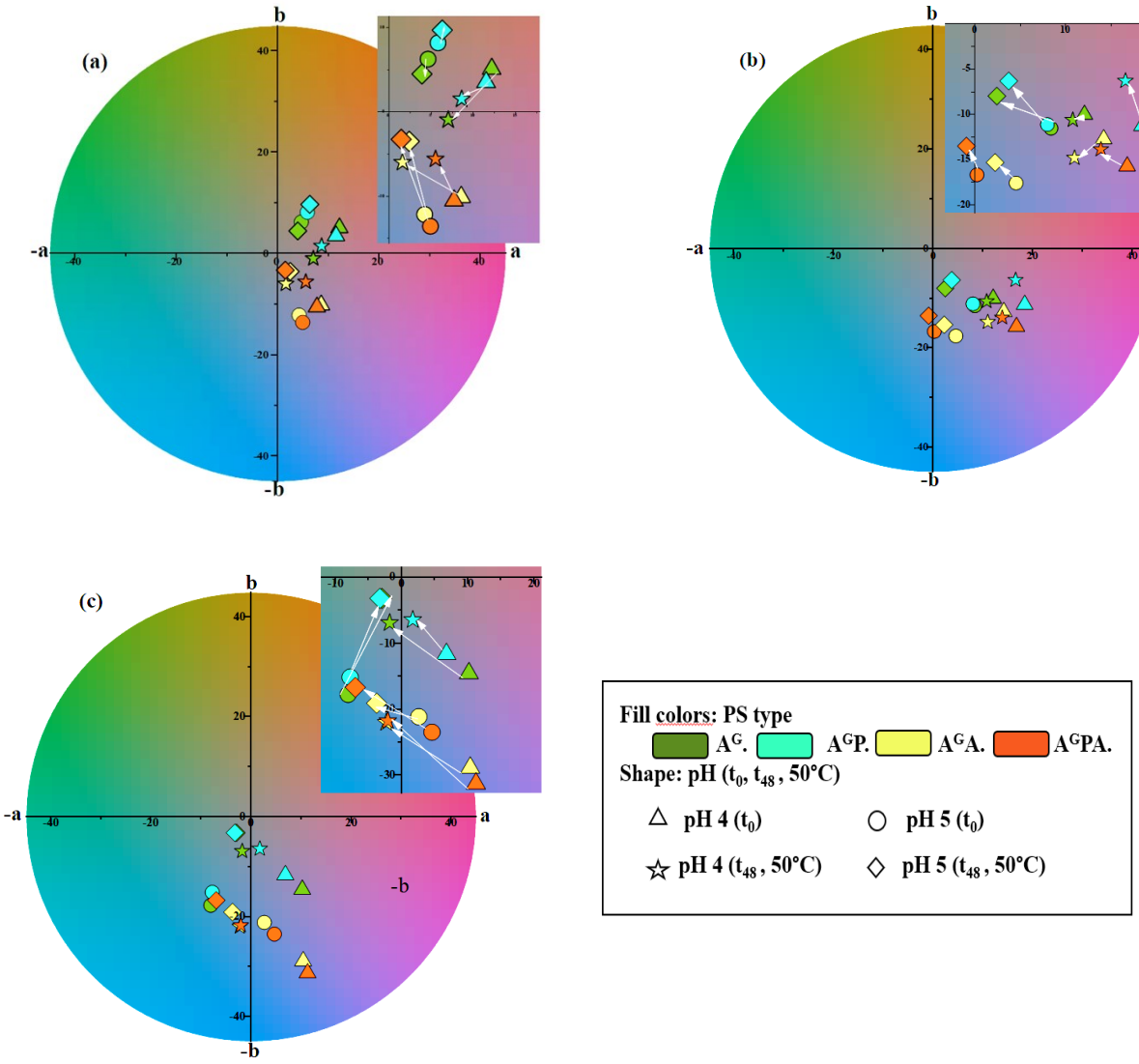

Figure 24. Two-dimensional scatter plot of CIELAB colorimetric data in the a*b* space with L* fixed at 60 for improved visualization, generated using OriginPro. (a) PGJ, (b) BOJ, and (c) EPP extracts.

3.4. Thermal stability of color and pigments

The effect of heating at moderate temperature (50°C) was evaluated on each formulation to assess the stability and protective capacity of the encapsulation system. Pigment loss is expressed as a percentage of the initial concentration prior to heating **(Table 8).** Color changes during heating was assessed by colorimetry **(Table 7, line 2)**. ΔE*, the total color difference, calculated relative to the initial color (before heating), was assumed to reflect the extend of color degradation.

Color changes upon heating consist of a reversible process (flavylium ion hydration leading to hemiketal and chalcone) and an irreversible process of pigment degradation by autoxidation and/or hydrolysis. The latter is evaluated by reversing the former through acidification to pH 1 (conversion of all ACN forms to the flavylium ion), followed by quantification of the residual flavylium ion released from dissociated gel beads. However, under heat treatment, water loss from the beads caused anthocyanin diffusion into the external phase, as indicated by the colored supernatant and bead shrinkage. Thus, the reduction in pigment content measured in the beads after heating is not solely due to anthocyanin degradation but also to partial release into the external medium. Therefore, our quantification methods (ΔE* or residual ACN concentration) assess overall color loss without distinguishing between the two mechanisms. Diffusion within hydrogels relates to transport in porous media and is strongly influenced by particle porosity.

Based on the data in **Table 8**, pigment loss followed a similar trend across all matrices, with the extent varying depending on pH and the encapsulation system. Alginate-only beads showed the greatest pigment loss, especially at pH 5, where the higher proportion of colorless forms prone to autoxidation accelerated degradation. In contrast, at pH 4, the dominance of the more stable flavylium form favored pigment retention. Al^{3+}-containing beads consistently exhibited the best stability, particularly at pH 5, indicating that Al^{3+} binds both ACNs and polysaccharides under mildly acidic conditions, thus limiting thermal leakage and degradation. These results were confirmed by the colorimetric data. The addition of pectin appeared to further enhance pigment retention, likely by reducing pore size and compacting the network, thereby limiting diffusion. These structural effects contributed to improved encapsulation efficiency and greater thermal stability of anthocyanins within gel beads.

Matrix-specific differences were also evident. EPP showed the highest degradation, with the greatest pigment loss, particularly at pH 5 (60.6% and 62.9% in A^G and A^GP formulations, respectively, after 24 h, increasing to 87.0% and 81.1% after 48 h). This trend was consistent with EPP having the highest ΔE* values observed among the three extracts **(Table 7, line 2)**, and is probably linked to the instability of its caffeoyl derivatives, whose redox activity may accelerate thermal breakdown.

Table 8. Pigment loss in beads heated at 50 °C for 24 and 48 h. Thermal stability of anthocyanin extracts under heating at 50 °C (mean ± *SD*). Statistical significance was assessed using three-way ANOVA followed by Tukey's HSD post hoc test ($p < 0.05$). Means having different letters are significantly different.

Samples	pH	Beads type	Pigment loss 24*h*	Pigment loss 48*h*
BOJ	4	A^G	$26.0 \pm 1.2^{e,f}$	40.8 ± 0.1^{j}
		A^GP	$23.3 \pm 0.5^{f,g}$	39.9 ± 0.1^{j}
		A^GA	$21.0 \pm 0.9^{g,h,i}$	34.5 ± 1.3^{k}
		A^GPA	8.13 ± 0.1^{l}	24.0 ± 0.3^{l}
	5	A^G	49.1 ± 0.8^{b}	61.7 ± 2.4^{c}
		A^GP	33.7 ± 2.0^{d}	$53.4 \pm 1.7^{f,g}$
		A^GA	$16.7 \pm 0.5^{j,k}$	35.5 ± 1.6^{k}
		A^GPA	6.6 ± 0.7^{l}	21.1 ± 1.2^{l}
EPP	4	A^G	32.0 ± 0.2^{d}	$59.8 \pm 0.7^{c,d,e}$
		A^GP	28.3 ± 0.5^{e}	$57.1 \pm 1.6^{d,e,f}$
		A^GA	$26.2 \pm 1.0^{e,f}$	55.6 ± 0.8^{f}
		A^GPA	$22.3 \pm 0.1^{g,h}$	$49.8 \pm 2.0^{g,h}$
	5	A^G	60.6 ± 2.0^{a}	87.0 ± 2.0^{a}
		A^GP	62.9 ± 1.0^{a}	81.1 ± 0.1^{b}
		A^GA	$19.2 \pm 2.0^{h,i,g}$	$49.0 \pm 1.4^{h,i}$
		A^GPA	$19.0 \pm 0.6^{i,j,k}$	$55.8 \pm 0.7^{e,f}$
PGJ	4	A^G	28.1 ± 0.2^{e}	45.6 ± 0.6^{i}
		A^GP	$18.0 \pm 1.2^{i,j,k}$	$45.9 \pm 0.3^{h,i}$
		A^GA	$16.7 \pm 0.2^{j,k}$	32.8 ± 0.8^{k}
		A^GPA	$18.0 \pm 0.3^{i,j,k}$	32.7 ± 0.5^{k}
	5	A^G	40.1 ± 2.0^{c}	62.5 ± 0.4^{c}
		A^GP	34.8 ± 1.2^{d}	$61.1 \pm 3.5^{c,d}$
		A^GA	$20.5 \pm 1.8^{g,h,i}$	32.6 ± 1.4^{k}
		A^GPA	15.8 ± 0.6^{k}	24.5 ± 0.1^{l}

BOJ exhibited the highest thermal stability over 24 h with low pigment loss (26% and 23% for A^G and A^GP formulations at pH 4, respectively) and limited color degradation. This stability is likely due to a synergistic effect between the polymers and flavonoid copigments, which restricted hydration and ring opening. PGJ showed even lower pigment loss in some cases, for instance, only 18% after 24 h at pH 4 in the A^GP formulation, but nevertheless suffered from markedly greater color degradation. This may be attributed to the prevalence of 3,5-O-diglucosides, known to be less thermally stable than their 3-O-glucoside homologs due to their higher sensitivity to water addition. Moreover, the presence of ellagitannins as copigments in the matrix, which are only modest copigments, further contributed to this instability **(section 2.3).** Marked discoloration was already evident at t_0, especially at pH 5, and was further accentuated by heating. The low ΔE* values observed in alginate and alginate–pectin beads at pH 5 (2.4 and 2.7, respectively) may misleadingly suggest good stability, whereas they in fact reflect an already severe loss of color occurring at the initial stage due to hydration. In the case of PGJ, Al^{3+} - ACN complexes also appeared weaker (compared to those formed with EPP and BOJ), probably because ellagitannins compete with ACNs for Al^{3+}.

These findings indicate that while simple encapsulation procedures can protect anthocyanins, differentiating pigment diffusion from true degradation remains challenging, thus highlighting the need for more refined methods. However, it can be noted that leakage of encapsulated ACNs through water release is expected to be severely limited when beads are previously incorporated into water-rich food matrices for coloring purposes.

Whatever the methods used, data interpretation is complicated by the presence of several compounds other than ACNs in the extracts, especially phenolic compounds, which interact not only with anthocyanins, but also with metal ions and polysaccharides. Extensive research is still required to unravel these interactions both individually and collectively.

Despite these challenges, the use of ionic gelation remains advantageous, as it relies on mild and eco-friendly conditions (no need of heating or vigorous stirring, no organic solvents) allowing the encapsulation of thermally sensitive compounds such as ACNs. These findings justify the subsequent evaluation of pigments in confectionery systems, where stability during thermal treatment and storage is critical.

4. Anthocyanin-Rich Extract in Hard Candy Formulation

The physicochemical investigation of anthocyanin equilibria within the extracts, together with the stability and encapsulation results, have highlighted that the anthocyanins are particularly sensitive to aqueous environments (water addition to the flavylium ion, exposure of ACNs to transition metal traces). To address this constraint, we explored their incorporation into a formulation with minimal water content, namely hard candy. This work represents a preliminary attempt to evaluate the potential of these extracts (as powders) as natural colorants in confectionery. The results are therefore intended as an initial proof-of-concept, providing insight into their possible use in future industrial applications.

4.1. Hard candy characterization

Hard candy was prepared and enriched with ACN-rich extracts. **Figure 25** shows the final appearance of hard candies formulated with anthocyanin-rich extracts, artificial Allura Red, and the control. Only one concentration of extract was tested in order to compare with Allura Red, an azo dye widely used in the confectionery industry **(Barciela et al., 2023).**

Depending on the type of candy produced, the processing temperature can vary. Most hard candies are boiled to 145–155 °C under normal atmospheric pressure to ensure that the mixture reaches the *hard crack* stage **(Ozel et al., 2024)** . In our study, the samples were boiled to 145 °C to obtain a final moisture content below 5% (**Table 9**). However, the confectionery industry generally uses vacuum processing, which reduces the boiling temperature by 11–20 °C. This method is more economical than bench-top preparation, as it consumes less energy, reduces the risk of caramelization or Maillard reactions, and increases production capacity by shortening processing time. This efficiency arises because vacuum processing evaporates water from the confectionery mixture more rapidly than boiling under open atmosphere **(McDonald & Sun, 2000; Ozel et al., 2024; Piri et al., 2024**).

In our formulation, the sugar-to-syrup ratio was approximately 54% to 43%, close to the commonly used 60:40 ratio **(Spanemberg et al., 2019)**. The mixture was added to a flask and boiled on a hot plate to 145 °C, the standard *hard crack* temperature. Once removed from the heat, the colorant and citric acid, previously dissolved in 2–3 mL of water, were added between 115 and 121 °C, then mixed thoroughly with a glass rod to maximize dissolution. This temperature range

was chosen because the candy must remain hot enough to vaporize the added liquid and disperse the powders, yet not so hot as to degrade the natural compounds **(Ozel et al., 2024)**.

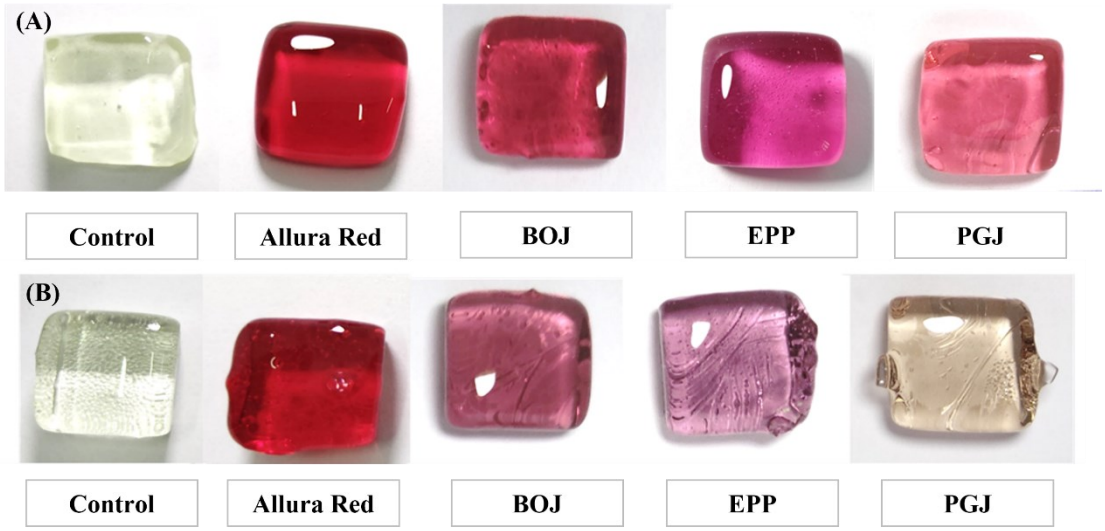

Figure 25. Hard candies formulated with anthocyanin-rich extracts, Allura Red, and the control: (A) acidified (0.15% citric acid) and (B) non-acidified.

Although anthocyanin loss may occur during processing, their relative heat stability ensures that degradation remains limited when exposure to high temperatures is short. Gu et al. **(2015)** demonstrated that incorporating freeze-dried black raspberry powder (22%) directly into the sugar mass at 150 °C resulted in 59% anthocyanin retention, indicating that a significant proportion of pigments can withstand confectionery processing. In our approach, the extract and citric acid were added at 115–121 °C, providing gentler conditions likely to further preserve pigment integrity. After incorporation, the mass was cooled in silicone molds and then placed in a refrigerator at 4°C, a step that helped control stickiness and moisture. In line with industrial quality requirements, the final moisture content of our samples ranged from 1.05% to 3.17%. Such control of processing and storage conditions is critical to ensure both the visual appeal of hard candies and the functional retention of anthocyanins for industrial applications.

Citric acid was incorporated into the formulation to lower the pH below 3.5, thereby enhancing anthocyanin stability. Pre-dissolving citric acid together with the colorant ensured homogeneous

dispersion and prevented the formation of a gritty texture in the candy. The final pH of the acidified samples was around 3.3, consistent with the recommended interval (3.0–3.5) for acidified hard candies **(Ozel et al., 2024).**

The incorporation of anthocyanin-rich extracts into the hard candy formulation resulted in products with visually appealing colors, ranging from bright red under acidic conditions (pH ≈ 3) to purple hues at pH ≈ 5 **(Figure 25)**. These shades contrasted strongly with the control samples, which remained nearly colorless to slightly yellow, confirming that the observed coloration was primarily attributable to the added pigments.

Colorimetric analysis supported these observations: L* values ranged from 31.43 to 47.25 and hue angles from 3.50 to 359.60, reflecting the broad chromatic diversity of the extracts across pH levels **(Table 9)**. Acidification with citric acid enhanced the redness and saturation of the candies, consistent with the stabilization of the flavylium cation at low pH. This effect was particularly pronounced for BOJ, whose chromatic profile at pH 3 closely resembled that of Allura Red ($\Delta E^* = 4.32$), highlighting its strong potential as a natural substitute for synthetic dyes.

At pH 5, the extracts shifted toward purple tones, in line with the predominance of neutral quinonoidal bases. These colors diverged substantially from Allura Red, as indicated by the highest ΔE^* values. Clear differences among matrices were also evident: EPP and BOJ retained a vivid purple coloration, whereas PGJ exhibited pronounced discoloration, with candies turning golden to brown.

The high sugar concentration in hard candies is known to lower water activity, which delays the hydration of anthocyanins and limits their conversion to colorless hemiketals **(Moldovan & David, 2020)**. In our case, the measured residual moisture content (1.05–3.17%) supports such a protective effect, consistent with the good color stability observed in most formulations. Such an effect likely contributed to the retention of strong hues in BOJ and EPP, even under high-temperature processing, though to a lesser extent for PGJ at pH 5.

However, it should also be considered that sugars and their degradation products may negatively influence pigment stability. During candy cooking, thermal decomposition of sugars can lead to the formation of 5-hydroxymethylfurfural (HMF). At moderate levels, HMF exerts only limited effects on anthocyanin degradation and may even transiently enhance stability **(Calvi & Francis, 1978)**. At higher concentrations, however, HMF is known to impair both pigment content

and color expression **(Song et al., 2023)**. Although HMF was not quantified in this study, the preservation of distinct hues in most of our formulations suggests that its accumulation did not reach destabilizing levels.

As expected for a synthetic dye, Allura a Red maintained visually strong and stable coloration under both pH conditions. By comparison, anthocyanin-rich extracts provided a remarkable diversity of natural shades. BOJ emerged as the most promising candidate for confectionery coloration, while PGJ illustrated the strong pH-dependence of anthocyanin-based pigments.

Table 9. Characteristics of the hard candies' formulation

Sample	**Acidified hard candy (0.15% citric acid)**					**Non Acidified hard candy**				
	Control	**All red**	**BOJ**	**PGJ**	**EPP**	**Control**	**All red**	**BOJ**	**PGJ**	**EPP**
pH	3.29 ± 0.01	3.29 ± 0.02	3.29 ± 0.02	3.3 ± 0.03	3.3 ± 0.01	5.20 ± 0.18	5.05 ± 0.13	5.01 ± 0.07	5.5 ± 0.12	4.9 ± 0.21
Humidity %	1.05 ± 0.04	1.09 ± 0.02	2.33 ± 0.16	2.91 ± 0.19	1.30 ± 0.10	2.40 ± 0.24	1.05 ± 0.09	1.91 ± 0.13	2.82 ± 0.20	3.17 ± 0.12
L*	53.23 ± 1.60	32.00 ± 0.90	32.55 ± 0.07	39.65 ± 0.92	40.00 ± 0.85	53.70 ± 0.28	32.95 ± 0.49	31.43 ± 0.54	47.25 ± 0.78	36.90 ± 0.57
a*	-1.80 ± 0.17	28.35 ± 0.07	25.20 ± 1.13	27.85 ± 1.34	35.45 ± 2.76	-1.95 ± 0.07	30.50 ± 0.28	17.58 ± 0.33	5.30 ± 0.35	11.20 ± 0.14
b*	2.77 ± 0.06	10.80 ± 0.14	7.90 ± 0.28	10.00 ± 0.14	-0.25 ± 0.07	2.05 ± 0.07	12.85 ± 0.49	3.78 ± 0.10	9.50 ± 0.28	0.70 ± 0.00
c	3.30 ± 0.10	30.20 ± 0.28	26.35 ± 1.20	29.60 ± 1.27	35.45 ± 2.76	2.85 ± 0.07	33.05 ± 0.49	17.98 ± 0.33	11.00 ± 0.42	11.20 ± 0.14
H_0	123.20 ± 2.86	20.90 ± 0.14	17.35 ± 0.07	19.70 ± 0.57	359.60 ± 0.14	133.70 ± 2.12	22.85 ± 0.64	12.43 ± 0.56	59.70 ± 1.27	3.50 ± 0.28
ΔE*	0.87_{C}	3.12_{AR}	$4.32_{\ddagger}$	$7.71_{\ddagger}$	$15.38_{\ddagger}$	0.87_{C}	3.12_{AR}	$15.86^{\ddagger}_{\ddagger\ddagger}$	$29.17^{\ddagger}_{\ddagger\ddagger}$	$23.15^{\ddagger}_{\ddagger\ddagger}$

ΔE_C : Control pH 3 vs. Control pH 5, ***ΔE_{AR}***: Allura Red pH 3 vs. Allura Red pH 5, ***$\Delta E_{\ddagger}$:*** Acidified matrix (pH 3) vs. Allura Red pH 3, ***$\Delta E^{\ddagger}_{\ddagger\ddagger}$:*** Non-acidified matrix (pH 5) vs. Allura Red pH 5.

4.2. Sensory analyses

A sensory evaluation of the hard candies was carried out to assess visual attributes (color and brightness), overall visual acceptability, and purchase intention. The scores for each attribute represent the proportion of affirmative responses (yes), while Product appreciation was directly rated on a nine-point hedonic scale.

The radar plot in **Figure 26** shows that colors and brightness were generally well accepted across samples, with two exceptions: Allura Red and PGJ_{pH5} were judged less attractive in terms of color. However, PGJ_{pH5} stood out for its brightness. When combining both attributes into overall visual acceptability, BOJ_{pH5} received the highest score, whereas Allura Red was least appreciated. Purchase intention diverged from color appreciation: it was highest for PGJ_{pH5}, suggesting that consumers valued aspects beyond visual intensity. Among the samples, Allura R was distinctly perceived as an artificial color, whereas PGJ_{pH3} was judged to have the most natural appearance.

The observation from the radar plots was confirmed by the statistical analysis conducted after the sensory characterization of the products. The discriminant attribute power **(Figure 27)** revealed that artificial color perception was the most discriminating attribute (test value = 14.050, $p < 0.001$). Purchase intention also differed significantly (test value = 2.877, $p = 0.002$). Visual acceptability was not significant at 5% (test value = 1.326, $p = 0.092$) but became discriminating at the 10% level. Glossiness (test value = 0.232, $p = 0.408$) and color acceptability (test value = 0.186, $p = 0.426$) showed no significant differences. Adjusted proportions of attributes **(Table10)** show that values highlighted in blue are significantly higher, while those in red are significantly lower than the global average, confirming that natural extracts were consistently perceived as less artificial than the synthetic dye. BOJ_{pH5} combined strong visual acceptability with high preference, whereas PGJ_{pH5}, despite lower color ratings, showed the highest purchase intention.

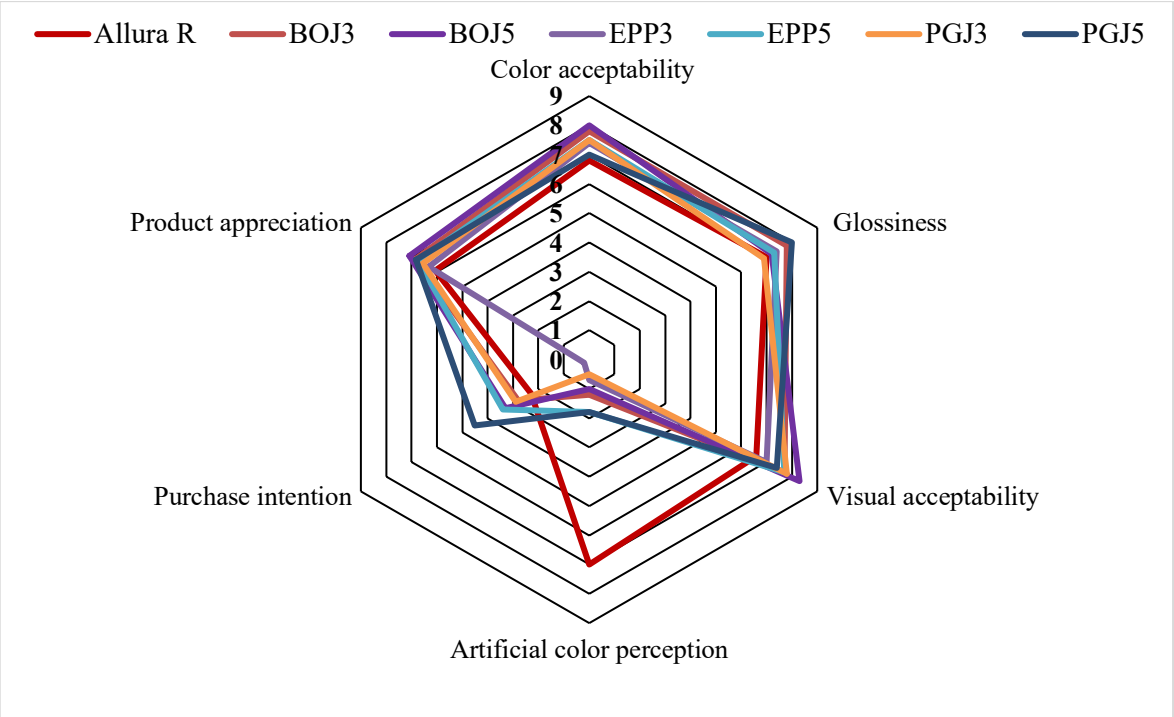

Figure 26. Radar plot of the visual sensory profile of candy samples.

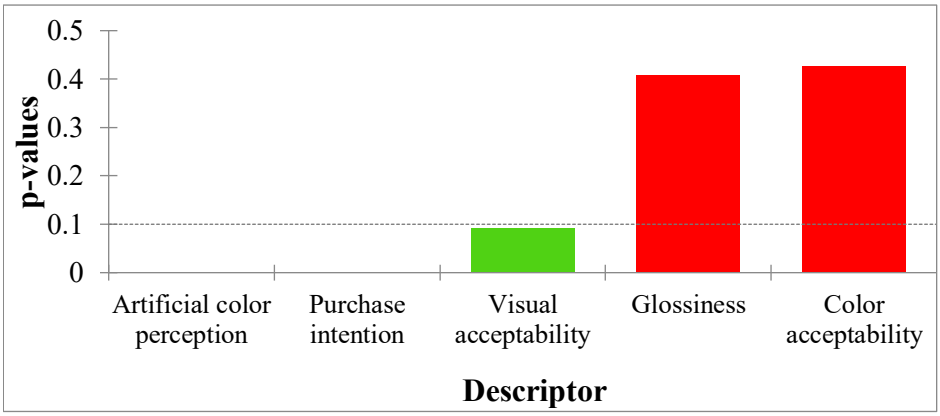

Figure 27. Discriminating power by descriptor for the sensorial analysis.

Table 10. Adjusted proportion sensory attributes by product.

Hard candy	Visual acceptability	Color acceptability	Purchase intention	Glossiness	Artificial color perception
BOJ_{pH5}	0.83	0.80	0.33	0.72	0.10
BOJ_{pH3}	0.77	0.78	0.28	0.78	0.12
PGJ_{pH3}	0.78	0.75	0.29	0.69	0.05
EPP_{pH5}	0.77	0.75	0.34	0.73	0.18
PGJ_{pH5}	0.74	0.70	0.45	0.80	0.18
EPP_{pH3}	0.70	0.74	0.20	0.74	0.07
Allura R	0.66	0.68	0.23	0.70	0.70

To explore the relationship between sensory attributes and consumer preferences, a preference mapping (PREFMAP) analysis was performed. This approach combines sensory profiles with preference data to identify the attributes driving consumer choices and to position the products according to their level of acceptance. To generate PREFMAP results, panelists were first grouped into clusters using Agglomerative Hierarchical Clustering (AHC), while Principal Component Analysis (PCA) was applied to reduce dimensionality and provide a visual representation of the relationships between sensory attributes and products. The PREFMAP PCA biplot (**Figure 28**) explains 82.34% of the total variance (F1 = 52.89%, F2 = 29.45%), effectively capturing the main sensory differences among the seven candy products. Glossiness and purchase intention are strongly and positively correlated, as are visual and color acceptability, while visual acceptability shows a strong negative correlation with artificial color perception.

Preference mapping revealed that Allura Red, closely associated with artificial color perception, was located in the lower preference area (20–40%). In contrast, candies made with natural extracts were placed in the moderate preference zone (40–60%), particularly BOJ_{pH5}, which aligned strongly with visual appeal, and PGJ_{pH5}, which was more related to purchase intention and glossiness. EPP_{pH5}, BOJ_{pH3}, and PGJ_{pH3} showed balanced but moderate associations, while EPP_{pH3} remained closer to the lower preference area.

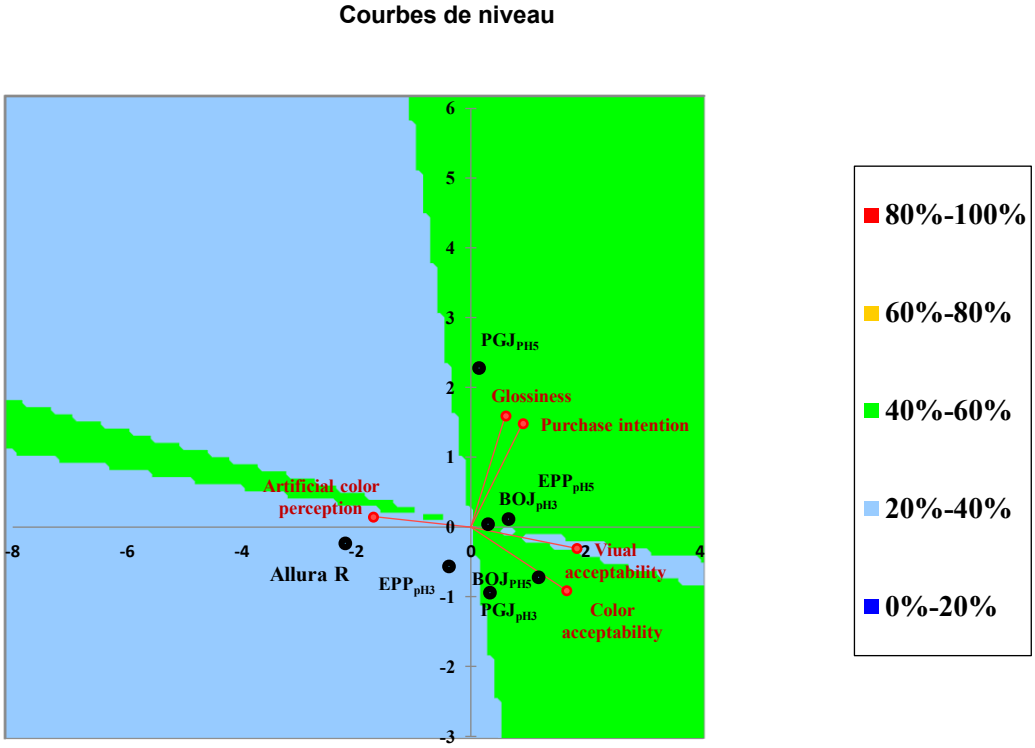

Figure 28. External preference mapping (PREFMAP) biplot based on principal component analysis (PCA) of sensory attributes of hard candies.

The preference ranking **(Figure 29)** further confirmed this trend: natural colorants, particularly BOJ_{pH5} and PGJ_{pH5}, were most preferred, while Allura R received the lowest acceptance. Open-ended questions provided additional insights into these choices. When asked what makes a candy appear more natural, most participants answered that a **"**softer color**"** and a hue **"**similar to a real fruit**"** were key indicators. The preference for BOJ_{pH5} and PGJ_{pH5} was often justified by their reassuring and natural tones, with PGJ_{pH5} specifically described as reminiscent of caramel, a familiar and appealing association in confectionery. In contrast, the color of Allura Red was perceived as excessively intense, which made its artificial nature evident to consumers and consequently lowered its acceptability. All candies formulated with natural extracts were positively evaluated, supporting their potential as commercial products. However, for EPP_{pH3} and EPP_{pH5}, although their color was appreciated, they appeared more suitable for other applications, such as cosmetics, as highlighted by panelists' comments.

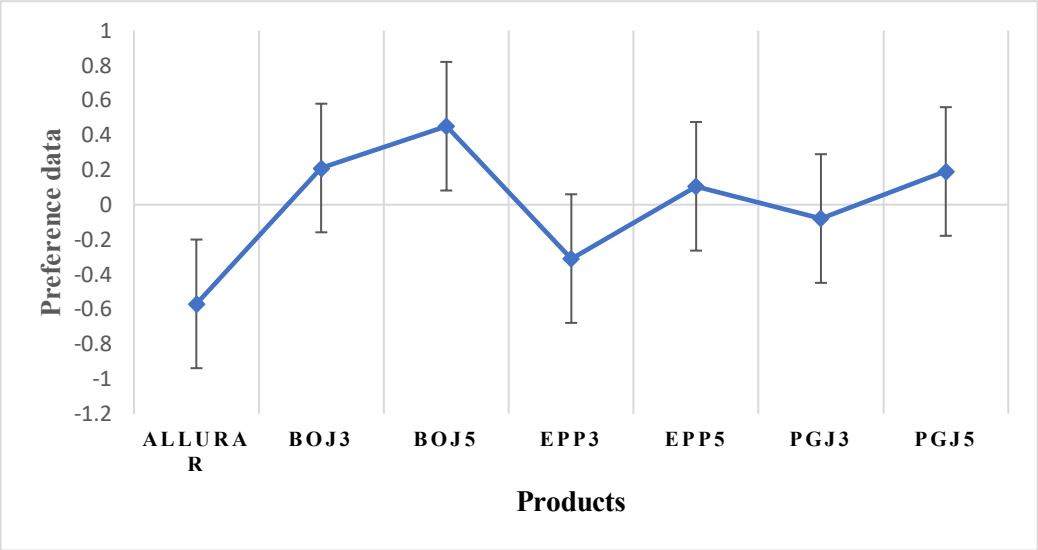

Figure 29. Preference DATA Product.

Conclusion and perspectives

Conclusion and Perspectives

The overall objective of this work was to bridge fundamental knowledge on anthocyanin chemistry with applied strategies for food formulation, thereby contributing to the valorization of natural colorants as sustainable alternatives to synthetic dyes. This objective was at the core of the partnership expertise and represents an extension of the research carried out at Avignon University, which has for the past years focused on acylated anthocyanins, particularly those derived from red cabbage and purple sweet potatoes, with very promising results in the context of food applications. At the same time, drawing on the fundamental investigations conducted at Porto University on purified anthocyanins, our study was able to position its findings within a broader framework, allowing for direct comparison between extract-based data and literature values on pure compounds. This approach highlights how semi-purified extracts can serve as an intermediate level of complexity between purified standards and real food systems, thus reinforcing their relevance for both fundamental understanding and industrial application due to their economic and practical advantages.

Extracts from common plant foods were easily prepared, enriched in anthocyanins, and extensively characterized. Their phenolic composition revealed a broad diversity, including mono- and di-O-glucosides of delphinidin and cyanidin (including, in the case of BOJ, a fraction of pigments with malonyl and/or oxalyl acylation) known to be vulnerable to hydration, along with distinctive copigments, such as flavonoids in BOJ, ellagitannins in PGJ, and spermidine derivatives in EPP. This diversified composition, in terms of both anthocyanin structures and copigment types, provides a solid basis for mapping the mechanisms of anthocyanin stabilization and interactions, thereby strengthening the relevance of our study.

Building on this compositional diversity, a more detailed physicochemical investigation was undertaken to clarify how these structural features and copigment profiles translate into stability mechanisms under different conditions.

On this basis, kinetic studies on the selected extracts were carried out to identify the key mechanisms governing their stability and to place the investigation on more rigorous physicochemical grounds, thereby enabling a deeper interpretation of color data. This approach

proved useful for selecting extracts in which specific pigment–copigment combinations enhance stability, while also providing practical guidelines for storage and formulation. Beyond liquid systems, their reactivity was further demonstrated in semi-solid matrices through encapsulation in natural polymers, and their susceptibility to hydration, thermal degradation, and metal binding was systematically assessed. Finally, their incorporation into a low-moisture confectionery matrix (hard candy) was explored, extending the relevance of these findings to real food applications.

Color Expression and Stability of Anthocyanins in aqueous Solution

Speciation diagrams derived from thermodynamic acidity and hydration constants revealed clear differences in color expression among the extracts. Above pH 3, PGJ solutions became almost colorless, whereas EPP and particularly BOJ retained part of their color, in line with their visual appearance. These differences reflect the influence of glycosylation patterns and potent copigments on anthocyanin stability. At pH 5, all extracts formed Al^{3+} complexes, which reversed hydration equilibria and efficiently regenerated color. Complex hues were observed, with EPP forming blue complexes and BOJ and PGJ forming purple ones.

Thermal treatments at 50 °C further confirmed BOJ as the most stable extract, while EPP degraded more rapidly, likely due to autoxidation of its caffeoyl derivatives. Notably, Al^{3+}–anthocyanin binding markedly reduced both color loss and pigment degradation, with BOJ again emerging as the most stable system.

It has been reported that increasing anthocyanin structural complexity through acylation results in more bluish hues and higher color stability, mainly owing to intramolecular copigmentation and self-association **(Pereira et al., 2024)**. Our findings place anthocyanin-rich extracts in an intermediate position between pure non-acylated anthocyanins and the highly acylated pigments extensively described in red cabbage and purple sweet potato, the latter being particularly resistant to water addition **(Fenger et al., 2021a; Fenger et al., 2021b; Moloney et al., 2018)**. In these acylated systems, multiple hydroxycinnamic acids—particularly when positioned on the external glucose of the sophorose unit—stabilize the chromophore through sandwich-type conformations, conferring exceptional resistance to hydration and thermal degradation. By contrast, the anthocyanins in our extracts are non-acylated or acylated by non-phenolic acids, yet they display higher stability than pure homologues forms **(Leydet et al., 2012; Mazza & Brouillard, 1987)**

due to intermolecular copigmentation with co-occurring phenolics, such as dicaffeoylspermidine derivatives in EPP or flavonoids in BOJ. This highlights that, although less intrinsically protected than multi-acylated pigments, anthocyanin-rich extracts provide valuable insight into stabilization mechanisms mediated by the plant matrix.

Ionic Gelation Encapsulation

In this work, we also sought to understand the subtle influence of biopolymers on anthocyanins in the presence or absence of metal ions, as well as the underlying physicochemical mechanisms of their interactions. Preliminary kinetic analyses carried out at the University of Porto (data not reported) with different alginic acid calcium salts at varying concentrations did not reveal any significant stabilizing effect. Moreover, high alginate concentrations induced viscosity-related interferences, with baseline distortions due to light scattering in the 700–800 nm region compromising spectral measurements. These limitations in liquid systems also prevented the evaluation of higher polysaccharide concentrations, which could potentially have produced more pronounced effects. For these reasons, we shifted the focus toward encapsulation approaches, where biopolymers can be applied at higher effective levels and act through entrapment mechanisms that restrict pigment exposure to destabilizing factors. Within this framework, alginate and pectin emerged as particularly promising anionic polysaccharides, with additional potential arising from their combination with natural endogenous antioxidants (phenols within the selected matrices) to further improve oxidative stability.

Simple ionic gelation encapsulation protocols yielded colored anthocyanin-rich extract beads, though the encapsulation effectiveness and stability strongly depended on matrix composition and gel properties. BOJ, for instance, showed the lowest encapsulation efficiency (EE%), possibly due to preferential pigment–copigment interactions in solution, or competition between pigments and copigments for the gel matrix. Nevertheless, the encapsulated fraction showed a higher color and pigment stability, as if the copigmentation complexes were transferred to the hydrogel beads. A limitation, however, is that highly hydrophilic anthocyanins may diffuse relatively rapidly from the ionic gel network at elevated temperatures (e.g., 50 °C), thereby reducing the hydrogel's protective effect. Encouragingly, preliminary release experiments showed that anthocyanins incorporated in alginate–pectin gels were released slowly under acidic conditions (0.1 M HCl), mimicking gastric digestion. This finding suggests that encapsulation can modulate anthocyanin

bioaccessibility, which is highly relevant for functional food design. Furthermore, Al^{3+}–anthocyanin complexation occurred at both pH values tested (4 and 5), but the complexes were markedly more stable at pH 5, where high EE% and improved thermal stability were achieved, with an additional protective effect conferred by pectin.

Hard Candy Formulation

The formulation of hard candies with anthocyanin-rich extracts demonstrated that anthocyanins can be successfully incorporated into confectionery products to achieve brilliant red and purple hues. Owing to the low water content of this matrix, these natural pigments effectively imparted color, though their intensity and stability were strongly dependent on pH. The addition of citric acid promoted more vivid red coloration, whereas its absence led to purple shades accompanied by partial browning and color loss, particularly for the PGJ extract. Sensory evaluation further revealed that the natural colors were well perceived, despite their lower saturation compared with synthetic dyes.

Potential Experimental Directions

These perspectives aim to: (i) verify the hypotheses put forward in this work; (ii) explore the potential of the main stabilization strategies identified, namely the preservation of endogenous copigments, encapsulation, and the binding of catechol rings by Al^{3+} ions or other biocompatible metal ions, either in solution or within encapsulated systems; and (iii) define appropriate analytical methods to further advance this research.

Preparation of the Extracts

- Future work should investigate green extraction strategies, such as supercritical CO_2 extraction, which offers high selectivity, reduced solvent residues, and the possibility of tuning extraction conditions through pressure and cosolvent adjustments. Enzyme-assisted extraction could also be applied to degrade cell wall polysaccharides and enhance pigment release. In parallel, open-column chromatography using low-cost stationary phases (e.g., silica gel, Sephadex, or C18 resins) represents a practical fractionation method to enrich extracts in anthocyanins or copigments, and potentially increase overall yields. Such approaches would combine environmentally friendly extraction with cost-effective preparative separation, thereby facilitating the production of standardized anthocyanin-rich extracts at laboratory or pilot scale.

Stability Mechanisms and Processing Conditions

- Future research should include a broader diversity of anthocyanin-rich plant sources. This would help generalize the findings of this work and, above all, identify the most favorable anthocyanin–copigment combinations for achieving optimal stability and applicability in food systems. Explore the role of endogenous copigments, not as impurities to be removed, but as valuable contributors to stabilization.

- Conduct systematic studies of anthocyanin stability under a wider range of pH values, temperatures, and food-processing scenarios (e.g., frying, microwave heating).

- Design experiments to evaluate the long-term stability of plant extracts under different storage conditions (such as light exposure, temperature, and humidity) to determine their feasibility in practical applications.

Metal Complexation and Safety Control

- Further investigate the use of Al^{3+} or other food-compatible metal ions to enhance anthocyanin stability in both solutions and encapsulated systems, while carefully assessing their potential toxicity and ensuring that such strategies can be safely and effectively scaled up in food products.

Perspectives for Anthocyanin Encapsulation

- Optimize encapsulation conditions by adjusting polymer type, concentration, and bead morphology to improve stabilization and control release kinetics.

- Apply the developed encapsulation protocol to various anthocyanin sources, and explore the use of specialized encapsulators to better control particle size and morphology, as smaller beads could facilitate dispersion in food.

- Explore advanced micro- and nanoencapsulation systems, such as natural surfactants, micelles, and liposomes, with an emphasis on food-grade and consumer-safe carriers, and compare their performance with conventional techniques like the atomization method.

- Evaluate the anthocyanin release profile of particles under simulated gastric (pH 2 - 5) and intestinal (pH 6 - 7) conditions.

- Employ advanced analytical tools (light scattering, zeta potential, electron microscopy, DSC, FTIR, CD spectroscopy, XRD) to better characterize anthocyanin–biopolymer interactions.

Formulation

- Optimize sugar composition (sucrose / glucose / fructose) and explore natural substitutes such as honey, fruit syrups, or stevia, with the aim of lowering the glycemic index while preserving the desired texture and visual aspect.

- Investigate the effect of natural organic acids (malic, tartaric, ascorbic acid) on anthocyanin stability and sensory perception, in order to achieve more vivid and stable coloration.

- Compare alternative cooking or concentration processes, such as vacuum cooking or low-temperature methods, to minimize pigment degradation and preserve bioactive compounds during formulation.

- Evaluate storage stability under various environmental conditions (temperature, light, humidity) to determine the optimal shelf life and ensure consistent product quality.

- Further enhance thermal and oxidative protection during processing by incorporating encapsulated anthocyanin (micro- or nano-) extracts.

- Expand applications to jelly candy and beyond confectionery to a broader range of food matrices (ex: baked goods, dairy systems).

Taken together, these perspectives emphasize the dual importance of fundamental understanding and applied research. By integrating stabilization strategies, such as copigmentation, metal complexation, and encapsulation, while also addressing consumer perception and industrial feasibility, future work can accelerate the transition toward sustainable, anthocyanin-based food colorants.

References

Azhar, M. F., Haris, M. S., Mohamad, I., Ismadi, M. N. S., Yazid, A. A. H., Rahman, S. R., & Azlan, N. H. (2021). Optimisation of alginate-pectin bead formulation using central composite design guided electrospray technique. *International Food Research Journal*, *28*(4), 860-870.

Barciela, P., Perez-Vazquez, A., & Prieto, M. A. (2023a). Azo dyes in the food industry : Features, classification, toxicity, alternatives, and regulation. *Food and Chemical Toxicology*, *178*, 113935. https://doi.org/10.1016/j.fct.2023.113935

Barreca, D., Bellocco, E., Caristi, C., Leuzzi, U., & Gattuso, G. (2011). Distribution of C- and O-glycosyl flavonoids, (3-hydroxy-3-methylglutaryl)glycosyl flavanones and furocoumarins in Citrus aurantium L. juice. *Food Chemistry*, *124*(2), 576-582. https://doi.org/10.1016/j.foodchem.2010.06.076

Cai, D., Li, X., Chen, J., Jiang, X., Ma, X., Sun, J., Tian, L., Vidyarthi, S. K., Xu, J., Pan, Z., & Bai, W. (2022). A comprehensive review on innovative and advanced stabilization approaches of anthocyanin by modifying structure and controlling environmental factors. *Food Chemistry*, *366*, 130611. https://doi.org/10.1016/j.foodchem.2021.130611

Calvi, J. p., & Francis, F. j. (1978). STABILITY OF CONCORD GRAPE (V. labrusca) ANTHOCYANINS IN MODEL SYSTEMS. Journal of Food Science, 43(5), 1448-1456. https://doi.org/10.1111/j.1365-2621.1978.tb02517.x

Cao, L., Lu, W., Mata, A., Nishinari, K., & Fang, Y. (2020). Egg-box model-based gelation of alginate and pectin : A review. *Carbohydrate Polymers*, *242*, 116389. https://doi.org/10.1016/j.carbpol.2020.116389

Cao, S., Liu, L., Pan, S., Lu, Q., & Xu, X. (2009). A Comparison of Two Determination Methods for Studying Degradation Kinetics of the Major Anthocyanins from Blood Orange. *Journal of Agricultural and Food Chemistry*, *57*(1), 245-249. https://doi.org/10.1021/jf8021964

Catania, P., Comparetti, A., De Pasquale, C., Morello, G., & Vallone, M. (2020). Effects of the extraction technology on pomegranate juice quality. *Agronomy*, *10*(10), 1483. https://doi.org/10.3390/agronomy10101483

Cebadera-Miranda, L., Domínguez, L., Dias, M. I., Barros, L., Ferreira, I. C. F. R., Igual, M., Martínez-Navarrete, N., Fernández-Ruiz, V., Morales, P., & Cámara, M. (2019). Sanguinello and Tarocco (Citrus sinensis [L.] Osbeck) : Bioactive compounds and colour appearance of blood oranges. *Food Chemistry*, *270*, 395-402. https://doi.org/10.1016/j.foodchem.2018.07.094

Cheng, Y., Liu, J., Li, L., Ren, J., Lu, J., & Luo, F. (2023). Advances in embedding techniques of anthocyanins : Improving stability, bioactivity and bioavailability. *Food Chemistry: X*, *20*, 100983. https://doi.org/10.1016/j.fochx.2023.100983

Ćorković, I., Pichler, A., Ivić, I., Šimunović, J., & Kopjar, M. (2021). Microencapsulation of Chokeberry Polyphenols and Volatiles : Application of Alginate and Pectin as Wall Materials. *Gels*, *7*(4), Article 4. https://doi.org/10.3390/gels7040231

Cruz, L., Basílio, N., Mateus, N., de Freitas, V., & Pina, F. (2022). Natural and Synthetic Flavylium-Based Dyes : The Chemistry Behind the Color. *Chemical Reviews*, *122*(1), 1416-1481. https://doi.org/10.1021/acs.chemrev.1c00399

Dangles, O., & Fenger, J.-A. (2018). The Chemical Reactivity of Anthocyanins and Its Consequences in Food Science and Nutrition. *Molecules*, *23*(8), 1970. https://doi.org/10.3390/molecules23081970

Dangles, O., Dufour, C., Tonnelé, C., & Trouillas, P. (2016). The Physical Chemistry of Polyphenols : Insights into the Activity of Polyphenols in Humans at the Molecular Level. In K. Yoshida, V. Cheynier, & S. Quideau (Éds.), *Recent Advances in Polyphenol Research* (p. 1-35). John Wiley & Sons, Ltd. https://doi.org/10.1002/9781118883303.ch1

de Oliveira, I. R. N., Teófilo, R. F., de Oliveira, E. B., Ramos, A. M., de Barros, F. A. R., Maia, M. de P., & Stringheta, P. C. (2017). Evaluation of potential interfering agents on *in vitro* methods for the determination of the antioxidant capacity in anthocyanin extracts. *International Journal of Food Science & Technology*, *52*(2), 511-518. https://doi.org/10.1111/ijfs.13307

Denish, P. R., Fenger, J.-A., Powers, R., Sigurdson, G. T., Grisanti, L., Guggenheim, K. G., Laporte, S., Li, J., Kondo, T., Magistrato, A., Moloney, M. P., Riley, M., Rusishvili, M., Ahmadiani, N., Baroni, S., Dangles, O., Giusti, M., Collins, T. M., Didzbalis, J., …

Robbins, R. J. (2021). Discovery of a natural cyan blue : A unique food-sourced anthocyanin could replace synthetic brilliant blue. *Science Advances*, *7*(15), eabe7871. https://doi.org/10.1126/sciadv.abe7871

Díaz-Mula, H. M., Tomás-Barberán, F. A., & García-Villalba, R. (2019). Pomegranate Fruit and Juice (cv. Mollar), Rich in Ellagitannins and Anthocyanins, Also Provide a Significant Content of a Wide Range of Proanthocyanidins. *Journal of Agricultural and Food Chemistry*, *67*(33), 9160-9167. https://doi.org/10.1021/acs.jafc.8b07155

Dranca, F., & Oroian, M. (2017). Total Monomeric Anthocyanin, Total Phenolic Content and Antioxidant Activity of Extracts from Eggplant (*S olanum Melongena* L.) Peel Using Ultrasonic Treatments : Eggplant antioxidants extraction. *Journal of Food Process Engineering*, *40*(1), Article 1. https://doi.org/10.1111/jfpe.12312

Fenger, J.-A., Moloney, M., Robbins, R. J., Collins, T. M., & Dangles, O. (2019). The influence of acylation, metal binding and natural antioxidants on the thermal stability of red cabbage anthocyanins in neutral solution. *Food & Function*, *10*(10), Article 10. https://doi.org/10.1039/C9FO01884K

Fenger, J.-A., Roux, H., Robbins, R. J., Collins, T. M., & Dangles, O. (2021a). The influence of phenolic acyl groups on the color of purple sweet potato anthocyanins and their metal complexes. Dyes and Pigments, 185, 108792. https://doi.org/10.1016/j.dyepig.2020.108792

Fenger, J.-A., Sigurdson, G. T., Robbins, R. J., Collins, T. M., Giusti, M. M., & Dangles, O. (2021b). Acylated Anthocyanins from Red Cabbage and Purple Sweet Potato Can Bind Metal Ions and Produce Stable Blue Colors. International Journal of Molecular Sciences, 22(9), 4551. https://doi.org/10.3390/ijms22094551

Ferarsa, S., Zhang, W., Moulai-Mostefa, N., Ding, L., Jaffrin, M. Y., & Grimi, N. (2018). Recovery of anthocyanins and other phenolic compounds from purple eggplant peels and pulps using ultrasonic-assisted extraction. *Food and Bioproducts Processing*, *109*, 19-28. https://doi.org/10.1016/j.fbp.2018.02.006

Fernandes, A., Brás, N. F., Mateus, N., & de Freitas, V. (2014). Understanding the Molecular Mechanism of Anthocyanin Binding to Pectin. *Langmuir*, *30*(28), 8516-8527. https://doi.org/10.1021/la501879w

Fischer, U. A., Carle, R., & Kammerer, D. R. (2011). Identification and quantification of phenolic compounds from pomegranate (Punica granatum L.) peel, mesocarp, aril and differently produced juices by HPLC-DAD–ESI/MSn. *Food Chemistry*, *127*(2), 807-821. https://doi.org/10.1016/j.foodchem.2010.12.156

Forner-Giner, M. Á., Ballesta-de los Santos, M., Melgarejo, P., Martínez-Nicolás, J. J., Melián-Navarro, A., Ruíz-Canales, A., Continella, A., & Legua, P. (2023). Fruit Quality and Primary and Secondary Metabolites Content in Eight Varieties of Blood Oranges. *Agronomy*, *13*(4), Article 4. https://doi.org/10.3390/agronomy13041037

García-Salas, P., Gómez-Caravaca, A. M., Morales-Soto, A., Segura-Carretero, A., & Fernández-Gutiérrez, A. (2014). Identification and quantification of phenolic compounds in diverse cultivars of eggplant grown in different seasons by high-performance liquid chromatography coupled to diode array detector and electrospray-quadrupole-time of flight-mass spectrometry. *Food Research International*, *57*, 114-122. https://doi.org/10.1016/j.foodres.2014.01.032

Gil, M. I., Tomás-Barberán, F. A., Hess-Pierce, B., Holcroft, D. M., & Kader, A. A. (2000). Antioxidant Activity of Pomegranate Juice and Its Relationship with Phenolic Composition and Processing. *Journal of Agricultural and Food Chemistry*, *48*(10), 4581-4589. https://doi.org/10.1021/jf000404a

Gu, J., Ahn-Jarvis, J. H., & Vodovotz, Y. (2015). Development and characterization of different black raspberry confection matrices designed for delivery of phytochemicals. *Journal of Food Science*, *80*(3), E610-618. https://doi.org/10.1111/1750-3841.12808

Guo, J., Giusti, M. M., & Kaletunç, G. (2018). Encapsulation of purple corn and blueberry extracts in alginate-pectin hydrogel particles : Impact of processing and storage parameters on encapsulation efficiency. *Food Research International*, *107*, 414-422. https://doi.org/10.1016/j.foodres.2018.02.035

Hillebrand, S., Schwarz, M., & Winterhalter, P. (2004). Characterization of anthocyanins and pyranoanthocyanins from blood orange [Citrus sinensis (L.) Osbeck] juice. *Journal of Agricultural and Food Chemistry*, *52*(24), 7331-7338. https://doi.org/10.1021/jf0487957

Ichiyanagi, T., Kashiwada, Y., Shida, Y., Ikeshiro, Y., Kaneyuki, T., & Konishi, T. (2005). Nasunin from Eggplant Consists of Cis − Trans Isomers of Delphinidin 3-[4-(*p*- Coumaroyl)- L -rhamnosyl (1→6)glucopyranoside]-5-glucopyranoside. *Journal of Agricultural and Food Chemistry*, *53*(24), 9472-9477. https://doi.org/10.1021/jf051841y

Kacjan Maršić, N.; Mikulič-Petkovšek, M.; Štampar, F. Grafting Influences Phenolic Profile and Carpometric Traits of Fruits of Greenhouse-Grown Eggplant (*Solanum Melongena* L.). *J. Agric. Food Chem.* **2014**, *62*, 10504–10514. doi.org/10.1021/jf503338m

Kanha, N., Surawang, S., Pitchakarn, P., Regenstein, J. M., & Laokuldilok, T. (2019). Copigmentation of cyanidin 3-O-glucoside with phenolics : Thermodynamic data and thermal stability. *Food Bioscience*, *30*, 100419. https://doi.org/10.1016/j.fbio.2019.100419

Kiaei Pour, P., Alemzadeh, I., Vaziri, A. S., & Beiroti, A. (2020). Potential effects of alginate–pectin biocomposite on the release of folic acid and their physicochemical characteristics. *Journal of Food Science and Technology*, *57*(9), 3363-3370. https://doi.org/10.1007/s13197-020-04369-7

Koh, J., Xu, Z., & Wicker, L. (2020). Blueberry pectin and increased anthocyanins stability under *in vitro* digestion. *Food Chemistry*, *302*, 125343. https://doi.org/10.1016/j.foodchem.2019.125343

Kopač, T., Krajnc, M., & Ručigaj, A. (2021). A mathematical model for pH-responsive ionically crosslinked TEMPO nanocellulose hydrogel design in drug delivery systems. *International Journal of Biological Macromolecules*, *168*, 695-707. https://doi.org/10.1016/j.ijbiomac.2020.11.126

Legua, P., Melgarejo, P., Martínez, J. J., Martínez, R., & Hernández, F. (2012). Evaluation of Spanish Pomegranate Juices : Organic Acids, Sugars, and Anthocyanins. *International Journal of Food Properties*, *15*(3), 481-494. https://doi.org/10.1080/10942912.2010.491931

Legua, P., Modica, G., Porras, I., Conesa, A., & Continella, A. (2022). Bioactive compounds, antioxidant activity and fruit quality evaluation of eleven blood orange cultivars. *Journal of the Science of Food and Agriculture*, *102*(7), 2960-2971. https://doi.org/10.1002/jsfa.11636

Leydet, Y., Gavara, R., Petrov, V., Diniz, A. M., Jorge Parola, A., Lima, J. C., & Pina, F. (2012). The effect of self-aggregation on the determination of the kinetic and thermodynamic constants of the network of chemical reactions in 3-glucoside anthocyanins. *Phytochemistry*, *83*, 125-135. https://doi.org/10.1016/j.phytochem.2012.06.022

Lin, Z., Fischer, J., & Wicker, L. (2016). Intermolecular binding of blueberry pectin-rich fractions and anthocyanin. *Food Chemistry*, *194*, 986-993. https://doi.org/10.1016/j.foodchem.2015.08.113

Liudvinaviciute, D., Rutkaite, R., Bendoraitiene, J., Klimaviciute, R., & Dagys, L. (2020). Formation and characteristics of alginate and anthocyanin complexes. *International Journal of Biological Macromolecules*, *164*, 726-734. https://doi.org/10.1016/j.ijbiomac.2020.07.157

Mazza, G., & Brouillard, R. (1987). Color stability and structural transformations of cyanidin 3,5-diglucoside and four 3-deoxyanthocyanins in aqueous solutions. *Journal of Agricultural and Food Chemistry*, *35*(3), 422-426. https://doi.org/10.1021/jf00075a034

McDonald, K., & Sun, D.-W. (2000). Vacuum cooling technology for the food processing industry : A review. *Journal of Food Engineering*, *45*(2), 55-65. https://doi.org/10.1016/S0260-8774(00)00041-8

Mena, P., Calani, L., Dall'Asta, C., Galaverna, G., García-Viguera, C., Bruni, R., Crozier, A., & Del Rio, D. (2012). Rapid and Comprehensive Evaluation of (Poly)phenolic Compounds in Pomegranate (Punica granatum L.) Juice by UHPLC-MSn. *Molecules*, *17*(12), 14821-14840. https://doi.org/10.3390/molecules171214821

Menegatti, T., Kopač, T., & Žnidaršič-Plazl, P. (2024). Tuning Mechanical Characteristics and Permeability of Alginate Hydrogel by Polyvinyl Alcohol and Deep Eutectic Solvent Addition. *Bioengineering*, *11*(4), 371. https://doi.org/10.3390/bioengineering11040371

Menegatti, T., Kopač, T., & Žnidaršič-Plazl, P. (2024). Tuning Mechanical Characteristics and Permeability of Alginate Hydrogel by Polyvinyl Alcohol and Deep Eutectic Solvent Addition. *Bioengineering*, *11*(4), 371. https://doi.org/10.3390/bioengineering11040371

Mohammadalinejhad, S., Kurek, M., Jensen, I.-J., & Lerfall, J. (2023). The potential of anthocyanin-loaded alginate hydrogel beads for intelligent packaging applications : Stability and sensitivity to volatile amines. *Current Research in Food Science*, *7*, 100560. https://doi.org/10.1016/j.crfs.2023.100560

Moldovan, B., & David, L. (2020). Influence of Different Sweeteners on the Stability of Anthocyanins from Cornelian Cherry Juice. *Foods*, *9*(9), 1266. https://doi.org/10.3390/foods9091266

Moloney, M., Robbins, R. J., Collins, T. M., Kondo, T., Yoshida, K., & Dangles, O. (2018). Red cabbage anthocyanins : The influence of d-glucose acylation by hydroxycinnamic acids on their structural transformations in acidic to mildly alkaline conditions and on the resulting color. *Dyes and Pigments*, *158*, 342-352. https://doi.org/10.1016/j.dyepig.2018.05.057

Morales, J., Bermejo, A., Navarro, P., Forner-Giner, M. Á., & Salvador, A. (2021). Rootstock effect on fruit quality, anthocyanins, sugars, hydroxycinnamic acids and flavanones content during the harvest of blood oranges 'Moro' and 'Tarocco Rosso' grown in Spain. *Food Chemistry*, *342*, 128305. https://doi.org/10.1016/j.foodchem.2020.128305

Nayak, B., Berrios, J. D. J., Powers, J. R., & Tang, J. (2011). Thermal Degradation of Anthocyanins from Purple Potato (Cv. Purple Majesty) and Impact on Antioxidant Capacity. *Journal of Agricultural and Food Chemistry*, *59*(20), 11040-11049. https://doi.org/10.1021/jf201923a

Ozel, B., Kuzu, S., Marangoz, M. A., Dogdu, S., Morris, R. H., & Oztop, M. H. (2024). Hard Candy Production and Quality Parameters : A review. *Open Research Europe*, *4*, 60. https://doi.org/10.12688/openreseurope.16792.1

Patras, A., Brunton, Nigel. P., O'Donnell, C., & Tiwari, B. K. (2010). Effect of thermal processing on anthocyanin stability in foods; mechanisms and kinetics of degradation. *Trends in Food Science & Technology*, *21*(1), Article 1. https://doi.org/10.1016/j.tifs.2009.07.004

Pereira, A. R., Fernandes, V. C., Delerue-Matos, C., de Freitas, V., Mateus, N., & Oliveira, J. (2024). Exploring acylated anthocyanin-based extracts as a natural alternative to synthetic

food dyes : Stability and application insights. *Food Chemistry*, *461*, 140945. https://doi.org/10.1016/j.foodchem.2024.140945

Piri, A., Fanaei, A. R., & Rostampour, V. (2024). Thermodynamic Analysis of a Continuous Vacuum Pan in the Crystallization Process of Sugar Beet Syrup. *Journal of Food Processing and Preservation*, *2024*(1), 2245675. https://doi.org/10.1155/2024/2245675

Riso, P., Visioli, F., Gardana, C., Grande, S., Brusamolino, A., Galvano, F., Galvano, G., & Porrini, M. (2005). Effects of blood orange juice intake on antioxidant bioavailability and on different markers related to oxidative stress. *Journal of Agricultural and Food Chemistry*, *53*(4), 941-947. https://doi.org/10.1021/jf0485234

Sadilova, E., Carle, R., & Stintzing, F. C. (2007). Thermal degradation of anthocyanins and its impact on color and in vitro antioxidant capacity. *Molecular Nutrition & Food Research*, *51*(12), 1461-1471. https://doi.org/10.1002/mnfr.200700179

Said, N. S., Olawuyi, I. F., & Lee, W. Y. (2023). Pectin Hydrogels : Gel-Forming Behaviors, Mechanisms, and Food Applications. *Gels*, *9*(9), 732. https://doi.org/10.3390/gels9090732

Šamec, D., Karalija, E., Šola, I., Vujčić Bok, V., & Salopek-Sondi, B. (2021). The Role of Polyphenols in Abiotic Stress Response : The Influence of Molecular Structure. *Plants*, *10*(1), 118. https://doi.org/10.3390/plants10010118

Sandoval-Castilla, O., Lobato-Calleros, C., García-Galindo, H. S., Alvarez-Ramírez, J., & Vernon-Carter, E. J. (2010). Textural properties of alginate–pectin beads and survivability of entrapped *Lb. Casei* in simulated gastrointestinal conditions and in yoghurt. *Food Research International*, *43*(1), 111-117. https://doi.org/10.1016/j.foodres.2009.09.010

Santiago, M. C. P. D. A., Gouvêa, A. C. M. S., Godoy, R. L. D. O., Borguini, R. G., Pacheco, S., Nogueira, R. I., Nascimento, L. D. S. D. M. D., & Freitas, S. P. (2014). Analytical standards production for the analysis of pomegranate anthocyanins by HPLC. *Brazilian Journal of Food Technology*, *17*(1), 51-57. https://doi.org/10.1590/bjft.2014.008

Seco, A., Pereira, A. R., Camuenho, A., Oliveira, J., Dias, R., Brás, N. F., Basílio, N., Parola, A. J., Lima, J. C., de Freitas, V., & Pina, F. (2024). Comparing the Chemistry of Malvidin-3-O-glucoside and Malvidin-3,5-O-diglucoside Networks : A Holistic Approach to the Acidic

and Basic Paradigms with Implications in Biological Studies. Journal of Agricultural and Food Chemistry, 72(13), 7497-7510. https://doi.org/10.1021/acs.jafc.4c00552

Shi, C., Guo, C., Wang, S., Li, W., Zhang, X., Lu, S., Ning, C., & Tan, C. (2024). The mechanism of pectin in improving anthocyanin stability and the application progress of their complexes : A review. *Food Chemistry: X*, *24*, 101955. https://doi.org/10.1016/j.fochx.2024.101955

Silva, V. G. da, Nogueira, G. F., Soares, C. T., & Oliveira, R. A. de. (2023). Anthocyanin-Rich Jamun (Syzygium cumini L.) Pulp Transported on Protein-Coated Ionic Gelation Microparticles of Calcium Alginate : Production and Morphological Characteristics. *Polysaccharides*, *4*(1), 33-50. https://doi.org/10.3390/polysaccharides4010002

Singh, J., Kaur, K., & Kumar, P. (2018). Optimizing microencapsulation of α-tocopherol with pectin and sodium alginate. *Journal of Food Science and Technology*, *55*(9), 3625-3631. https://doi.org/10.1007/s13197-018-3288-6

Song, B., Li, H., Tian, J., Zhang, Y., Li, Z., Wang, J., Wang, Y., Si, X., & Li, B. (2023). Mechanism of sugar degradation product 5-hydroxymethylfurfural reducing the stability of anthocyanins. Food Chemistry, 419, 136067. https://doi.org/10.1016/j.foodchem.2023.136067

Spanemberg, F. E. M., Korzenowski, A. L., & Sellitto, M. A. (2019). Effects of sugar composition on shelf life of hard candy : Optimization study using D-optimal mixture design of experiments. Journal of Food Process Engineering, 42(6), e13213. https://doi.org/10.1111/jfpe.13213

Sun, J., Song, Y.-L., Zhang, J., Huang, Z., Huo, H.-X., Zheng, J., Zhang, Q., Zhao, Y.-F., Li, J., & Tu, P.-F. (2015). Characterization and Quantitative Analysis of Phenylpropanoid Amides in Eggplant (Solanum melongena L.) by High Performance Liquid Chromatography Coupled with Diode Array Detection and Hybrid Ion Trap Time-of-Flight Mass Spectrometry. *Journal of Agricultural and Food Chemistry*, *63*(13), 3426-3436. https://doi.org/10.1021/acs.jafc.5b00023

Tan, C., Dadmohammadi, Y., Lee, M. C., & Abbaspourrad, A. (2021). Combination of copigmentation and encapsulation strategies for the synergistic stabilization of

anthocyanins. Comprehensive Reviews in Food Science and Food Safety, 20(4), 3164-3191. https://doi.org/10.1111/1541-4337.12772

Trouillas, P., Sancho-García, J. C., De Freitas, V., Gierschner, J., Otyepka, M., & Dangles, O. (2016a). Stabilizing and Modulating Color by Copigmentation : Insights from Theory and Experiment. *Chemical Reviews*, *116*(9), Article 9. https://doi.org/10.1021/acs.chemrev.5b00507

Yang, P., Basílio, N., Liao, X., Xu, Z., Dangles, O., & Pina, F. (2024). Influence of Acylation by Hydroxycinnamic Acids on the Reversible and Irreversible Processes of Anthocyanins in Acidic to Basic Aqueous Solution. *Journal of Agricultural and Food Chemistry*, *72*(46), 25955-25971. https://doi.org/10.1021/acs.jafc.4c06847

Zearah, S. A. (2024). Assessment of the Antioxidant Potential of Anthocyanin-Rich Extract of Eggplant (Solanum melongena L.) and Evaluation of its Antimicrobial Activity. *Tropical Journal of Natural Product Research*, *8*(3), 6558-6562. https://doi.org/10.26538/tjnpr/v8i3.13

Zhang, Y., Deng, Z., Li, H., Zheng, L., Liu, R., & Zhang, B. (2020). Degradation Kinetics of Anthocyanins from Purple Eggplant in a Fortified Food Model System during Microwave and Frying Treatments. *Journal of Agricultural and Food Chemistry*, *68*(42), 11817-11828. https://doi.org/10.1021/acs.jafc.0c05224

Zhao, C. L., Chen, Z. J., Bai, X. S., Ding, C., Long, T. J., Wei, F. G., & Miao, K. R. (2014). Structure–activity relationships of anthocyanidin glycosylation. *Molecular Diversity*, *18*(3), 687-700. https://doi.org/10.1007/s11030-014-9520-z

APPENDICES

Appendix 1. Calibration curve of Gallic acid

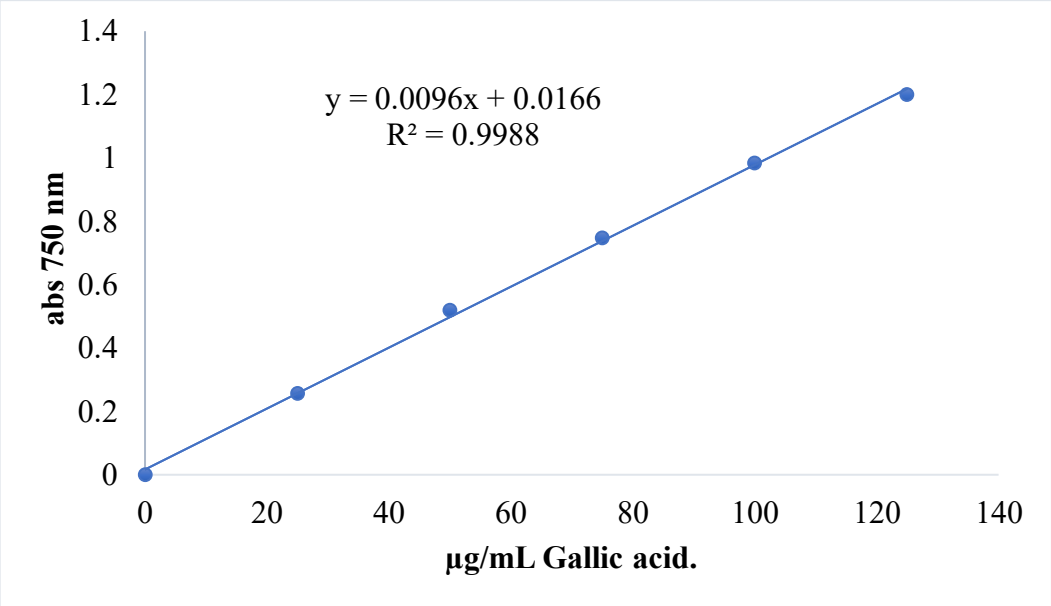

Appendix 2. Mean molecular weight (HPLC) and apparent molar absorption coefficient at λ_{max} (pH 1) of extracts.

Table A2-1. Anthocyanin composition of the eggplant peel extract.

#	RT	Compound	MW* (g/mol)	Area (%)
1	17.3	Delphinidin-3-O-rutinoside-5-O-galactoside	773	7.36
2	24.28	Delphinidin-3-O-rutinoside-5-O-glucoside	773	4.43
3	29.62	Delphinidin-3-O-glucoside	465	2.76
4	31.01	Delphinidin-3-O-rutinoside	611	85.45
Total			**626**	**100**

*Calculated MW from the composition and mass of individual pigments (see table 2 & appendix 3).

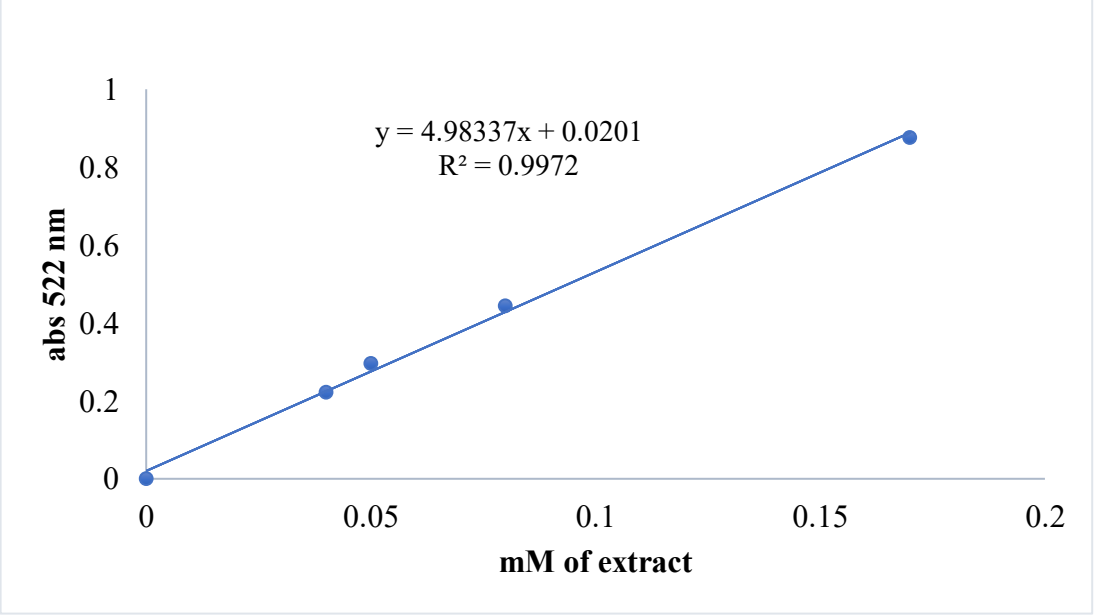

Figure A2-1. Apparent molar absorption coefficient (ε) at λ_{max} (522 nm) and pH 1 (flavylium form), determined from Beer's law assuming 100% anthocyanin content in the EPP extract.

Table A2-2. Anthocyanin composition of the pomegranate juice (*Punica granatum*) extract.

#	RT	Compound	MW* (g/mol)	Area (%)
1	19.56	Delphinidin-3,5-di-O-glucoside	627	6.86
2	24.51	Cyanidin-3,5-di-O-glucoside	611	37.89
3	29.26	Delphinidin-3-O-glucoside	465	7.94
4	34.53	Cyanidin-3-O-glucoside	449	42.23
5	39.73	Pelargonidin-3-O-glucoside	433	5.09
Total			**523**	**100**

*Calculated MW from the composition and mass of individual pigments (see table 2 & appendix 3).

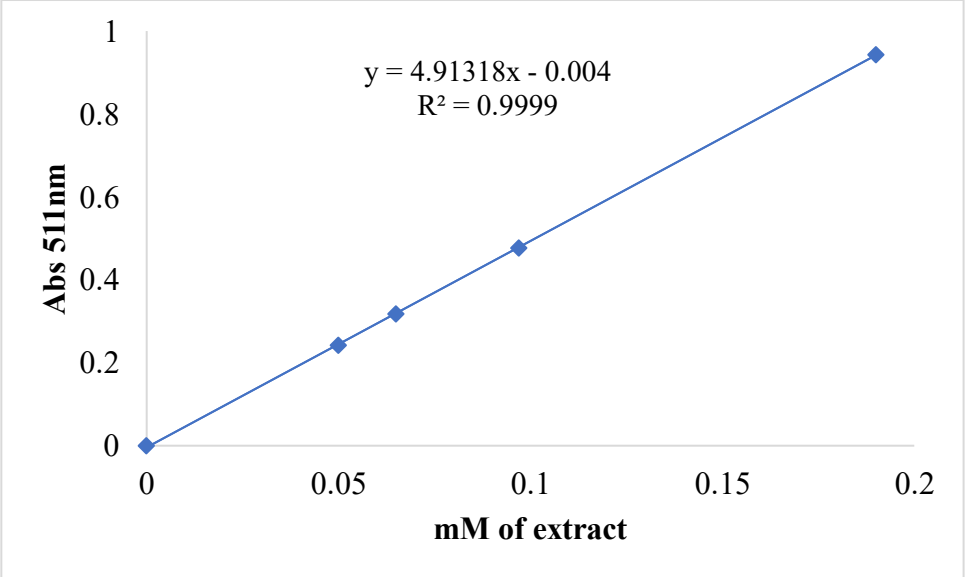

Figure A2-2. Apparent molar absorption coefficient (ε) at λ_{max} (512 nm) and pH 1 (flavylium form), determined from Beer's law assuming 100% anthocyanin content in the PGJ extract.

Table A2-3. Anthocyanin composition of the Blood orange juice (*Citrus sinensis (L.)* extract.

#	RT	Compound	MW* (g/mol)	Area (%)
1	29.47	Delphinidin-3-O-glucoside	465	0.95
2	31.18	Cyanidin-3-O-sophoroside	611	0.76
3	32.34	Cyanidin-3-O-galactoside	449	0.92
4	34.73	Cyanidin-3-O-glucoside	449	57.1
5	42.89	Peonidin-3,5-di-O-glucoside	625	3.76
6	46.27	Cyanidin-3-O-dioxalylglucoside	593	1.61
7	47.56	Cyanidin-3-O-(6˝-malonyl)glucoside	535	27.96
8	50.55	Cyanidin-3-O-dioxaloylglucoside	593	3.6
9	55.21	Peonidin-3-O-(6˝-malonyl)glucoside	549	1
10	57.63	Cyanidin-3-O-(malonyl, dioxalyl)glucoside	679	2.34
Total			**495**	**100**

*Calculated MW from the composition and mass of individual pigments (see table 2 & appendix 3).

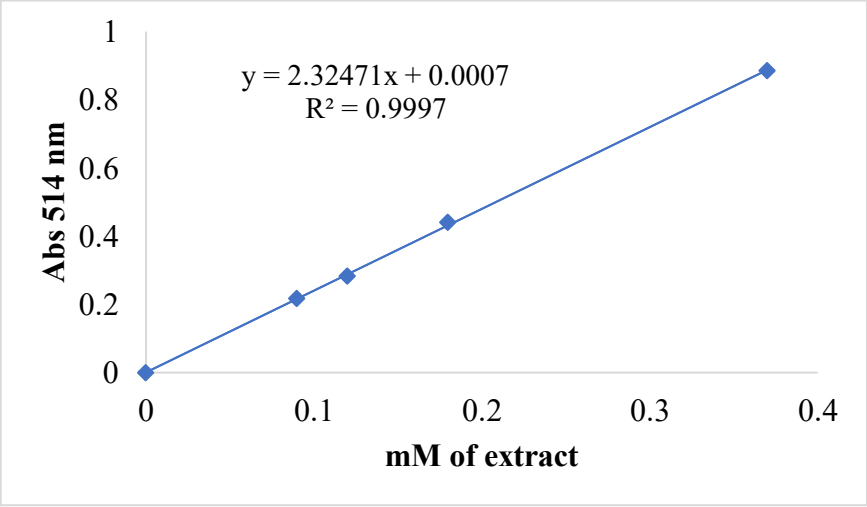

Figure A2-3. Apparent molar absorption coefficient (ε) at λ_{max} (514 nm) and pH 1 (flavylium form), determined from Beer's law assuming 100% anthocyanin content in the BOJ extract.

Appendix 3. HPLC chromatograms and MS spectra of pigments and copigments in the extracts.

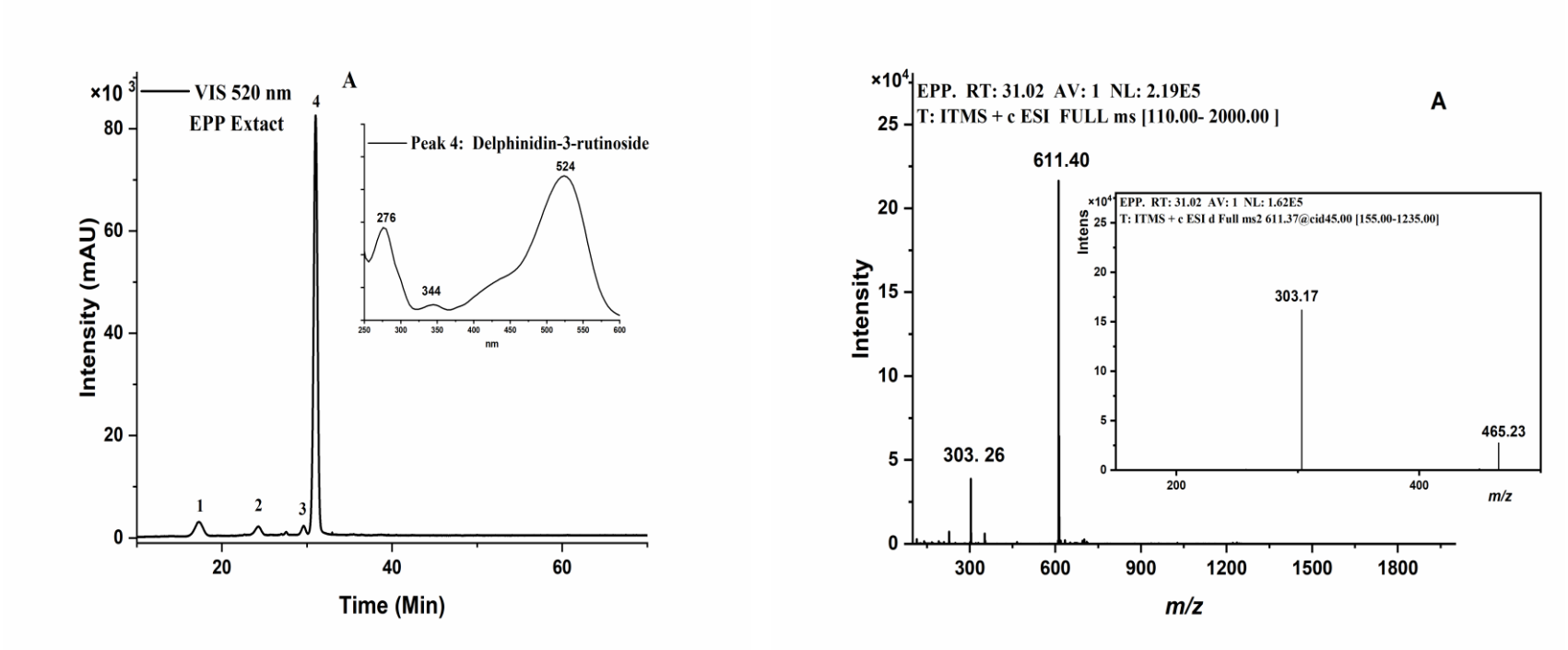

Figure A3-1. *Left:* HPLC chromatogram showing the anthocyanin profile of eggplant peel (**A**). *Right:* MS data of major anthocyanins. Peak 4 in eggplant peel (**A).**

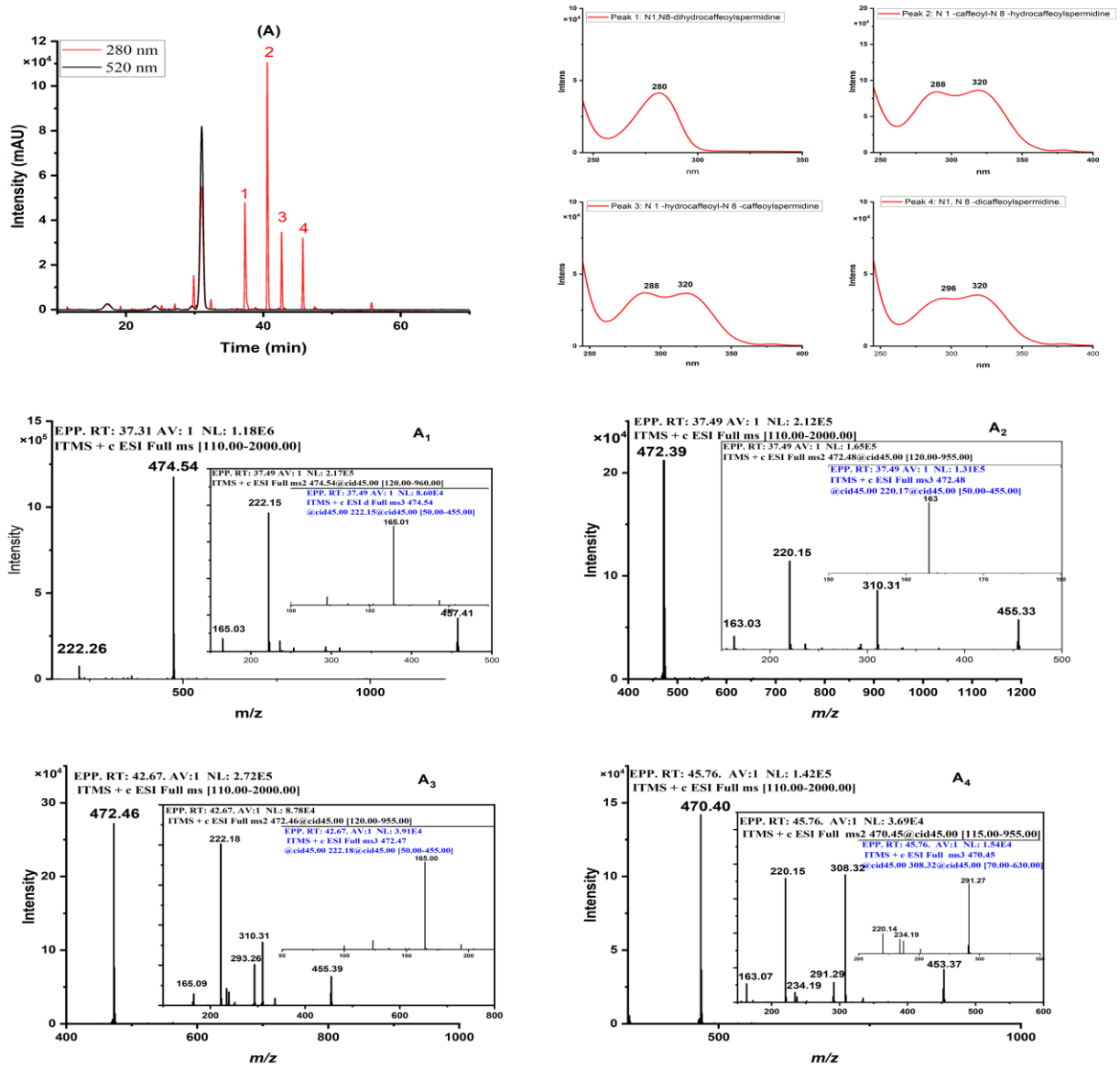

Figure A3-2. *Top*: HPLC chromatograms showing the copigment profile of eggplant peel (**A**). See Table 2 for identification of each numbered peak. *Down*: MS data of the main copigments of eggplant peel. Peak 1: N_1,N_8-di-dihydrocaffeoylspermidine (**A1**), peak 2: N_1-caffeoyl-N_8-dihydrocaffeoylspermidine (**A_2**), peak 3: N_1-dihydrocaffeoyl-N_8-caffeoylspermidine (**A_3**), peak 4: N_1,N_8-dicaffeoylspermidine (**A_4**).

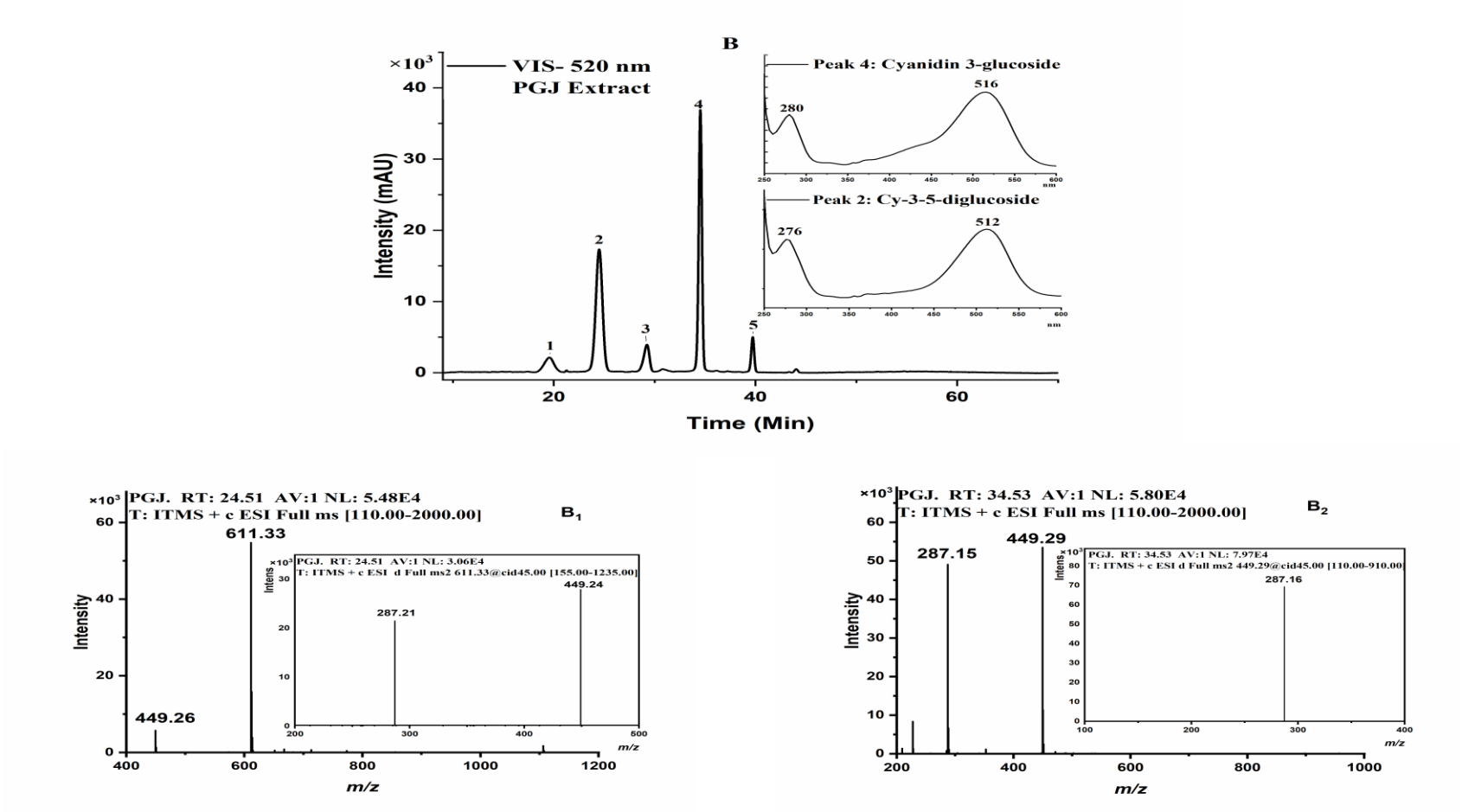

Figure A3-3. *Top:* HPLC chromatogram showing the anthocyanin profile of pomegranate juice (**B**). *Down*: MS spectra of the major anthocyanins, peaks 2 (B1) and 4 (B2).

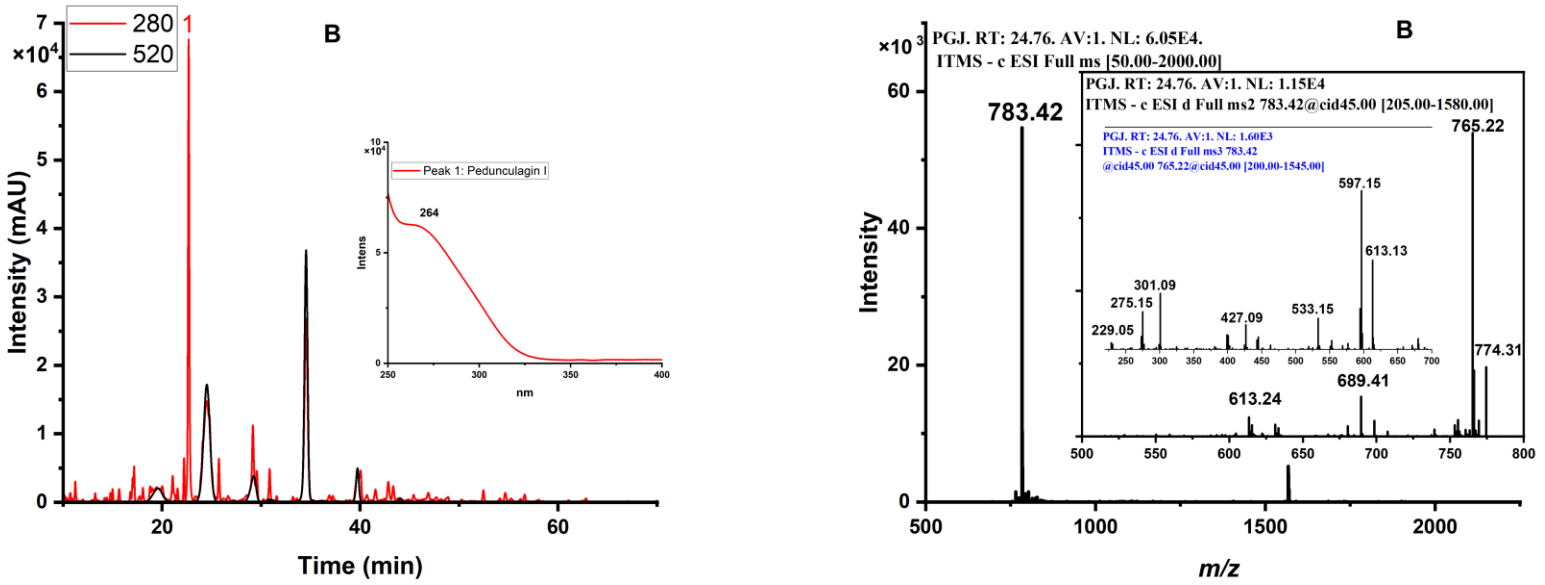

Figure A3-4. *Left*: HPLC chromatograms of pomegranate juice. *Right*: MS data of the main copigment, peak 1: pedunculagin I.

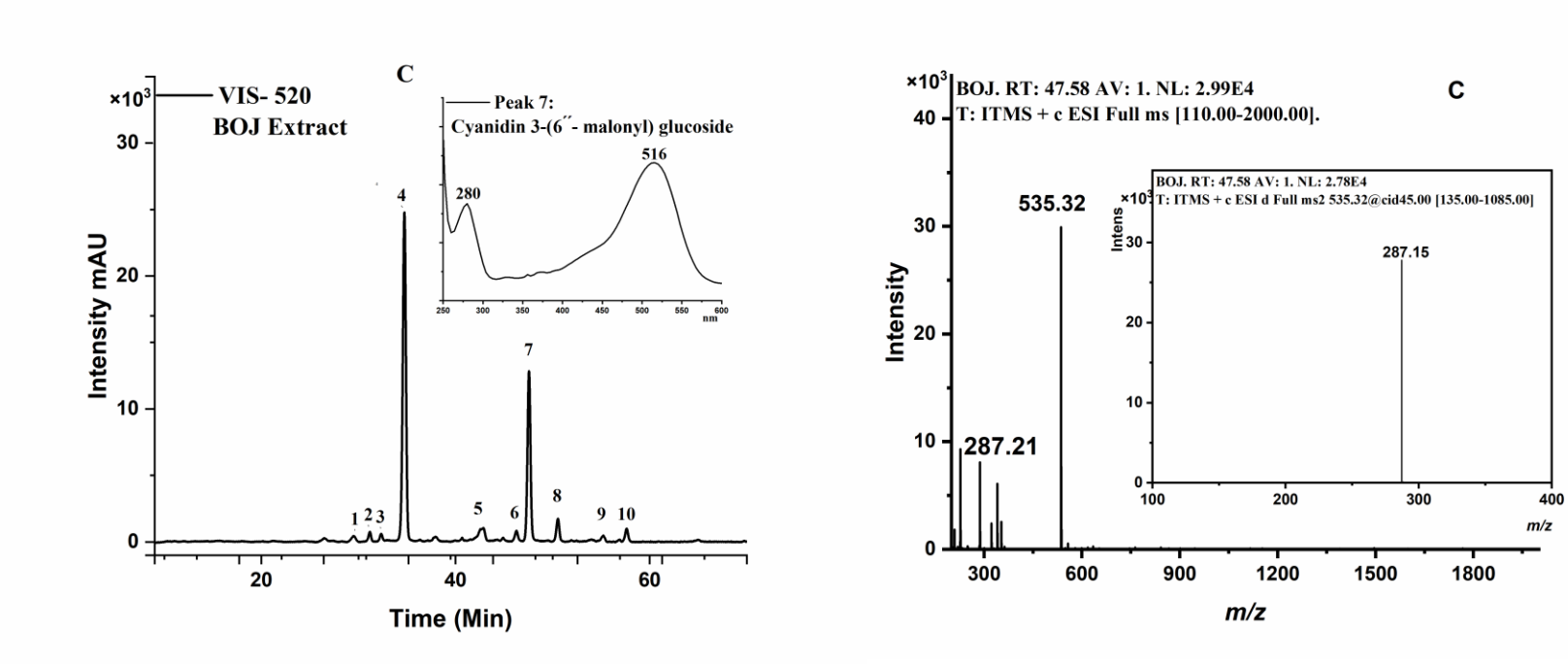

Figure A3-5. *Left*: HPLC chromatogram showing the anthocyanin profiles of blood orange juice (**C**). *Right*: MS data of major anthocyanins, peak 7 in blood orange juice, (**C**).

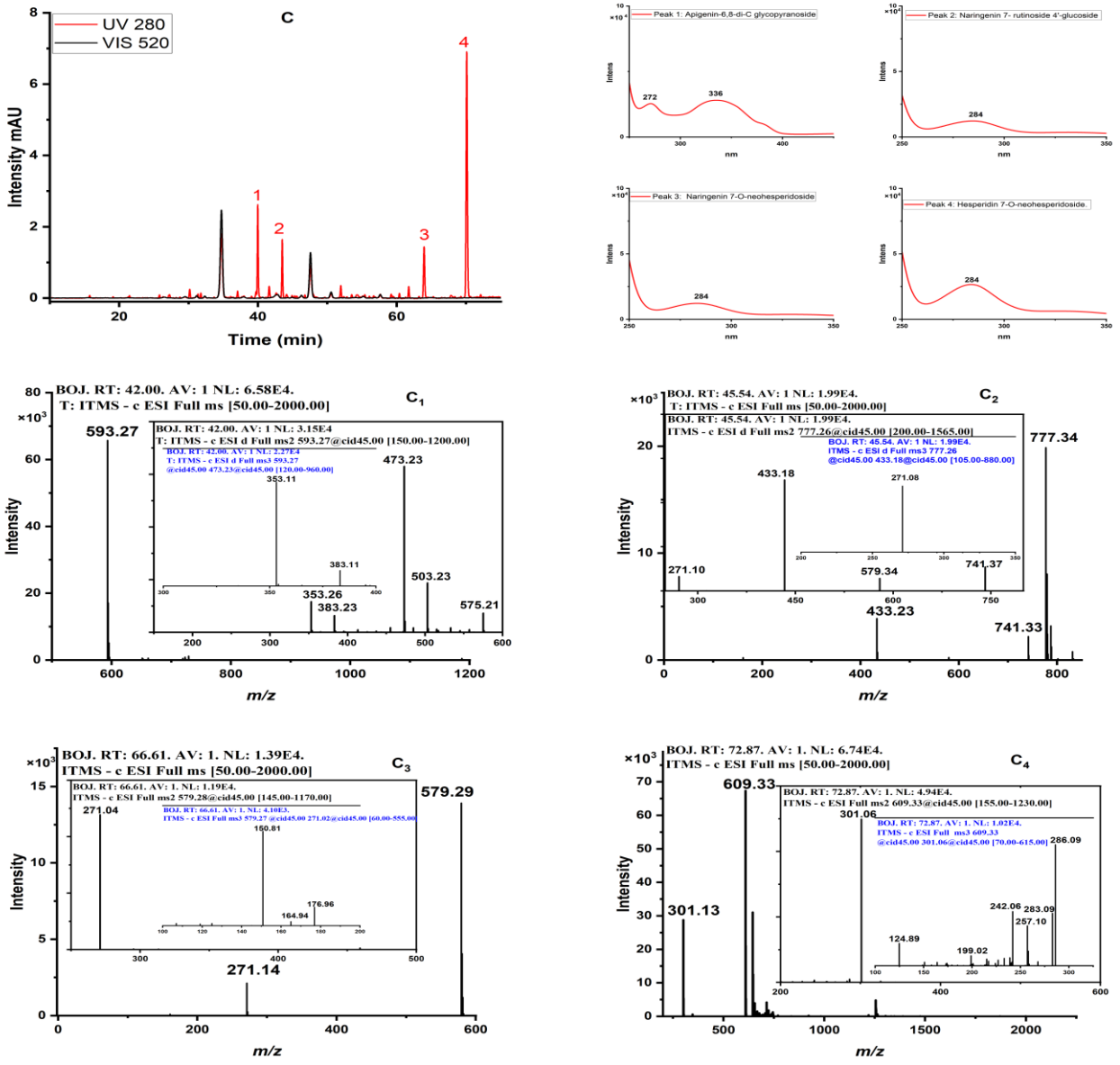

Figure A3-6. *Top*: HPLC chromatograms showing the main copigments of blood orange juice. See Table 2 for identification of each numbered peak. *Down*: MS data of the main copigments in blood orange juice. (**C1**), peak 1: apigenin 6,8-di-C-glucoside (**C2**), peak 2: naringenin 7-O-rutinoside-4'-O-glucoside (**C3**), peak 3: naringenin 7-O-neohesperidoside (**C4**), peak 4: hesperidin 7-O-neohesperidoside.

Appendix 4. Kinetic monitoring of anthocyanin hydration at λ_{max} for each extract, with determination of k_{obs} as a function of pH. Exemples for pH 3, 4 and 5 are shown in the figure, fitted using a monoexponential model.

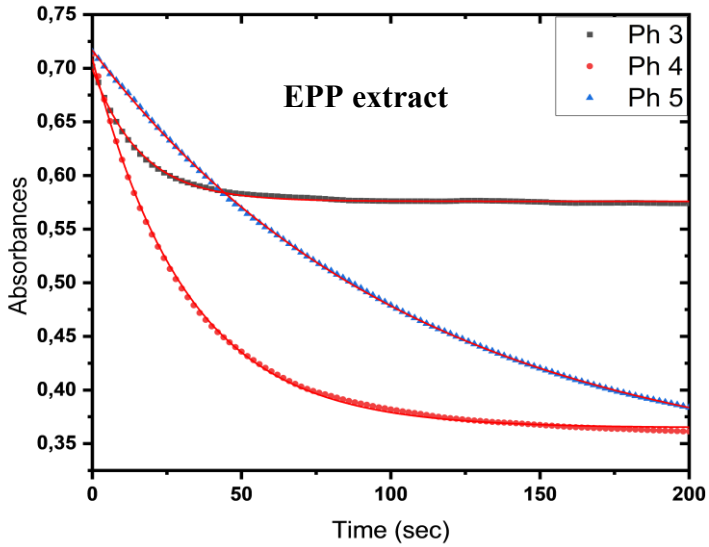

***Kobs* vs. pH**

Final pH	k_{obs} (s^{-1})	sd
2.52	0.282610	0.002740
2.89	0.169170	0.001710
3.44	0.115110	0.000544
3.81	0.068320	0.000594
4.24	0.040860	0.001923
4.56	0.025640	0.001358
4.88	0.014210	0.000014
5.35	0.005380	0.000219
5.66	0.002910	0.000071
5.94	0.001610	0.000002

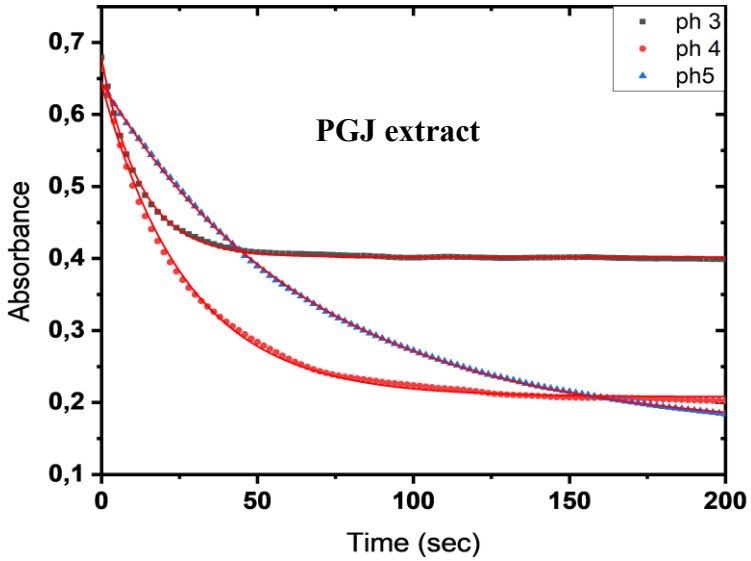

***K**obs* *vs.* pH**

Final pH	k_{obs} (s^{-1})	sd
2.57	0.3186	0.0720
2.97	0.2688	0.0045
3.43	0.1427	0.0122
3.82	0.1048	0.0097
4.23	0.0727	0.0024
4.55	0.0442	0.0010
4.86	0.0283	0.0022
5.34	0.0117	0.0002
5.63	0.0055	0.0001
5.97	0.0036	0.0001

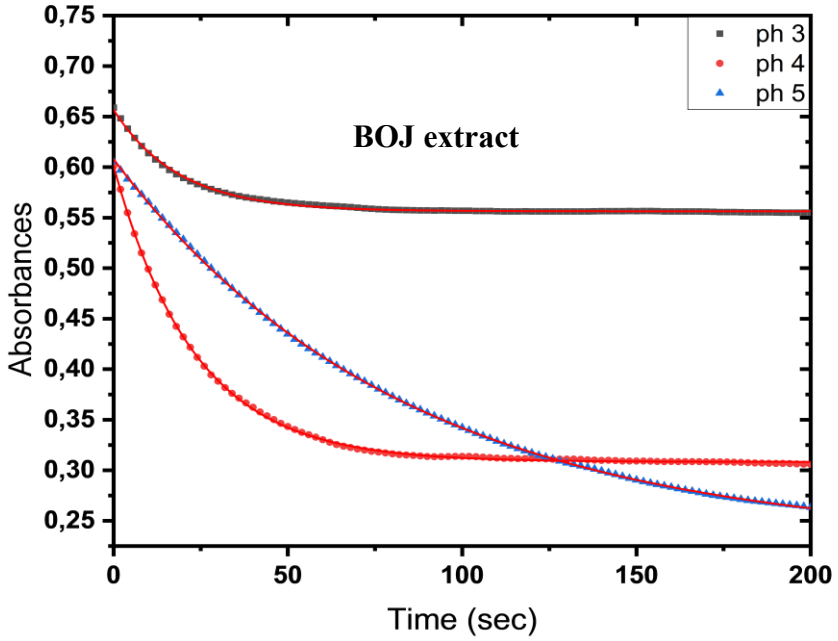

***K**obs* **vs. pH**

Final pH	k_{obs} (s^{-1})	sd
3.23	0.13642	0.00422
3.81	0.07851	0.00271
4.39	0.04491	0.00190
4.65	0.02859	0.00004
4.95	0.01869	0.00220
5.35	0.00652	0.00002
5.5	0.00753	0.00028
6.14	0.00213	0.00004

Appendix 5. Color loss (A_1, B_1, C_1), and Pigment loss (A_2, B_2, C_2), in anthocyanin-rich extracts at pH 5 and 50°C as a function of time: A) EPP, B) PGJ, C) BOJ.

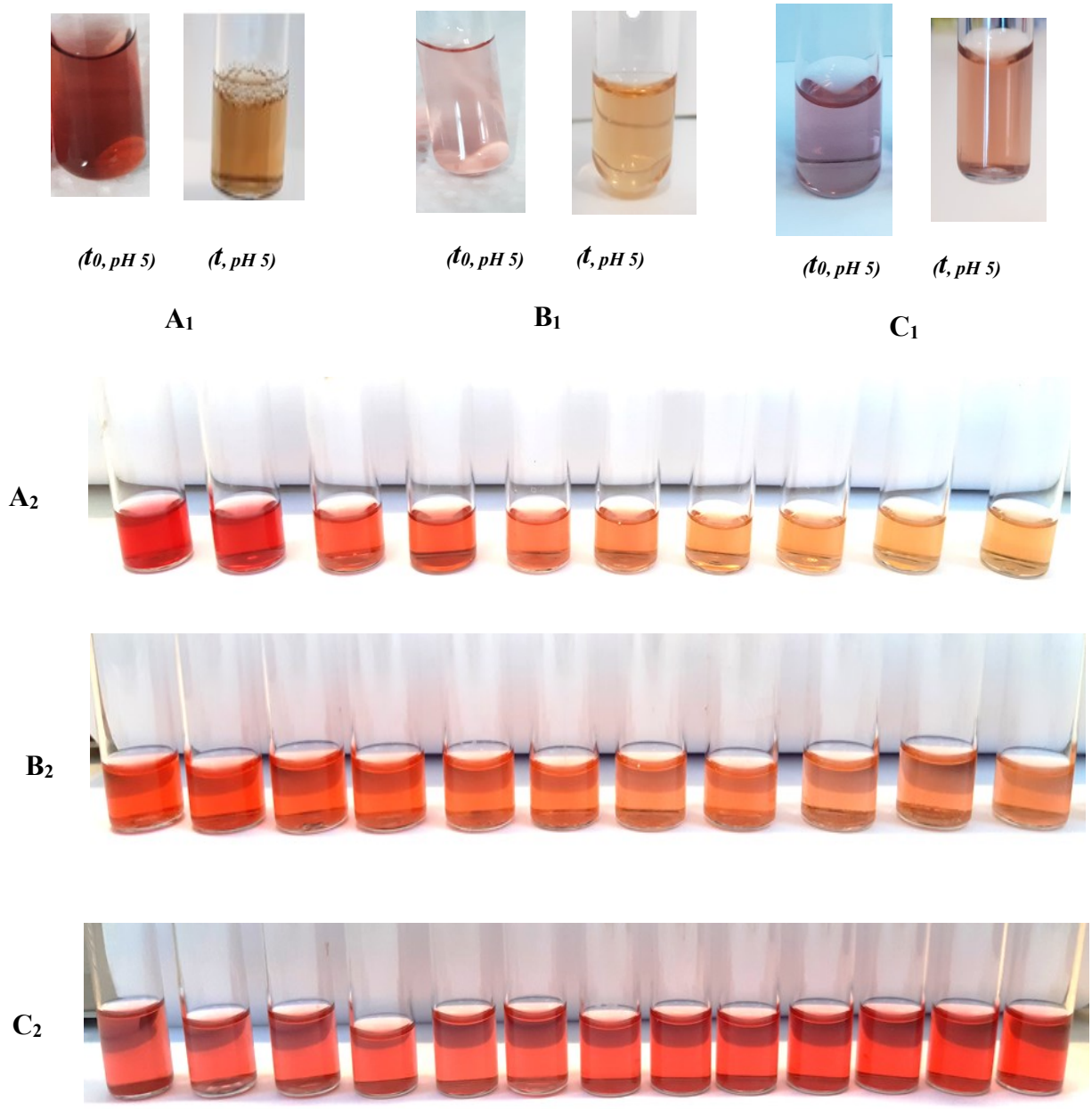

Appendix 6. Moisture content of anthocyanin-encapsulated beads.

Billes	BOJ (%)	PGJ (%)	EPP (%)
A pH 4	95.3 ± 0.4	96.2 ± 0.2	94.8 ± 0.4
A pH 5	96.4 ± 0.2	98.3 ± 2.9	95.6 ± 0.3
AP pH 4	97.9 ± 2.8	96.4 ± 0.1	95.5 ± 0.2
AP pH 5	95.7 ± 2.9	96.2 ± 0.4	95.4 ± 0.0
AA pH 4	96.8 ± 0.8	96.3 ± 0.7	93.7 ± 2.2
AA pH 5	96.7 ± 0.3	97.3 ± 0.4	95.8 ± 0.3
APA pH 4	95.9 ± 0.7	96.3 ± 0.4	96.8 ± 0.2
APA pH 5	96.7 ± 0.6	95.4 ± 0.6	94.8 ± 0.4

Appendix 7. Alginate and Pectin structure.

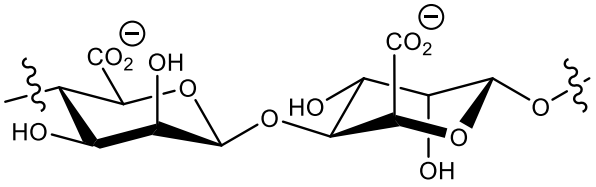

Alginate

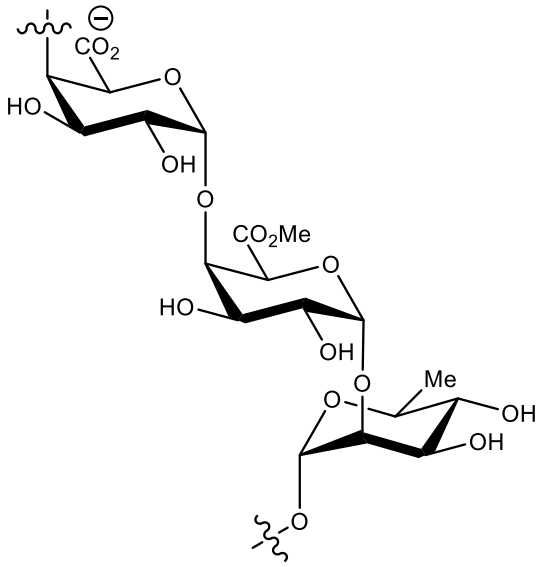

Pectin

Appendix 8. Al^{3+} - cyanidin 3-O-glycoside complex stabilized by anionic polysaccharide.

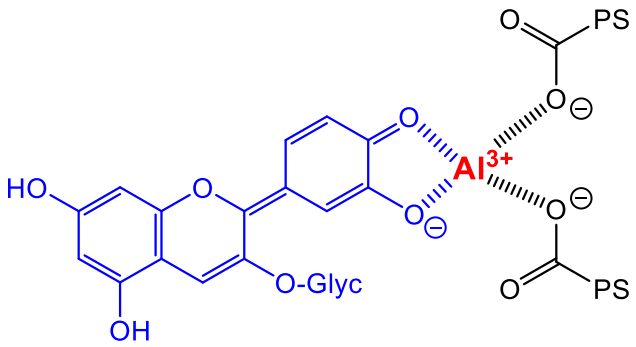

Appendix 9. Sensory Evaluation Form – Visual Aspect of Candies.

Age: _____ Sexe: _____

In this visual evaluation, you will examine a series of candy samples (A to G) prepared with either natural or artificial colorants. Please focus only on their color: pay attention to the intensity, brightness, uniformity, and overall visual impression. You are not asked to taste the candies or to judge their shape or texture. The purpose of this evaluation is to determine whether the color appears appealing, appetizing, and visually pleasant.

1. For each candy sample (A to G), please answer, Yes or No:

Product	**Color appreciation**	**Glossiness**	**Appearance acceptability**	**Artificial color perception**	**Purchase intention**
A	☐ Yes ☐ No	☐ Yes ☐ No	☐ Yes ☐ No	☐ Yes ☐ No	☐ Yes ☐ No
B	☐ Yes ☐ No	☐ Yes ☐ No	☐ Yes ☐ No	☐ Yes ☐ No	☐ Yes ☐ No
C	☐ Yes ☐ No	☐ Yes ☐ No	☐ Yes ☐ No	☐ Yes ☐ No	☐ Yes ☐ No
D	☐ Yes ☐ No	☐ Yes ☐ No	☐ Yes ☐ No	☐ Yes ☐ No	☐ Yes ☐ No
1	☐ Yes ☐ No	☐ Yes ☐ No	☐ Yes ☐ No	☐ Yes ☐ No	☐ Yes ☐ No
2	☐ Yes ☐ No	☐ Yes ☐ No	☐ Yes ☐ No	☐ Yes ☐ No	☐ Yes ☐ No
3	☐ Yes ☐ No	☐ Yes ☐ No	☐ Yes ☐ No	☐ Yes ☐ No	☐ Yes ☐ No

2. Overall product acceptability: Please rate each sample from 1 (least liked) to 9 (most liked).

Product	A	B	C	D	1	2	3
Rating							

3. In your opinion, what makes a candy look “natural”? (You can tick more than one box)

   ☐ Its color looks like a real fruit (e.g., strawberry, cherry)

   ☐ It has a very bright and flashy color

   ☐ It looks very shiny

   ☐ It has a soft and light color

4. Does the visual appearance of candies influence your purchasing decision?

   ☐ Yes ☐ No ☐ Sometimes

5. Do you think that colors made from natural extracts are attractive enough to make you want to buy the candies?

   ☐ Yes, definitely

   ☐ Yes, but a bit less than artificial colors

   ☐ No, I prefer the brighter colors of artificial candies

   ☐ I don’t know

Comment: .....

Équipe d’encadrement

Pr. Sabiha ACHAT, directeur de thèse, Professeur, Laboratoire Biomathématique, Biophysique, Biochimie et Scientométrie (L3BS). Sciences Alimentaires.

Pr. Olivier DANGLES, Co-directeur de thèse, Professeur, UMR 408 SQPOV (Sécurité et qualité des produits d’origine végétale), Equipe Micronutriments, Réactivité et digestion.

Abstract

Anthocyanins are natural red–purple–blue pigments of interest as alternatives to synthetic dyes. However, their sensitivity to pH, temperature, dioxygen, light, and matrix composition limits their industrial applications, particularly under near-neutral conditions. In this work, anthocyanin-rich extracts from eggplant peel (EPP), pomegranate juice (PGJ), and blood orange juice (BOJ) were enriched and characterized by HPLC-MS and UV–visible spectroscopy. Their composition, hydration susceptibility (reversible color loss), thermal stability (irreversible degradation), and metal-binding capacity were investigated as key determinants of color diversification and stabilization. BOJ and EPP were more resistant to hydration than PGJ. All extracts formed Al^{3+} complexes at pH 5, reversing hydration equilibria and regenerating color: EPP produced blue complexes, whereas BOJ and PGJ produced purple ones. At 50 °C, BOJ showed the highest stability, while EPP degraded rapidly. To better approximate food-like environments, the extracts were encapsulated in alginate–pectin beads at pH 4 and 5. Encapsulation efficiency ranged from 17.9 to 82.1 %, with the highest values for EPP and PGJ and the lowest for BOJ. Thermal stability was greatest for BOJ, followed by PGJ, with EPP being the least stable. Al^{3+}–anthocyanin complexes provided the highest encapsulation efficiency and were especially stable at pH 5, with pectin further improving thermal resistance. BOJ, the most stable extract in both liquid and encapsulated forms, contains flavonoids, particularly flavones, whose planar structures promote strong π-stacking with anthocyanins, enhancing color stability by limiting hydration and the accumulation of thermally sensitive chalcones. Conversely, PGJ experienced greater color loss due to abundant hydration-prone anthocyanidin 3,5-diglucosides, only modestly protected by endogenous ellagitannins. The faster degradation of EPP anthocyanins likely results from their higher sensitivity to autoxidation driven by caffeoyl derivatives, which, although they mitigate hydration-induced color loss, can accelerate thermal breakdown. Finally, incorporation into hard candies confirmed practical relevance: acidified formulations produced vivid red hues, while non-acidified ones yielded purple tones for BOJ and EPP and nearly colorless PGJ. Despite lower color vividness than Allura Red, natural extracts were perceived as more authentic and were thus well appreciated by consumers.

Résumé

Les anthocyanes sont des pigments végétaux responsables des teintes rouge–pourpre–bleue et représentent une alternative prometteuse aux colorants synthétiques. Leur stabilité, fortement dépendante du pH, de la température, du dioxygène, de la lumière et de la composition matricielle, limite toutefois leur application industrielle, notamment en milieu neutre. Dans ce travail, des extraits riches en anthocyanes de pelure d'aubergine (EPP), jus de grenade (PGJ) et jus d'orange sanguine (BOJ) ont été enrichis et caractérisés par HPLC-MS et UV-Vis afin d'évaluer composition, stabilité thermique (dégradation irréversible), hydratation (perte de couleur réversible) et complexation métallique comme facteurs de stabilisation des couleurs. BOJ et EPP se sont révélés plus résistants à l'hydratation que PGJ. Tous les extraits ont formé des complexes avec Al^{3+} à pH 5, inversant l'équilibre d'hydratation et régénérant la couleur : EPP produisait des complexes bleus, tandis que BOJ et PGJ donnaient des complexes pourpres. À 50 °C, BOJ présentait la plus grande stabilité, alors qu'EPP se dégradait rapidement. Pour mieux simuler les environnements alimentaires, les extraits ont été encapsulés dans des billes d'alginate–pectine à pH 4 et 5. L'efficacité d'encapsulation variait de 17,9 à 82,1 %, avec les valeurs les plus élevées pour EPP et PGJ et les plus faibles pour BOJ. La stabilité thermique était toutefois la plus élevée pour BOJ, suivie de PGJ, EPP étant le moins stable. Les complexes Al^{3+}–anthocyanes présentaient la meilleure efficacité d'encapsulation et une stabilité accrue à pH 5, l'ajout de pectine renforçant encore la résistance thermique. BOJ, l'extrait le plus stable en solution comme encapsulé, contient des flavonoïdes, notamment des flavones, dont la structure plane favorise de fortes interactions π-empilement avec les anthocyanes, limitant l'hydratation et la formation de chalcones thermosensibles. À l'inverse, PGJ a montré une perte de couleur plus marquée en raison de la présence abondante d'anthocyanidines 3,5-diglucosides, très sensibles à l'hydratation et faiblement protégées par les ellagitannins endogènes. La dégradation plus rapide des anthocyanes d'EPP s'explique par leur sensibilité accrue à l'autoxydation induite par les dérivés caféoylés. Enfin, l'incorporation dans des bonbons durs a confirmé la pertinence pratique : les formulations acidifiées présentaient de vives teintes rouges, tandis que les non acidifiées donnaient des tons pourpres pour BOJ et EPP, et presque incolores pour PGJ. Malgré une couleur moins vive que l'Allura Red, les extraits naturels ont été perçus comme plus authentiques et en conséquence étaient bien appréciés par les consommateurs.

ملخص

الأنثوسيانين هي أصباغ نباتية طبيعية مسؤولة عن الألوان الحمراء–الأرجوانية–الزرقاء وتشكل بديلاً واعدًا للأصباغ الاصطناعية. غير أن حساسيتها تجاه درجة الحموضة والحرارة والأكسجين والضوء وتكوين المصفوفة تحد من استخدامها الصناعي، خصوصًا في البيئات شبه المحايدة. في هذا العمل، تم توصيف المستخلصات الغنية بالأنثوسيانين من قشر الباذنجان (EPP) وعصير الرمان (PGJ) وعصير البرتقال الدموي (BOJ) باستخدام HPLC-MS والتحليل الطيفي بالأشعة فوق البنفسجية والمرئية، لدراسة تركيبها، وقابليتها للترطيب (فقدان اللون القابل للعكس)، واستقرارها الحراري (تحلل غير قابل للعكس) ، وقدرتها على الارتباط بالمعادن كعوامل رئيسية لاستقرار الالوان. أظهر كل من BOJ وEPP مقاومة أعلى للترطيب مقارنة بـPGJ. جميع المستخلصات شكّلت مركبات مع Al^{3+}عند درجة حموضة 5 مما عكس توازن الترطيب وأعاد توليد اللون: أنتج EPP مركبات زرقاء، بينما شكّل BOJ وPGJ مركبات أرجوانية. عند 50 °م، أظهر BOJ أعلى استقرار حراري، في حين تدهور EPP بسرعة. لمحاكاة الظروف الغذائية، تم تغليف المستخلصات في حبيبات من الألجينات والبكتين عند درجة حموضة 4 و5. تراوحت فعالية التغليف بين 17.9 و82.1٪، وكانت الأعلى لـEPP وPGJ والأدنى لـBOJ. ومع ذلك، كان الاستقرار الحراري الأكبر لـBOJ، يليه PGJ، بينما كان EPP الأقل استقرارًا. أظهرت مركبات أنثوسيانين–Al^{3+} فعالي أفضل للتغليف واستقرارًا مرتفعًا عند درجة حموض 5 ، مع تعزيز البكتين للمقاومة الحرارية. يحتوي BOJ، الأكثر استقرارًا في الشكلين السائل والمغلف، على فلافونويدات، خصوصًا الفلافونات، التي تعزز هياكلها المستوية التراصّ π القوي مع الأنثوسيانين، عبر الحد من الترطيب وتكوّن الكالكونات الحساسة للحرارة. بالمقابل، فقد PGJ لونه بدرجة أكبر بسبب وفرة أنثوسيانيدين 3,5-ديجلوكوزيدات شديدة القابلية للترطيب وضعف حمايتها بالإيلاجيتانينات الذاتية. ويُعزى التحلل الأسرع لأنثوسيانين EPP إلى حساسيتها العالية للأكسدة الذاتية الناتجة عن المشتقات الكافيينية. أخيرًا، أكّد دمج المستخلصات في الحلوى الصلبة أهميتها التطبيقية: إذ أنتجت التركيبات المحمضة ألوانًا حمراء زاهية، بينما أعطت غير المحمضة ألوانًا أرجوانية لـBOJ وEPP، وشبه عديمة اللون بالنسبة لـPGJ. رغم أن حيوية الألوان أقل من Allura Red، فقد اعتُبرت المستخلصات الطبيعية حقيقية أكثر ونالت استحسان المستهلكين.